MAY. - AUG. 2002
Volume VIII Number II
ISSN 0859 144X

THE ASEAN JOURNAL OF RADIOLOGY

Published by The Radiological Society and
The Royal College of Radiologists of Thailand,
Bangkok, Thailand

Started through an educational grant from Bracco since 1995

Toshiba Medical Systems Group

contributes to the health and welfare of people all over the world through the development, production and servicing of advanced medical equipment. Toshiba Medical Systems Company has grown into one of the world's leading diagnostic imaging manufacturers, contributing to the advancement of medicine.

Its operations include Research & Development design, production, sales & services and support of diagnostic imaging equipment and systems. Based on the concept that only R & D carried out in full collaboration with worldwide medical circles can truly contribute to health care progress, Toshiba maintains constant contact with the real world of daily medical practice, receiving feed-back on clinical needs and incorporating it into R & D actvities. These and other activities have won the highest praise in the global medical market.

It is our commitment to bring high technology plus experience through the supply of a wide-range of Diagnostic X-ray, Ultrasound, Computerised Tomography and Magnetic Resonance Imaging Systems. Toshiba's vision is to provide solutions to the medical professionals that help save the patient's lives while offering reliable products with a long service life.

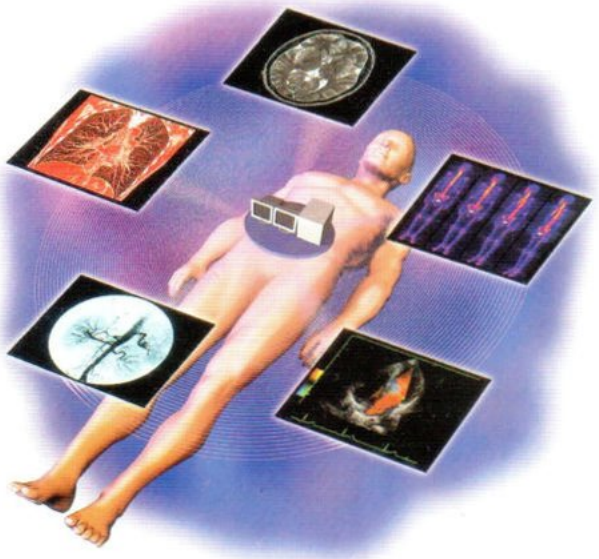

TOSHIBA
MEDICAL SYSTEMS

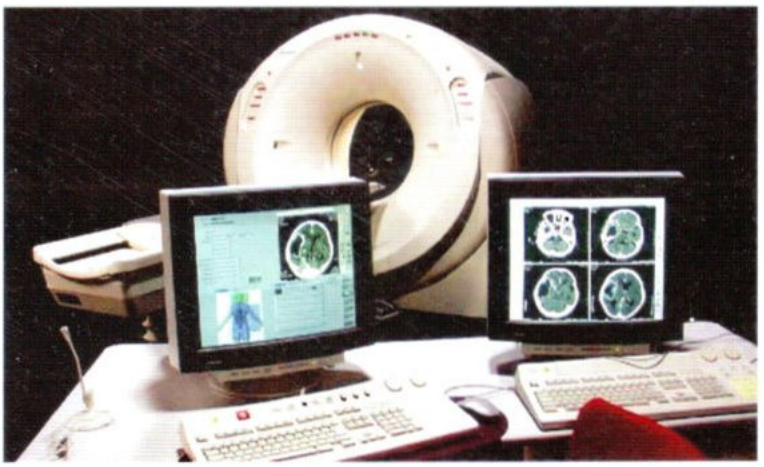

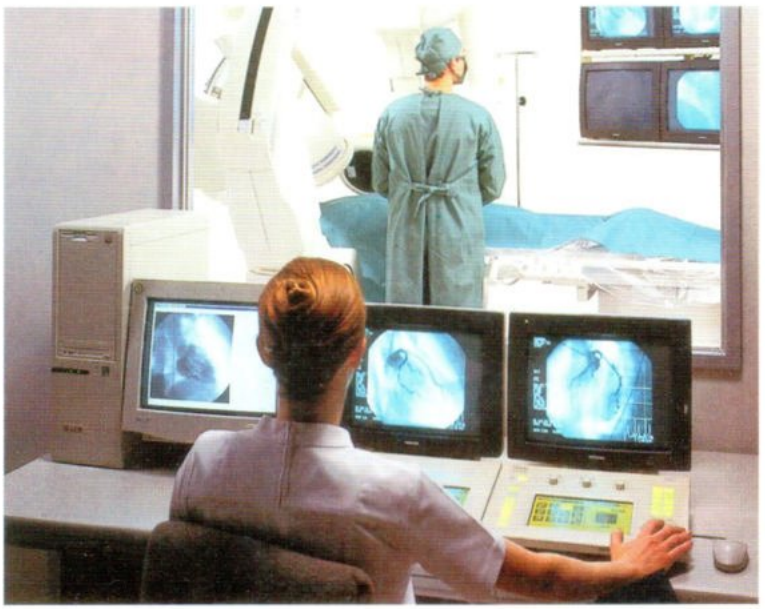

Sole Distributor

CMC Biotech Co., Ltd.

364 Muban Town-in-Town, Soi Ladphrao 94
Ladphrao Road, Wangthonglang, Bangkok 10310
Tel : 66 (0) 2530-4995 (Hunting 8 lines)
Fax: 66 (0) 2539-6903
E-mail address : cmcsales@cmcbiotech.co.th

- **Central Branch (Bangkok)**

Tel : 66 (0) 2530-4689, 2530-4995 Ext. 601
E-mail address: cmccb@cmcbiotech.co.th

- **Northern Branch (Chiangmai)**

Tel : 66 (0) 5328-3261 Fax : 66 (0) 5320-4463
E-mail address: cmcnb@cmcbiotech.co.th

- **North Eastern Branch (Khon Kaen)**

Tel : 66 (0) 4334-1642 Fax : 66 (0) 4334-1643
E-mail address: cmcneb@cmcbiotech.co.th

- **Southern Branch (Hadyai)**

Tel : 66 (0) 7442-9803 Fax : 66 (0) 7442-9804
E-mail address: cmcsb@cmcbiotech.co.th

Service Excellence with Professionalism

Made for Life

MAY. - AUG. 2002
Volume VIII Number II

ISSN 0859 144X

THE ASEAN JOURNAL OF RADIOLOGY

**Published by The Radiological Society and
The Royal College of Radiologists of Thailand,
Bangkok, Thailand**

Started through an educational grant from Bracco since 1995

www.bracco.com

Chief Editor

Professor Kawee Tungsubutra
Kaweevej Hospital, 318 Taksin Road, Dhonburi, Bangkok 10600, Thailand.

Asean Journal of Radiology.
Instructions for Authors.

1. The Asean Journal of Radiology publishes the papers on Radiological Sciences, such as research work, review articles, case reports, innovations in Medical Sciences related to all branches of Radiology, and letters to the editor. The aforementioned materials can be written in English only.

2. The authors have to submit 2 copies of the manuscript and a diskette: **to Prof. Dr. Kawee Tungsubutra.** 318 Kaweevej Hospital, Taksin Road, Dhonburi, Bangkok 10600, Thailand.

3. The original copy to be submitted must be typed in a double space on one side of the page of 8.1/2" x 11.1/2" paper.

4. The format of the article must include :

a. Title page and address of the author (s)
b. Abstract
c. Introduction (Background)
d. Material and Method
e. Results and discussion (Tables and Illustrations)
f. Acknowledgement (if any)
g. References (Follow the Vancouver style developed by ICMJE)

5. We will provide 5 copies of reprints for the author (s) who submit (s) an article for publication in the Asean Journal.

6. The illustrations and tables must be clearly prepared with legends in English as they are the art works to be reproduced.

7. The authors are responsible for the contents of the article as to its facts and findings.

8. Ethics.

Paper reporting studies which might be interpreted as human experimentation (e.g. controlled trials) should conform to the standards of the Declaration of Helsinki (see British Medical Journal 1964:2:177) and should indicate that, approval that such studies may proceed, has been granted by the local or hospital Ethics Committee.

When reporting experiments on animals indicate whether the institution's or the National Research Council's guide for, or any national law on, the care and use of laboratory animals was followed.

THE ASEAN JOURNAL OF RADIOLOGY

Volume VIII Number II MAY. - AUG. 2002

CONTENTS

THE ASEAN JOURNAL OF RADIOLOGY

Volume VIII Number II MAY. - AUG. 2002

CONTENTS

HYDRANENCEPHALY : CASE REPORT AND LITERATURE REVIEW

Parichad CHANPONG, M.D.[1]
Patama NAKBUMRUNG, M.D.[2]

ABSTRACT

Hydranencephaly is the total or virtually total absence of the cerebral hemispheres, which are reduced to membranous sac of glia tissue, with no ependymal coating, in an intact skull. This is rare disorder. It is classified as a circulatory encephalopathy from many causes (vascular, parasitic, viral,toxic,estrogenic,...).

It appears to be readily diagnoses prenatal by ultrasound. The neurological findings may be normal at birth. Transfrontanellar ultrasound,CT scanning and anatomical confirmation can established the diagnosis. The prognosis is hopeless and there is no treatment. Our report presents one case of hydranencephaly, clinical presentation and differential diagnosis from other common congenital diseases.

INTRODUCTION

"Hydranencephaly" is a term derived by the combination of two words, " hydrocephalus" and "anencephaly".[1] While hydrocephalic pathology is undoubtedly present in some cases, "anencephaly" is not quite appropriate, since the cranial vault and meninges are intact.[2-3] Hydranencephaly is a rare, isolated abnormality occuring in less than 1 per 10,000 births worldwide. It is the most severe form of bilateral cerebral cortical destruction. The exact etiology of hydranencephaly is unclear. The most popular etiological mechanism is intrauterine infarction of cerebral structures, primarily due to occlusion of the supraclinoid internal carotid artery.[4-7] The hydranencephalic infant may look remarkable normal at birth and demonstrated few neurologic abnormalities other than the lack of fixing and following an object with the eyes. CT scanning or cranial ultrasound examination should make the definitive diagnosis. CT offers a unique diagnostic tool for the evaluation of these infants. Most of the affected infants die within one year of life, but survival past three years has been reported.[1-3]

CASE PRESENTATION

This female infant was the first child of a 34 years old woman. Pregnancy was uncomplicated during antenatal care to term pregnancy about 39 weeks gestation. During delivery, poor maternal effort, so vacuum extraction (V/E) was performed. Cesarean section (C/S) was the final treatment due to fail V/E. At birth, Apgar score at one and five-minutes were nine and ten respectively, active child and normal in appearance. Her birth wedge and length were appropriate for gestational age. Two days after delivery, an abnormally slightly increasing head circumference was observed. Cranial ultrasound showed massive ventricular dilatation. A non-contrast enhanced CT scan demonstrated disruption of falx cerebri, absence of cerebral hemispheres, which were replaced by a large fluid-filled cavity, sparing normal thalamus and posterior fossa including the cerebellum, consistent with diagnosis of hydranencephaly.

[1] Division of Neuroradiology, Prasat Songkhla Hospital Thailand.
[2] Division of Radiology, Suratthanee Hospital Thailand.

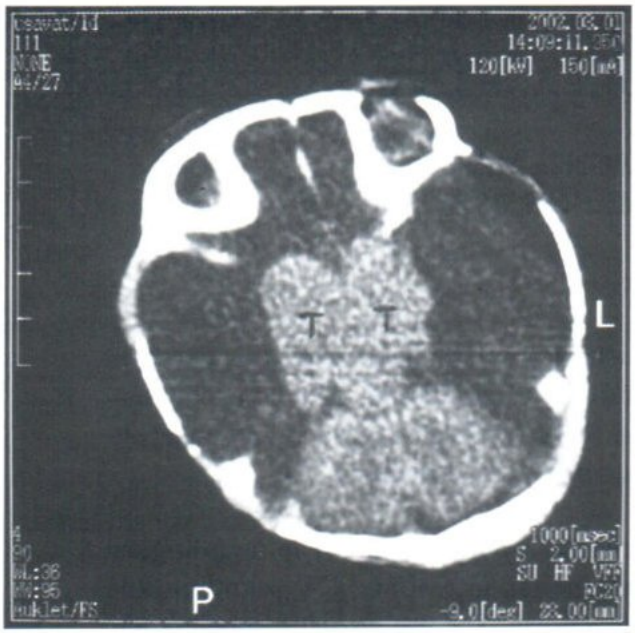

Slide 1 : CT scan of this newborn's head without use of Intravenous contrast axial slide 1 Transaxial view through the base shows normal thalami (T) and normal posterior fossa, including cerebellum.

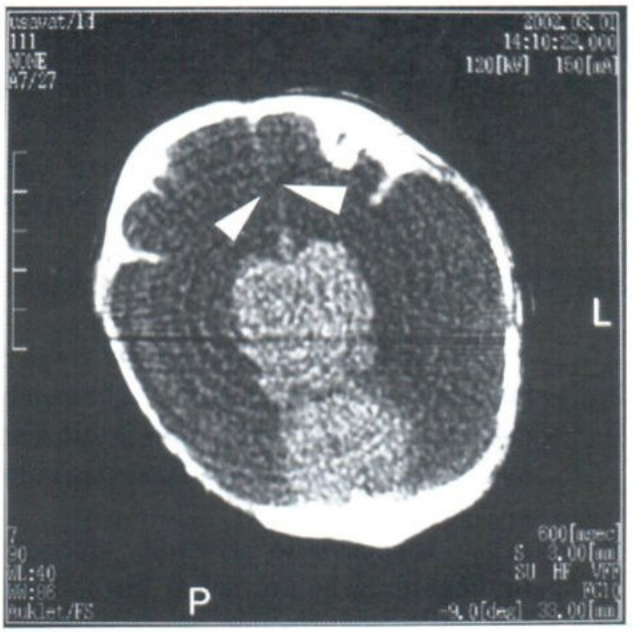

Slide 2 : Disrupted anterior falx is present (Arrow) Preservation of the falx cerebri helping to differentiate this from holoprosencephaly.

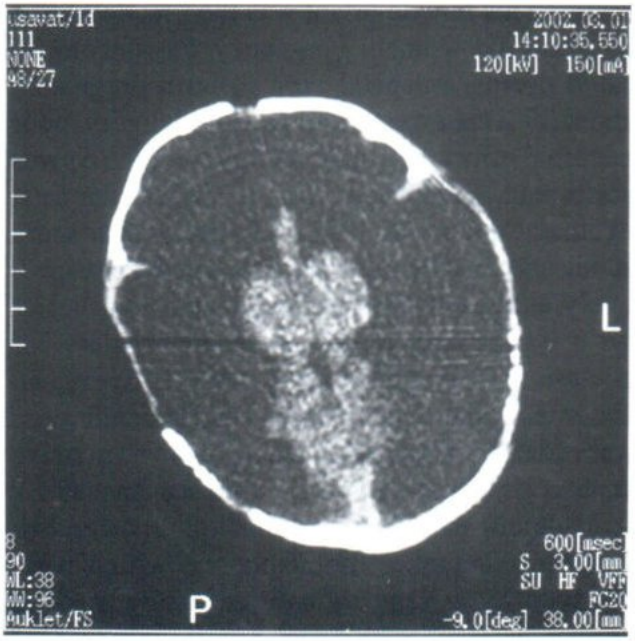

Slide 3 : A centrally placed tissue structure resembling a "brain stem model" represents diencephalic (thalamic and hypothalamic) and upper cerebellar and tentorial structures.

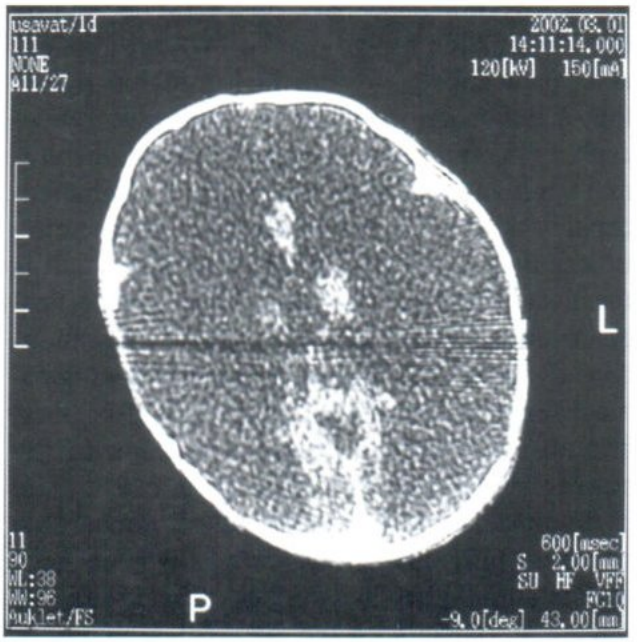

Slide 4 : A slightly higher levels show the falx intact posteriorly.

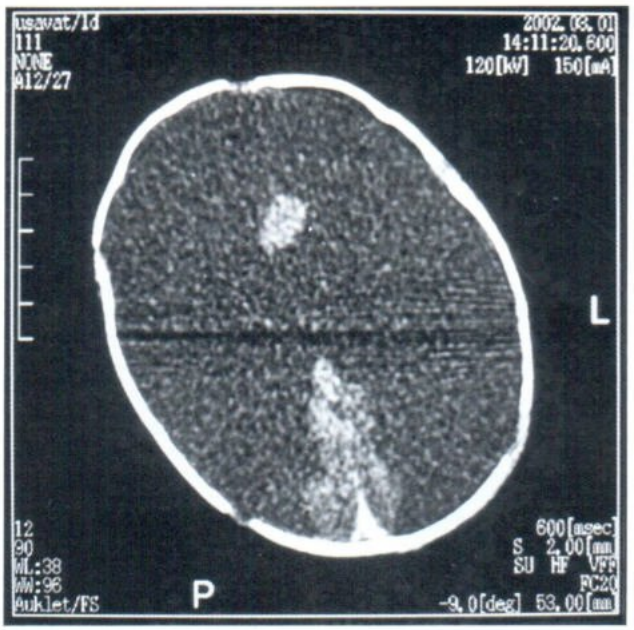

Slide 5 : This slide showing some occipital lobe preservation on either side of the posterior falx cerebri.

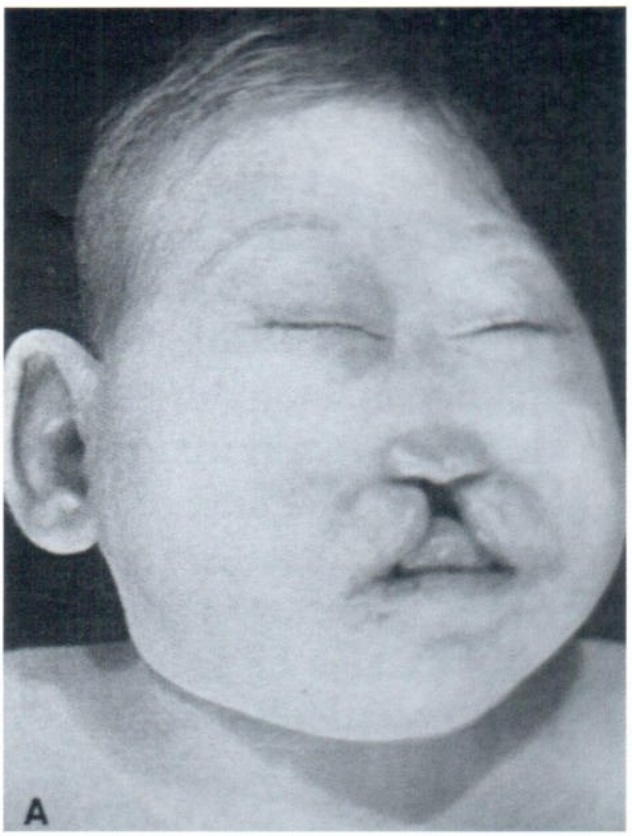

Slide 6 : Photograph of stillborn child with alobar holoprosencephaly shows low midline facial cleft, hypotelorism, and microcephaly. (Figure 6-9 from Diagnostic Pediatric Neuroradiology,1996)

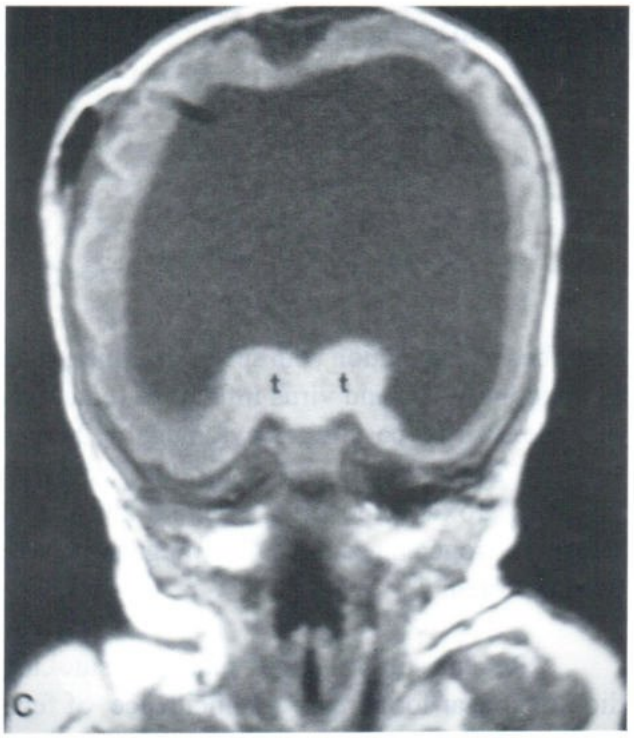

Slide 7 : Coronal MRI T1–weighted image showing horseshoe – shaped monoventricle with fused thalami (t). The corpus callosum is absent and there is con tinuation of gray and white matter across the midline. The interhemispheric fissure is rudimentary and the falx is absent.

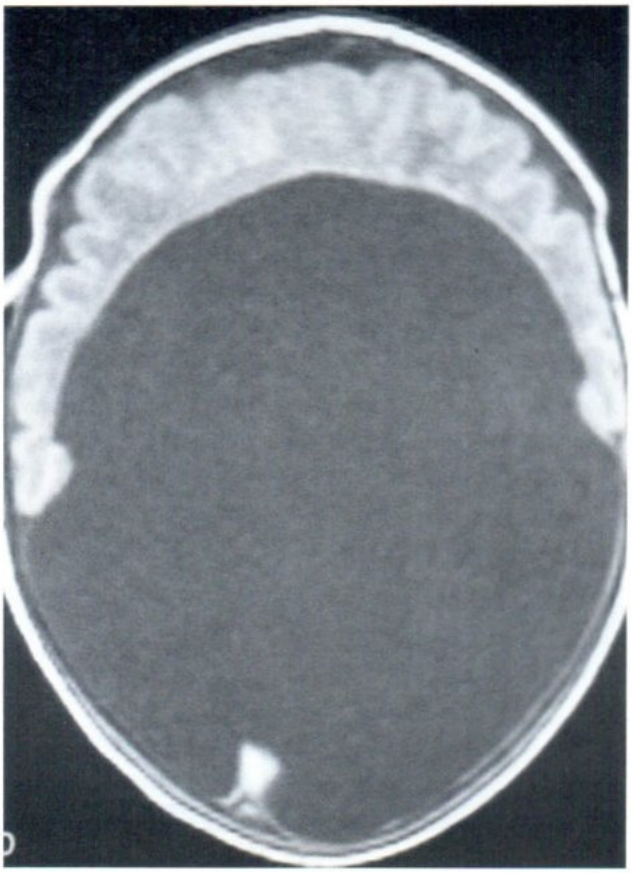

Slide 8 : Axial MR T1–weighted image in a different patient shows monoventicle and majority of residual cerebral tissues to be located rostrally. The interhemispheric fissure and falx are absent. There is a large dorsal midline cyst that is contiguous with the venticle

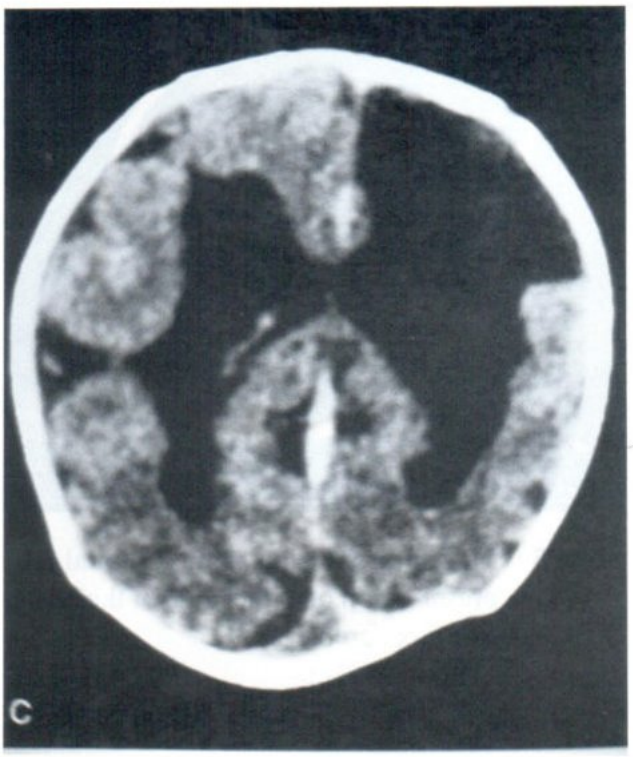

Slide 9 : Axial noncontrast computed tomography shows bilateral (left > right) open - lip schizencephalies.

DISCUSSION

Hydranencephaly is defined as the congenital absence of the cerebral hemispheres which are replaced by a large fluid - filled cavity but with intact cranial vault and meninges. A specific, clinical, nonradiographic diagnosis is usually impossible. The pathogenesis of hydranencephaly is thought to be a vascular accident, this cannot always be confirmed because internal carotid arteries are not always occluded at autopsy.[2] Massive cerebral destruction has been described in association with specific entities, such as, toxoplasmosis and virus infections (enterovirus, adenovirus, parvovirus,cytomegalic, herpes simplex, Epstein-Barr and respiratory syncytial visuses).[8] Toxic exposures, cocaine abuse and massive estrogen ingestion during pregnancy have been reported.[8-10]

Recent study[11] found maternal smoking did not appear to increase the incidence of fetal

congenital CNS anormalies overall, but might be associated with particular vascular patterns of damage to the developing brain that could predispose to a hydranencephalic malformtion. In monochorionic twin pregnancies, death of one twin in the second trimester may cause a vascular exchange to the living twin through the placental circulation, leading to hydranencephaly in the surviving fetus.[12]

Detection of hydranencephaly and other neural tube defects before birth has been enhanced by the development of a new screening technique for assaying the amniotic fluid. However, this test is not universally applied at present, and it is only accurate from the 16 th to the 22 nd week of pregnancy, a period dangerously close to the maximum allowable gestational age for legal abortion.[13-15] Thus, hydranencephalic fetuses continue to be carried to term, although there are no reliable statistics for the exact number. Table 1 summerized the clinical and radiographic finding hydra-nencephaly, severe bilateral porencephaly, and pictorially similar entities.

Clinically, hydranencephaly usually presents with normocephaly rather than macrocephaly, but occasionally may even be associated with microcephaly.[16-18] Transillumination of the head is nonspecific. The appearance of the child may be of some help in identifying infants with suspected hydranencephaly. Alobar holoprosencephaly always presents with midline cleft deformities such as fissured lips and/or palate, and hypotelorism.[17-18] A peculiar gyrated scalp was reported in one case of hydranencephaly but not with similar entities.[19] Previous recently reported one hydranencephalic infant associated with vascular malformation (port wine stains, generalized nevus flammeus, anormalous retinal vessels and absent internal carotid flow)[20] and one asscociated with dysplastic kidney and andramnios.[21]

Since hydranencephaly occurs after the brain and ventricle have fully performed, usually in the second trimester and the brain destruction is complete or almost complete in a bilateral internal carotid artery distribution with preservation of structure fed by posterior circulation. Plain radiograph findings of Hydranencephaly are usually nonspecific. Diagnostic ultrasound is useful in predicting the intrauterine process of macrocephaly, demonstrating abnormally increased echo-free areas of the intracranial contents, such as seen in hydranencephaly and hydrocephalus. Color Doppler ultrasound may shows absence of arterial flow above the supraclinoid portion of the internal carotid arteries, suggesting the diagnosis.[22]

CT and MRI help to accurate diagnosis and some authors suggested MRI is the modality of choice.[22] The cerebellum almost always intact, the brain stem usually atrophic, absence of cortical mantle, the thalamic, hypothalamic and mesencephalic structures are usually preserved and project into the cystic cavity. The choroid plexus,falx cerebri and tentorial cerebelli are usually intact but the falx cerebri may be deviated. With most of the cerebral cortex absent. The fetal head would be expected to be small. Although this may occur, the head is more often normal or increased in size because the choroid plexuses within the lateral ventricles continue to produce cerebral spinal fluid that is not adequately absorbed. This causes increased pressure, which may expand the head and lead to rupture of the falx cerebri.[23] Both of these findings were present in this case.

Angiographically, hydranencephaly demonstrates hypoplasia of the supraclinoid internal carotid arteries, with a normal external carotid vasculature. These changes were first described by Thelander et al in 1953 and later confirmed by others.[24-28] Remnants of subfrontal cortex may be present, supplied by a tangle of vessels in the anterior cerebral distribution. More

frequently, basal portions of the occipital or temporal lobes are present, along with relative normal hypothalamic and thalamic structures. There relative intact areas are supplied by normal posterior cerebral arteries. The cerebellum and vertebral-basilar arterial system are also intact.[7,16]

Pneumoencepahalography is rarely performed in hydranencephalic infants because of the danger of hydrocephalic mass effect and tonsillar or brain stem herniation. Ventriculography reveals no appreciable cerebral cortex, except for occasional remnants of occipital, temporal or subfrontal tissue.

An abnormal visual evoke response (VER) has been suggested in one case. It is not clear whether this infant was truly hydranencephalic. Two other patients had normal VER.[29] EEG measurements usually show diffusely abnormal patterns.[17,30]

Hydranencephaly may, on first impression, mimic severe hydrocephalus(dilated lateral ventricles).[3] Depending on the level of obstruction, concomitant dilatation of the third and fourth ventricles may be seen. The incidence of hydrocephalus approaches 1 in 1,000 births. Althrough there are many causes, the most common is an Arnold-Chiari typeII malformation secondary to a spina bifida. The most severe cases, however, are usually secondary to aqueductal stenosis. Hydrocephalus is often not isolated anormaly and can be associated with other intracranial abnormaities ,multiple anormaly syndromes, and abnormal karyotype.[31] With hydrocephalus, as with hydranencephaly, the head is normal to enlarged with an identifiable falx cerebri, which may be disruped in severe cases. Unlike in hydranencephaly, an intact rim of cortex is always present even in the most severe forms of hydrocephalus. It may, however, be difficult to identify prenatally. In aqueductal stenosis, a dilated third ventricle can often also be identified.[32]

Holoprosencephaly is developmental anormaly resulting from absent or incomplete diverticulation of the forebrain and occurs in 1 in 16,000 live births worldwide.[33] Holoprosencephaly is associated with a spectrum of facial anormalies and with visceral abnormalities with 75% of cases. The most severe form, alobar type, shows monoventricle communicates with a large dorsal cyst, no seperation of the ventricles, an absent falx, and fusion of the thalami. The convolutional markings are sparse and there is a smooth appearance to the brain surface. Migrational anormalies of the brain are often present. The cerebellum and brain stem are often spared. If the doppler is applied, absent anterior cerebral arteries or the occurrence of only a single vessel may be noted. There is absence of the internal cerebral veins, superior sinus, sagittal sinus and straight sinus.[34]

"Porencephaly", literally meaning" a hole in the brain," initially referred to cystic changes secondary to a vascular etiology.[17,23,35-36] However, the meaning of this word has been broadened to include any such changes from whatever cause. The porencephalic cyst is a focal area of cortical destruction.[2-3] When caused by middle cerebral artery infarctions, porencephalic cysts appear as bilateral fluid-filled clefts that communicate with the ventricles and is called schizencephaly. Unlike in hydranencepahly, both the frontal and parieto-occipital cortex are preserved. The falx cerebri is also preserved. The fetal head can be either normal or enlarged.

Other disesases such as massive congenital subdural hygromas and post-anoxic /infective encephalopathy may look like hydranencephaly as seen in table 1.

There are important reasons to differentiate hydranencephaly from hydrocephalus; these reasons related to prognosis and management.[35] Children with hydrocephalus, without chromo-

somal or other structural abnormalities, have an unpredictable prognosis. With proper ventricular shunt after birth, regrowth of the cortical mantle is usually evident of follow up imaging studies.[22] In contradistinction, hydranencephaly has an irretrievably poor prognosis, with only brain stem function remaining. Although most hydranencephalic children survive birth, they often die soon after. Rarely, these children may linger into their teenage years. If hydranencephaly were definitely diagnosed in utero, previous recently article[31] suggested cephalocentesis to decompress the fetal head, thus allowing a vaginal delivery to avoid the cesarean section, which thought to be unnecessary procedure, like in our case. On the other hand, if hydrocephalus were present, particularly without the presence of other anomalies, a cesarean section must be seriously considered.

SUMMERY

Hydranencephaly is rare disorder with poor prognosis and no treatment. The diagnostic ultrasound is helpful in screening intrauterine abnormality and children with abnormal cranial indices but non specific. The physical examination cannot suggest the disease due to the infant usually has normal face and less associated with other abnormalities. Nowadays CT or MRI are recommended for more precise differentiation and accurate diagnosis, angiography and other invasive procedures are unnecessary.

TABLE 1 : SUMMARY AND RADIOGRAPHIC FINDINGS IN HYDRANENCEPHALY AND PICTORIALLY SIMILAR ENTITIES

	Hydranencephaly (Classic)	Severe Hydrocephalus	Alobar Holoprosencephaly	Bilateral severe Porencephaly	Post- Anoxic/Infective Encephalopathy	Massive Congenital Subdural Hygroma
Clinical						
Cranial size at birth Or at discovery	Usually normal	Usually increased	Normal or microcephalic	Usually normal	Normal, micro-, or macrocephalic	Increased
Facial appearance	Normal, 1 case reported With gyrated scalp	Normal or with exophthalmos	Cleft palate defects, hypotelorism	Normal	Normal or "post viral"	Normal
Head Transillumination	4 +	4 +	3-4 +	3-4 +	1-4 +, depending on severity	4 +
Radiographic						
Plain skull Radiograph	Usually normal, occasionally macrocrania With open sutures	Sutures split. Associated abnormalities with Amold - Chiari syndrome (Lukenschadel)	Cleft defects, hypotelorism Normal or microcrania	Same as for hydranencephaly	With active disease, generalized cerebal swelling may split sutures. Inactive disease may present with split sutures (hydrocephalus) Or collapsed or overlapping sufures (atrophy)	Sutures split
Ultasonogram	Intact or partially intact falx with Echo - free fluid surrounding The central plexus cerebral tissue					
CT scan	Intact posterior fossa. intact or Relatively intact meninges & falx. falx may be midline or deviated But Not thickened. Majority of cranial vault is of CSF density, with remnants of temporal, occipital, or subfrontal cortex.	Some elements of cortex Usually identifiable. Massive CSF collection with intact falx	A frontal or occipital clump of Tissue. No falx. Generally intact posterior fossa. Midline osseous cleft defects	Wedge-shaped "infarcts" Without overlying cortex. Some identifiable ventricular remnants. Intact or relatively intact posterior fossa & meninges	Intact or peripheral areas of focal infaction. CT sequential changes in density with identifiable falx , ventricular structures, & areas of cerebral tissue	Mimics hydranencephaly. Wedge - shaped central collection of tissue
Pneumoencephalo-Gram and / or ventriculogram	Obstruction of the aqueduct or third ventricle	Variable		Same as for hydranencephaly		
Angiogram	Absence of supraclinoid Internal carotid arteries	Relatively intact cerebral vessels, massively compressed against the Cranial vault	Small, disordered tangle of vessels in frontal or occipital regions. Absence of falx vessels	Various degrees of midline or other focal arterial obstruction		Normal complement of supratentorial vessels compressed toward midline

REFERENCES

1. Dublin AB,French BN: Diagnostic image evaluation of hydranencephaly and pictorilly similar entities. Radiology;137: 81-91
2. Filly RA. Ultrasound evaluation of the fetal neural axis. In:Callen PW, ed. Ultrasonography in obstetrics and gynecology. 3rd ed. Philadelphia, Pa: Saunderds, 1994; 199-218
3. Nyberg DA, Pretorius DH. Cerebral malformations. In :Nyberg DA, Mahony BS, {retprois DH, eds. Diagnostic ultrasound of fetal anomalies: text and atlas. Chicago: Year book medical,1990;98-121
4. Yakovlev Pl, Wadsworth RC. Schizencephalies: a study of the congenital clefts in the cerebral mentle. J Neupathol Exp Neurol 1946;5:116-30
5. Linderberg R. Swanson PD: Infantile hydranencephaly. A report of five cases of infarction of both cerebral hemispheres in infancy. Brain 1967;90:839-50
6. Harwood-Nash DC, Fitz CR. Neuroradiology in infants and children. St. Louis, Mosby, 1976;98-9
7. Van HerzenJL, Berrirschke K. Unexpected disseminated herpes simplex infection in a newborn. Obstet Gynecol 1977;50:728-30
8. Kurtz AB, Johnson PT. Case 7 : Hydranencephaly. Radiology 1999;210:419-22 Blanc JF, Lapillonne A, Pouillaude JM, Badinand N. Hydranencephaly and ingestion of estrogens during pregnancy. Fetal cerebral vascular complication?. Arch Fr Pediatr 1988,45(7):483-5
9. Hoyme HE, Higginbottom MC, Jones KL. Vascular etiology of disruptive structural defects in monozygotic twins. Pediatrics 1981;67:288-91
10. To WW, Tang MH. The association between maternal smoking and fetal hydranencephaly. J Obstet Gynaecol Res 1999;25(1):39-42
11. Rais-Bahrami K, Naqvi M. Hydranencephaly andmaternalcocaine use:a case report.Clin Pediatr 1990:29:729-30
12. Wald N, Cuckle H, Stirrat G. Screening for neural-tube defects (letter). Lancet 1978;1:495
13. Bond EB, Thompson W, Elwood JH,et al. Evaluation of measurement of maternal plasmaalpha-fetoproteinlevels as a screening test for fetal neural tube defects. Br J Obstet Gynaecol. 1977;84:574-7
14. Clarke PC, Gordon YB, Kitau MJ, et al. Screening for fetal neural tube defect by maternal plasma alpha-fetoproteindetermination. Br J Obstet Gynaecol 1977;84: 568-73
15. Wolpert SM: Vascular studies of congenital malformations. In: Newton TH, Potts DG, eds: Radiology of the Skull and Brain. Angiography. St. Louis, Mosby, 1974 Vol 2, 2702-3
16. Crome L, Sylvester PE. Hydranencephaly. Arch Dis Child 1958;33:235-45
17. Harwood-Nash DC. Congenital craniocerebral abnormalities and computed tomography. Semin Roentgenol 1977;12:39-51
18. Bauer CR, Seastres L, Lorch V. Gyrated scalp associated with hydranencephaly in a newborn infant (letter). J Pediatr 1988; 90:492-3
19. Stevenson DA, Hart BL, Clericuzio CL. Hydranencephaly in an infant with vascular malformations. AM J med Genet 2001; 104(4):295-8

20. Lee TG, Warren BH. Antenatal diagnosis of hydranencephaly by ultrasound JCU 1979(5)271-323.
21. Casitillo M, Mukherji SK. Hydranencephaly. In: Casitillo M, Mukherji SK. Eds. Imaging of the Pediatric Head, Neck and Spine. Philladelphia, Lippincott-Raven, 1996; 518-9
22. Lees RF, Harrison RB,Sims TL: Gray scale ultrasonography in the evaluation of hydrocephalus and associated abnormalities in infant. Am J Dis Child 1978;132: 376-8
23. Mcabee GN, Chan A, Erde EL. Prolonged survival with hydranencephaly. Pediatr Neurol 2000;23(1): 80-4
24. Greco F, Finocchiaro M, Pavone P, et al. Hemihydranencephaly. J Child Neurol 2001;16(3):218-21
25. Green MF, Benacerraf B, Crawford JM. Hydranencephaly : US appearance during in utero evolution.] Radiology 1985;156: 779-80
26. Pangui E,Macumi E, Brinderrouch C,et al. Hydranencephaly: report of a new case. Rev Fr Gynecol Obstet 1991;86(5):401-5
27. Linuma K, Handa I, Kojima A, et al. Hydranencephaly and maximal hydrocephalus. J Child Neurol. 1898;4(2):114-7
28. Greco F, Finocchiaro M, Pavone P, et al. Hemihydranencephaly. J Child Neurol 2001;16(3):218-21
29. Calen off L. Hyfranencephaly : plain film findings.AJR 1961;86:453-5
30. Nicolaides KH, Snijders RJM, Gosden CM, et al. Ultrasonographically detectable markers of fetal chromosomal abnormalities. Lancet 1992;340:704-7
31. Kurtz AB, Johnson PT. Case 7 : Hydranencephaly. Radiology 1999;210:419-22
32. Appebzekkar O, Snyder R. Autonomic failure in hydranencephaly. J Neurol Neurosrg Psychiat 1970;33:532-43
33. Barr LL. Neonatal cranial Ultrasound. Radiologic Clinics of North America. 1999;37(6):1131-2
34. Strother CM, Harwood- Nash DC: Congenital malformations. In:Newtons TH, Potts DG, eds: Radiology of the Skull and Brain, Ventricles and Cisterns. St. Louis, Mosby ,1978 Vol 4:3734-5
35. Sutton LN, Bruce DA, Schut L. Hydranencephaly versus maximal hydrocephalus : an important clinical distinction. Neurosurgery 1980;6:34-8
36. Linuma K, Handa I, Kojima, et al. Hydranencephaly and maximal hydrocephalus : Usefulness of electrophysiological studies for their differentiation. J Child Neurol 1989;4 :114-7

BILATERAL NEPHROBLASTOMATOSIS: A ROLE FOR MULTISLICE CT

Jiraporn SRINAKARIN,[1] Suchart AREEMIT,[2] Churairat KULARBKAEW,[3] Nittaya CHAMADOL,[1] Apichart JIRAVUTTIPONG,[4] Surapon WIANGNON.[4]

ABSTRACT

Nephroblastomatosis is an abnormality of nephrogenesis characterized by incomplete maturation of the primitive nephrogenic cells. We report on one case of bilateral nephroblastomatosis in an 11-month-old boy who had an abdominal mass on the left side for 8 months. The boy had no other physical anomalies; he appeared healthy and had good development. A sonogram and an intravenous urogram revealed diffuse enlargement of both kidneys and ill-defined hyperechoic lesions covering both kidneys, except the lower pole of the right kidney. A multislice CT scan, performed with and without contrast medium, took no more than 10 minutes. We observed extensive enlargement of both kidneys and multiple solid masses throughout the left kidney and the upper half of the right kidney. Reconstruction on multi-planar views of both renal masses gave as good or better than MRI for displaying the extension of renal masses and renal vascular status. Surgical and pathologic findings are discussed in more detail.

INTRODUCTION

Nephroblastomatosis (NB) is an abnormality of nephrogenesis characterized by incomplete maturation of the primitive nephrogenic cells. The term was coined by HOU and Holman in 1961.[1] It also defines persistent metanephric blastema from infancy into childhood. In 1990, Bechwick et al. suggested that all foci of persistent metanephric tissue be referred to as nephrogenic rests and that the presence of a multiple nephrogenic rest be termed nephroblastomatosis.[2] The association of independent foci of persistent blastema with Wilms' tumor has been documented often. Minor degrees of NB are common with unilateral Wilms' tumour and are almost universal in bilateral Wilms' tumour. The most severe cases have features of both developmental malformation and neoplasia. Therefore, NB is widely accepted as a premalignant lesion.[3] The role of imaging in evaluating patients suspected of having NB, Wilms' tumour, or both, includes preoperative assessment of both kidneys, follow-up of the patient with known micro- or macroscopic NB to detect neoplastic changes, and screening of patients with syndromes associated with NB and Wilms' tumour. Microscopic foci of NB are not identified with any imaging modality.[3] In the case of macroscopic NB, diagnosis by ultrasound and excretory urography is less sensitive than computed tomography (CT) and magnetic resonance imaging (MRI). The use of spiral CT has definitely improved the efficacy of CT because of the more rapid scanning time, multi-planar reconstruction, and lower radiation doses particularly when multislice CT is performed.[4] We report one case of bilateral NB examined by multislice CT. We discuss the advantages of this technique in both diagnosing and preoperative assessment of tumor extension and its vascular supply of both kidneys.

CASE REPORT

An 11-month-old boy came to hospital with a left upper quadrant mass present since he

[1] Department of Radiology
[2] Department of Surgery
[3] Department of Pathology
[4] Department of Pediatric, Faculty of Medicine, Khon Kaen University, Khon Kaen, 40002, Thailand.

was 2-month-old. He had hyperpigmented skin and nevus of his back and neck, respectively. Other physical findings, laboratory tests, past medical and perinatal history were normal. There were no accompanying congenital abnormalites. The ultrasonogram revealed enlarged kidneys bilaterally with heterogeneous hyperechoic lesions covering the entire left kidney and the upper half of the right one (Fig.1a,b). Intravenous urography also revealed enlargement of both kidneys with compressed and distorted calices (Fig.2a,b). These findings were initially interpreted as polycystic kidney disease. At the follow-up three months later, the left kidney still had a hard consistency and irregular surface, so we performed a further multislice CT.

Sedation using oral chloral hydrate (0.5 mg/kg) was administrated before scanning. For the precontrast scan, the multislice CT (SOMATOM Plus 4 Volume Zoom, Siemens) was performed with 5-mm wide slices, 2.5-mm thick collimation, 12.5 mm/s table speed (pitch = 6) and 5 mm reconstruction interval. After intravenous administration of a nonionic contrast medium (2 mL/kg) performed using a mechanical injector at 2 mL/s, the volume scan began at the end of the mechanical injection and 70 seconds after the injection. The multislice CT scan was performed with 1.25-mm wide slices, 1-mm thick collimation, 5mm/s table speed (pitch = 5), and 5-mm reconstruction intervals. Fifty-five mAs and 120KV were performed for all three scans. The total scan time, including contrast medium injection, was less than 10 minutes. Multi planar reconstruction (MPR) and maximun intensity projection (MIP) were performed after finishing the axial image reconstruction. The CT of the abdomen revealed multiple nonenhancing cortical solid masses, an enlarged, surficially nodulated left kidney and upper half of the right (Fig.3). MIP and MPR clearly revealed the main renal arteries and veins and their branches into the renal masses (Fig.4). These images also showed the extension of the NB involving the entire left kidney and the upper half of the right kidney. A left nephrectomy was performed and revealed a10-cm, well encapsulated, nodular surficial mass covering the left kidney (Fig.5a,b). Cortical lobulated masses occupied the upper half of the right kidney and were biopsied. The histopathology was nephroblastomatosis (NB) of the left kidney with foci of Wilms' tumour and NB of a piece of the right kidney (Fig.6). Additional chemotherapy with vincristine and actinomycin was used to treat the stage I Wilms' tumour. The patient was referred to their nearest hospital for follow-up of the right kidney in case of tumour recurrence on left renal bed.

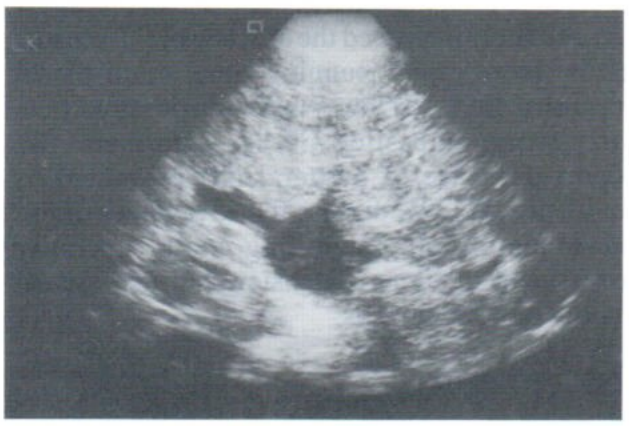

1A

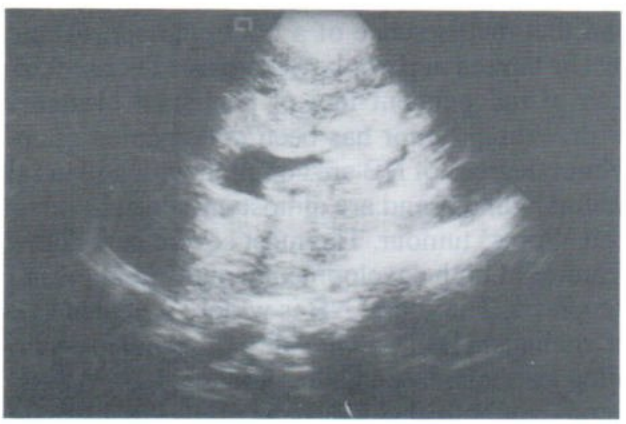

1B

Fig. 1 a,b. Sonogram reveals enlarged kidneys bilaterally with heterogeneously hyperechogenic lesions and some degree of caliectasis on the entire left kidney (a) and a mass at the upper pole of the right kidney (b).

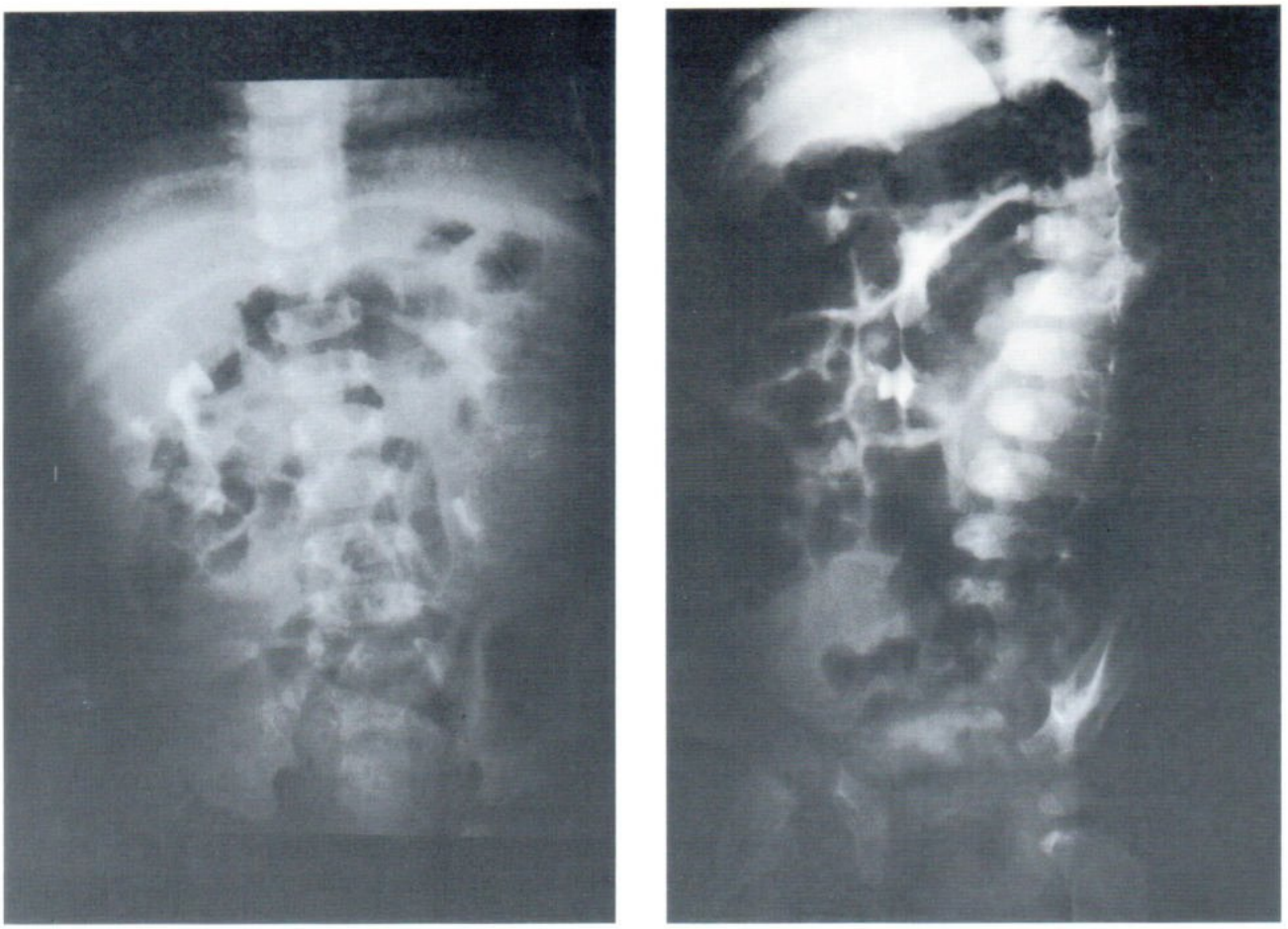

2A 2B

Fig. 2 a,b. Intravenous urography reveals an enlargement of both kidneys with compressed and distorted calices on the anteroposterior (a) and right posterior obligque (b) views.

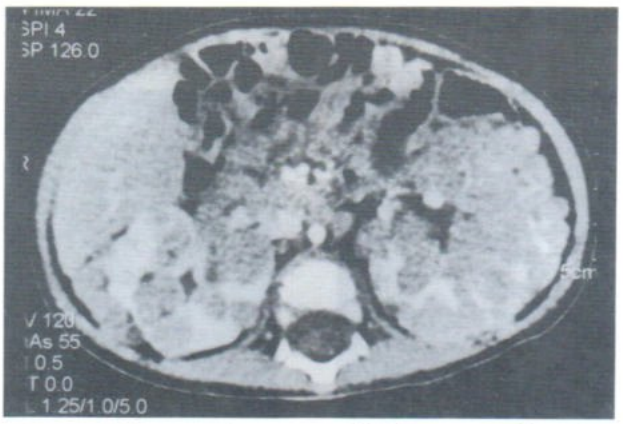

Fig. 3. CT scan shows multiple non-enhancing masses in the renal cortex of both kidneys, larger and more confluence in the left kidney with compressing and distorting of the collecting system.

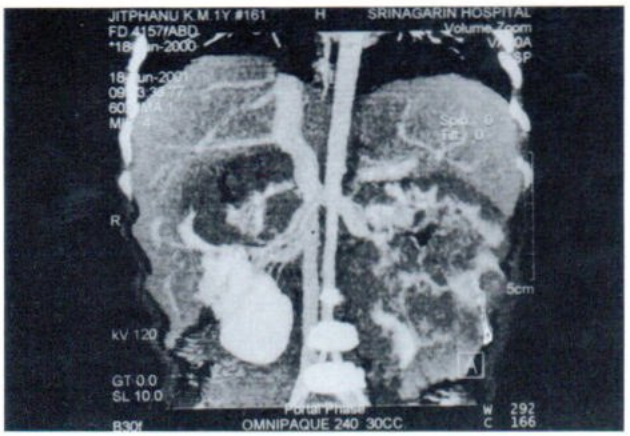

4A

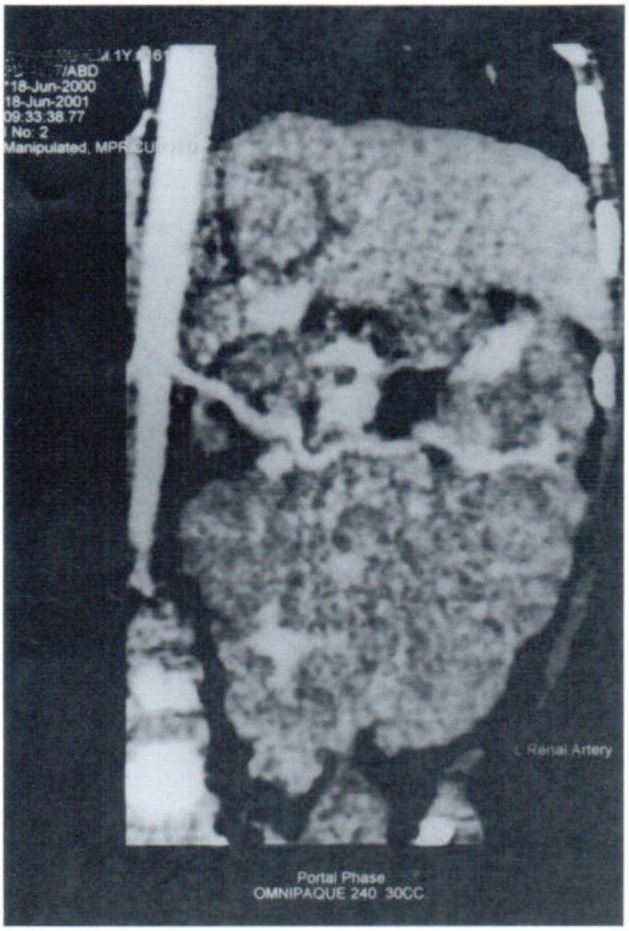

4B

Fig. 4 a,b. Maximum Intensity Projection (MIP) gives an excellent rendition of both renal arteries and veins (a). Multi-planar Reconstruction (MPR) reveals a branch of the left renal artery within NB of the left kidney (b). Both MIP and MPR also provide an extension of NB in both kidneys and the normal renal cortex at the lower pole of the right kidney.

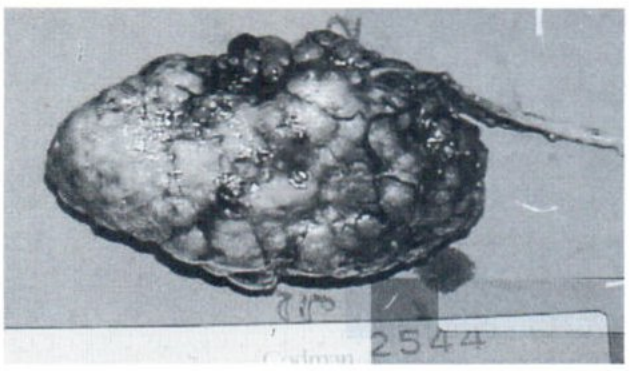

5A

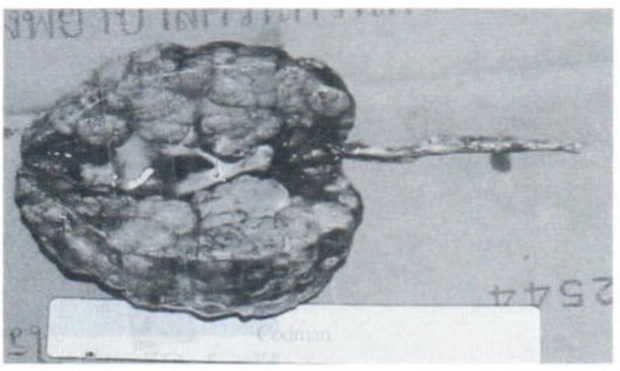

5B

Fig. 5 a,b. A left nephrectomy revealed a 10-cm well encapsulated, nodulated surface mass (a) while the cut surface revealed multiple masses throughout the entire renal cortex (b).

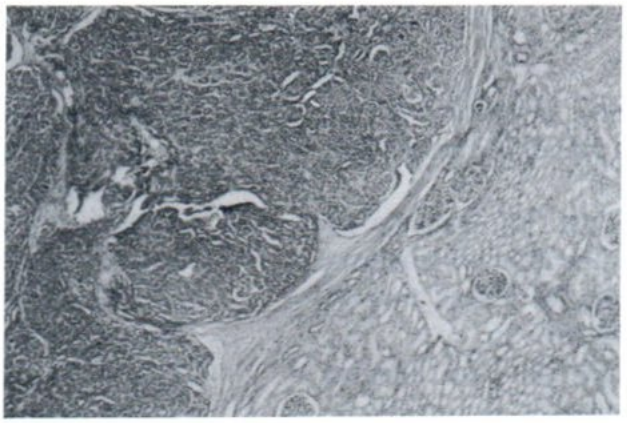

Fig. 6. Lower power photomicrograph shows multiple perilobar NB of variable sizes and well delineates from the normal renal parenchyma (right hand side).

DISCUSSION

The presence of multiple or diffuse nephrogenic rests define nephro-blastomatosis (NB). If nephrogenic rests persist until birth and during infancy, they usually form a Wilms' tumour so are regarded as precursor lesions.[3] Bechwith et al. suggested a modification in the classification of lesions with respect to their distribution within the renal lobe and classified NB as perilobar, intralobar and diffuse. The number of nephrogenic rests are classed: unifocal, multifocal, or diffuse.[2] In an attempt to divide lesions into clinically relevant groupings, the individual lesions are further subclassified as dormant, maturing/sclerosing, hyperplastic, and neoplastic. This subclassification requires both microscopic and gross pathologic evaluation of the lesions.[3]

Imaging findings of nephroblastomatosis (NB) typically reveal homogenously isoechogenic or slightly hypoechogenic nodules compared to the renal cortex[6,7,8] but unlike our case in whom that heterogeneously hyperechogenic lesions were demonstrated. The excretory urogram and CT findings of NB in our patient were similar to other reports.[3,4] Rohrschneider et al. reported 12 cases of NB checked with MRI, which revealed isointense or slightly hypointense to the cortex on T1W, T2W and proton-density images with poor delineation. Gadolineum-enhanced images were best used to detect lesions that remained homogeneously hypointense compared with the brightly enhancing cortex. They concluded, MR was the method of choice in view of significant radiation from serial CT.[6] Today CT scanners have been improved, particularly the multislice CT (SOMATOM Plus 4 Volume Zoom), in that one rotation produces 4 slices, so selecting a greater pitch to speed up acquisition and shorten scan time reduces radiation exposure. The authors also used low mAs in order to reduce radiation doses. The multislice CT provides thin slice reconstruction of the kidneys, which is an advantage in small NB thus allowing making possible a clear distinction between non-enhanced NB and enhanced normal renal parenchyma.

ACKNOWLEDGMENTS

The authors thank Mr. Bryan Roderick Hamman for assistance with the English-language presentation of the manuscript.

REFERENCES

1. Hou LT, Holman RL. Bilateral NB in a premature infant. J Pathol Bacteriol 1961; 82:244.
2. Bechwith JB, Kivial NB, Banadio JF. Nephrogenic rests, nephroblastomatosis, and the pathogenesis of Wilms' tumour. Pediatr Pathol 1990:10:1-36.
3. White KS, Kirks DR, Bove KE. Imaging of Nephroblastomatosis: An overview. Radiology 1992;182:1-5.
4. Merchant SA, Badhe PB. Nephroblastomatosis - Pathologic and Imaging Characteristics. J Postgrad Med 1995; 41 (3):72-80.
5. Miele V, Galluzzo M, Bellussi A, Valenti M. Spiral computed tomography in the study of renal neoplasms in children. Radiol Med (Torino) 1998;95(5):486-492.
6. Rohrschneider KW, Weirich A, Rieden K, et al. US, CT and MR imaging characteristics of nephroblastomatosis. Pediatr Radiol 1998;28:435-443.
7. Franken EA Jr, Yiu-Chiu V, Smith WL, et al. Nephroblastomatosis: clinicopathologic significance and imaging characteristics. AJR1982; 138:950-952.
8. Montgomery P, Kuhn JP, Berger PE, et al. Multifocal nephroblastomatosis: clinical significance and imaging. Pediatr Radiol 1984; 14:392-395.

CT FEATURES OF ADRENAL MASSES IN SRINAGARIND HOSPITAL

Warinthorn PHUTTHARAK[1], Jiraporn SRINAKARIN[2], Nittaya CHAMADOL[3], Chatlert PONGCHAIYAKUL[4], Jumpol MITRCHAI[5]

ABSTRACTS

Abdominal CT findings of 13 adrenal massses in 13 patients who had pathologically proven were reviewed. There were 4 cortical adenomas (3 Cushing's adenomas, 1 primary aldosteronism or Conn's adenoma) and 9 nonadenomas (4 pheochromocytomas, 2 adrenal cysts, 1 macronodular hyperplasia, 2 cortical carcinomas). Adrenalectomy were performed in all cases. All masses of cortical adenomas had smooth contour, size less than 5 cm., homogeneous density (less amount of attenuation number) and enhancement (mild to moderate degree). All pheochromocytomas had the same clinical presentation with smooth contour of masses, size less than 5 cm. and mainly had inhomogeneous density including enhancement pattern (moderate to marked degree). One from 2 cases of adrenal cysts and 1 macronodular hyperplasia could mimic adrenal tumor. All 2 cases of cortical carcinoma had large size masses , more than 5 cm. : 1 case had typical thick irregular rim enhancement and another case similar to benign tumor exceptional for the large size.

INTRODUCTION

The development of cross-sectional imaging technique has dramatically improved ability to examine the adrenal glands. No longer time –consuming or invasive investigations such as arteriography, venography, venous sampling were required, the adrenal glands are readily imaged with CT, sonography and MR imaging.

CT scanning has proved the most useful and most widely accepted imaging techniques, since it provides immediate and accurate diagnosis in all but the tiniest of adrenal masses.

Adrenal mass is an uncommon disease in general. The glands had varied tissue components, then the variety of masses could be occurred. The purpose of this study was to determine the causes of adrenal masses, described CT findings and determined whether there were characteristic features or overlapping findings of each group.

MATERIALS AND METHODS

We retrospectively reviewed the medical records and the available CT scans of 13 adrenal masses in 13 patients who had pathologically proven at Srinagarind Hospital, Khon Kaen University, during 1995-1999. CT examination were performed by using a 9800 GE Medical systems, Milwaukee, Wisconsin was used in 11

[1, 2, 3] Department of Radiology, Faculty of Medicine, Srinagarind Hospital, Khon Kaen University, Khon Kaen, Thailand 40002
[4] Department of Medicine, Faculty of Medicine, Srinagarind Hospital, Khon Kaen University, Khon Kaen, Thailand 40002
[5] Department of Pathology, Faculty of Medicine, Srinagarind Hospital, Khon Kaen University, Khon K aen, Thailand 40002

Correspondence to
Warinthorn PHUTTHARAK Department of Radiology, Faculty of Medicine, Srinagarind Hospital, Khon Kaen University, Khon Kaen, Thailand 40002 Telephone : 043-348389 Fax : 043-348389

patients, 3 mm. Collimation in 2 patients. All cases underwent CT before and after intravenous administration of contrast medium. The large group of neuroblastoma in pediatric patients were excluded from our study.

The patients were 4 men, 9 women with age range 13 – 67 years (mean age = 33.69 years). There were 4 cortical adrenomas (3 Cushing's and 1 Conn's adenomas) and 9 nonadenomas (4 pheochromocytomas, 2 adrenal cysts, 1 macronodular hyperplasia, 2 cortical carcinomas).

Shape, contour, size, density, enhancement pattern, calcification or necrosis within the masses, involvement adjacent organs were determined and analyzed.

Tissue diagnosis was obtained in all cases. All patients underwent adrenalectomy. (Laparoscopic adrenalectomy in one case)

RESULTS

CORTICAL ADENOMA

Four unilateral cortical adenomas were encountered in 4 patients. All patients had biochemical and/or clinical evidence of adrenal hyperfunction and were females. (table 1) All masses had smooth contours, homogeneous density and no calcification. Their diameter measured 2 – 4.5 cm. (average 2.78 cm.) The density of the masses was less than or equal to muscles. The available CT number of 2 cases was 5 H.U. and 17 H.U. respectively which is similar to fluid attenuation. (fig. 1, 2) Mild to moderate degree of homogeneous enhancement was evident

TABLE 1. Patient Data & CT features of cortical adenomas

Patient			Lesions					
Age (yr)	Sex	Clinical	Unenhanced CT				Enhanced CT	
			Size cm.	Contour	Homogeneity	Density	Homogeneity	Degree
25	F	Conn's	2	Smooth	Homogeneous	5 H.U.	Homogeneous	Mild
31	F	Cushing	3	"	"	= muscle	"	Mod.
31	F	"	2	"	"	= muscle	"	"
33	F	"	4.5	"	"	17 H.U.	"	"

● No calcification in all cases

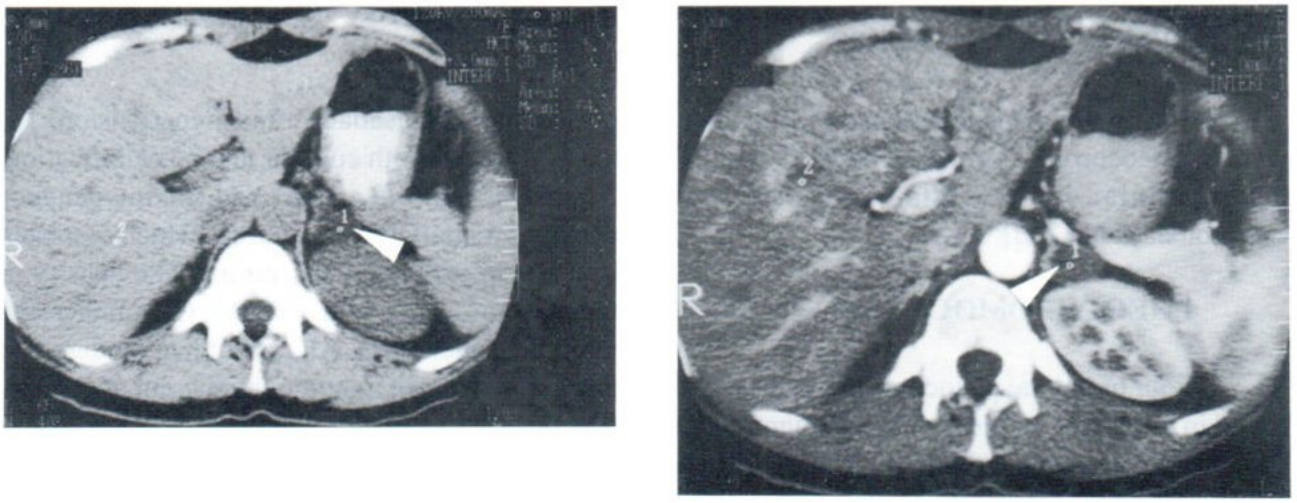

1A 1B

Fig. 1 Cortical Adenomas (Conn's adenoma) in a 25 – year – old woman with hypertension and an biochemical evidence of primary aldosteronism

A. Very small homogeneous hypodense LT.adrenal mass with smooth contour. Attenuation of mass is about 5 H.U. (arrow)

B. Moderate degree of homogeneous enhancement on post – contrast image (arrow)

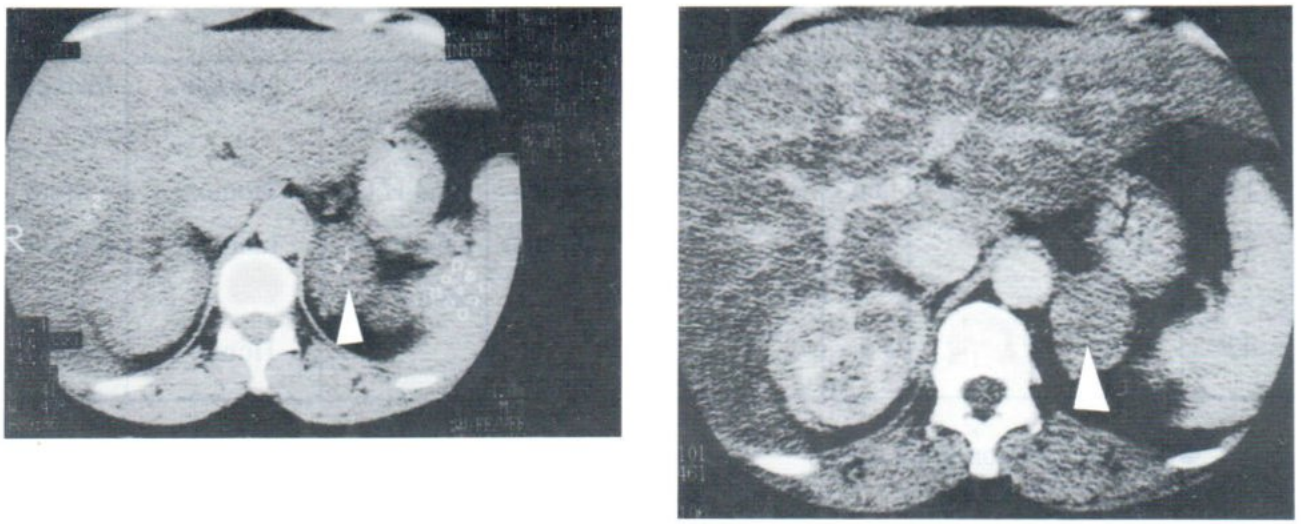

2A 2B

Fig. 2 Cortical Adenomas (Cushing's adenoma) in a 33 – year – old woman

A. LT.adrenal mass with smooth contour ,density is slightly less than muscles about 17 H.U. (arrow)

B. Moderate degree of enhancement on post contrast image (arrow)

NONADENOMATOUS MASSES

Of the 9 nonadenomatous patients, there were 4 pheochromocytoma, 2 adrenal cysts, 1 macronodular hyperplasia, and 2 cortical carcinoma. (table 2, 3)

PHEOCHROMOCYTOMA

Four unilateral pheochromocytomas were found in 4 patients. (table 2) Three patients were females. All patients had the same clinical presentation of headache and hypertension. All masses had smooth contour and no calcification. Almost of them (3 cases) had inhomogeneous density by small low dense areas which represent necrosis in pathological sections. The density of the mass in 2 cases with available CT number was more than adenomas. Almost all had moderate to marked degree of inhomogenous enhancement. (fig. 3, 4)

TABLE 2. Pheochromocytoma (4 cases)

Patient			Lesion					
Age (yr)	Sex	Clinical	Unenhanced CT				Enhanced CT	
			Size (cm.)	Contour	Homogeneity	Density	Homogeneity	Degree
13	M	Headache, hypertension	4	Smooth	Inhomogeneous	39.6 H.U.	Inhomo.	Marked
19	F	"	3.6	"	Homogeneous	48.4 H.U.	Homo.	Mod.
25	F	"	4.4	"	Inhomogeneous	= munscle central low	Inhomo.	Marked
42	F	"	4.5	"	"	"	Homo.	Mod.

● No calcification in all cases

ADRENAL CYSTS

They were encountered in 2 patients. One of them presented with RUQ abdominal pain, another one was asymptomatic. Both of them were reported as tumor, particularly primary malignancy or metastases because of her old ages. But the pathological sections were proven as adrenal cysts. One of them had well defined density mass without enhancement. (fig. 5) Another one had heterogeneous soft tissue density mass with lobulated contour, calcification and mild degree inhomogeneous enhancement. (fig. 6)

TABLE 3. Other nonadenomatous masses

	Adrenal cysts (n = 2)	Macronodular hyperplasia (n = 1)	Carcinoma (n = 2)
● Patient age	49 , 67	13	37 , 53
● Sex	F , F	M	F , M
● Presentation	RUQ pain , Asymptom	Precoccious Puberty and hypertension	Cushing 's , RUQ pain
Lesion size (cm.)	6 , 4 cm.	3 cm.	6 , 21 cm.
Unenhanced CT			
- Contour	smooth , lobulated	smooth	smooth , smooth
- Homogeneity	Homo , Inhomo.	Homo.	Homo. , Inhomo.
- Attenuation	= GB fluid , 37.9 H.U.	= muscle	= muscle , 28.57 H.U.
Enhanced CT			
- Homogeneity	no enhance , Inhomo.	Homo.	Thin septal & rim, thick irregular rim
- Degree	——— , Mild	Mild	Mild , Mod.
Calcification	None , septal Ca+	None	None , punctate
Involved adj. Organ	None , None	None	None , kidney

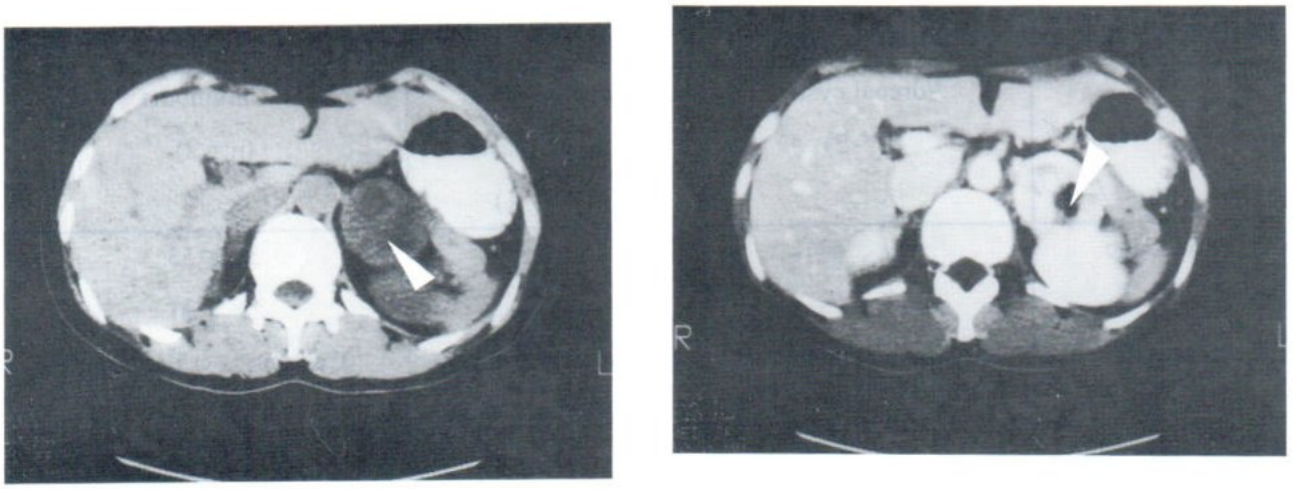

3A 3B

Fig. 3 Pheochromocytoma

A. Inhomogeneous hypodense mass of LT.adrenal gland with smooth contour (arrow)

B. Post contrast image show markedly enhancement of mass with more delineation of focal necrosis. (arrow)

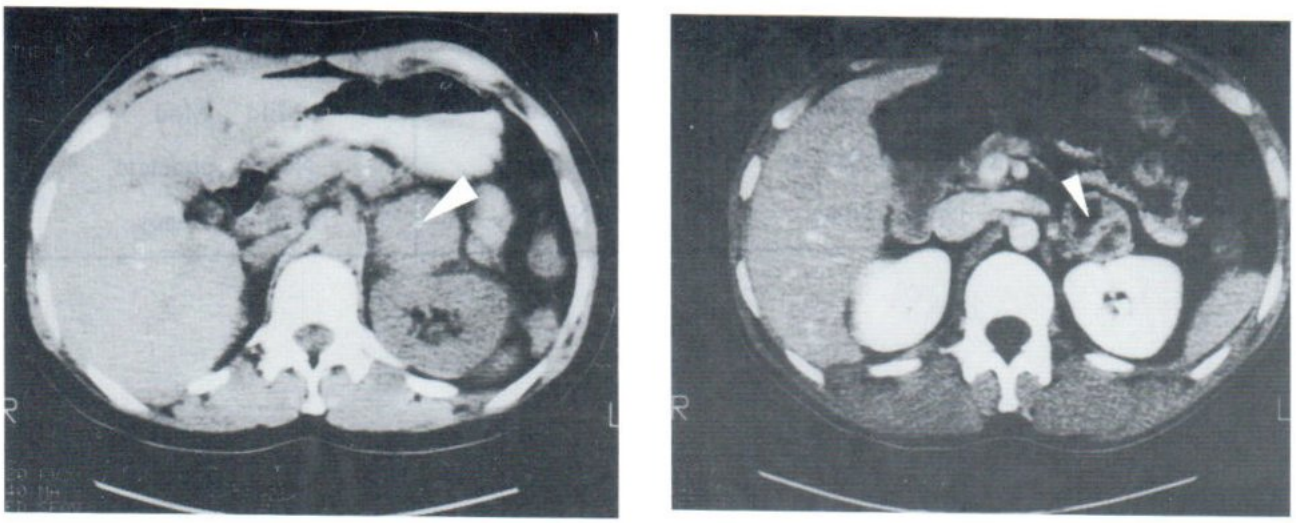

4A 4B

Fig. 4 Pheochromocytoma

A. Only one case of homogeneous density of LT.adrenal mass on pre – contrast image (arrow)

B. Heterogeneous moderate enhancement of the mass with small areas of necrosis (arrow)

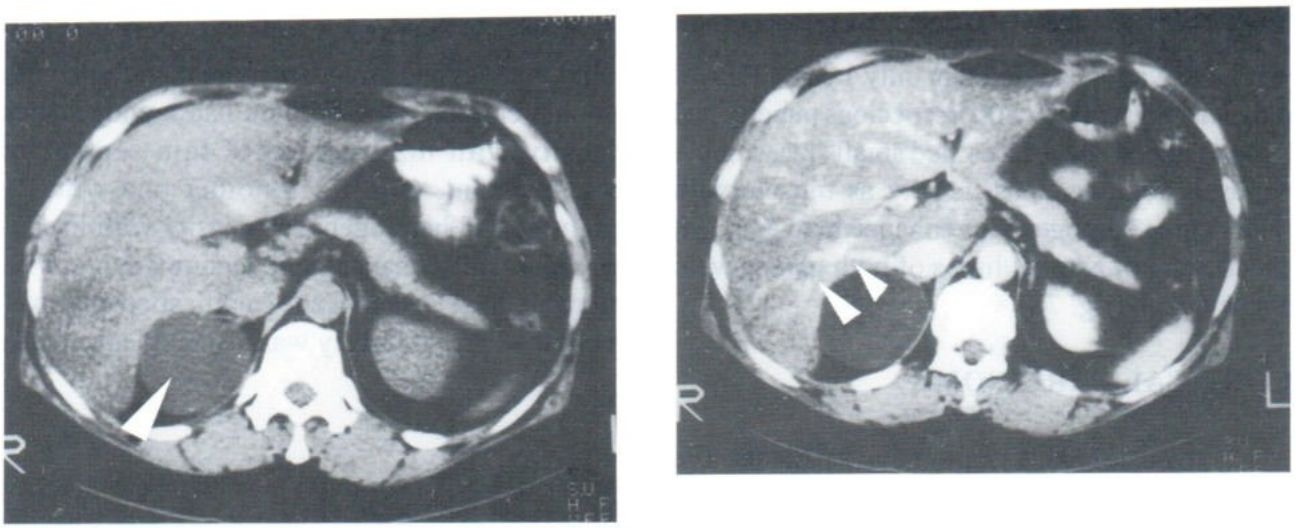

5A 5B

Fig. 5 Uncomplicated adrenal cyst

A Globular shape of hypodense mass (equal to GB fluid) with smooth contour at RT. adrenal gland (arrow)

B. No enhancement of this mass on post – contrast image, minimal pressure effect to adjacent liver is shown. (arrow)

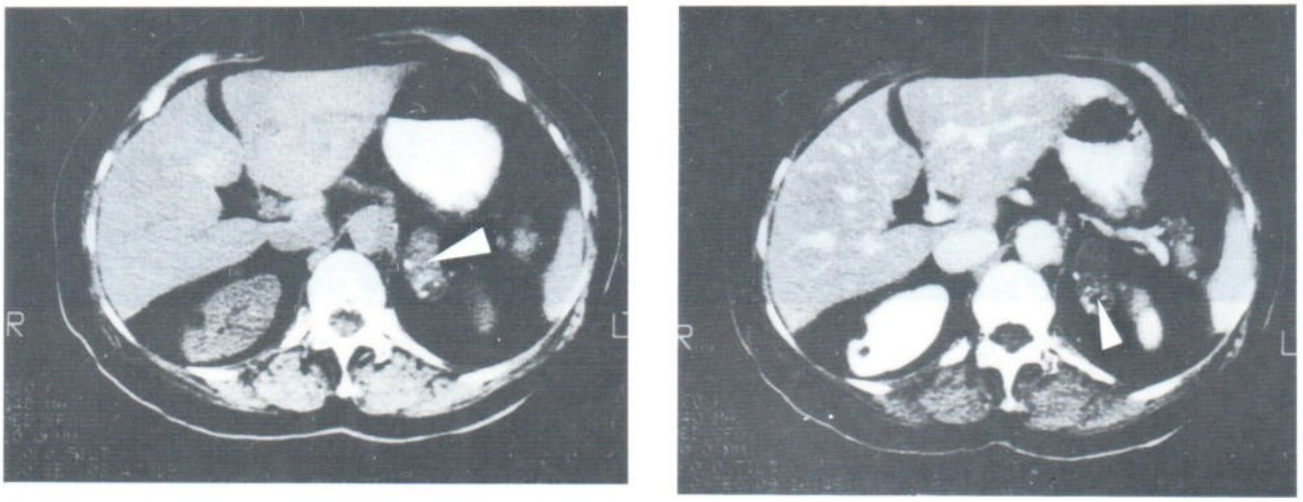

6A 6B

Fig. 6 Complicated adrenal cyst

A. Heterogeneous solid appearance of LT. adrenal mass (arrow) with calcification and lobulated contour which mimic tumor

B. Post contrast image show mild degree septal enhancement (arrow)

MACRONODULAR HYPERPLASIA

It was encountered in only 1 case, 13 year old male, presenting with precoccious puberty and hypertension. The masses had small size, smooth contour, homogeneous density as muscle with mild degree homogeneous enhancement. (fig. 7a) Thickening of adrenal limbs of both glands were also evident. (fig. 7b)

CORTICAL CARCINOMA

It occurred in symptomatic 2 patients. The tumor masses had large size more than 5 cm. with smooth contour. One of them had homogeneous density with mild degree of thin septal-rim enhancement. (fig. 8) Another one with 21 cm.mass had heterogeneous density with irregular thick rim enhancement,accompanying with mural nodules and punctate calcification. Involvement to adjacent kidney was also evident. (fig.9)

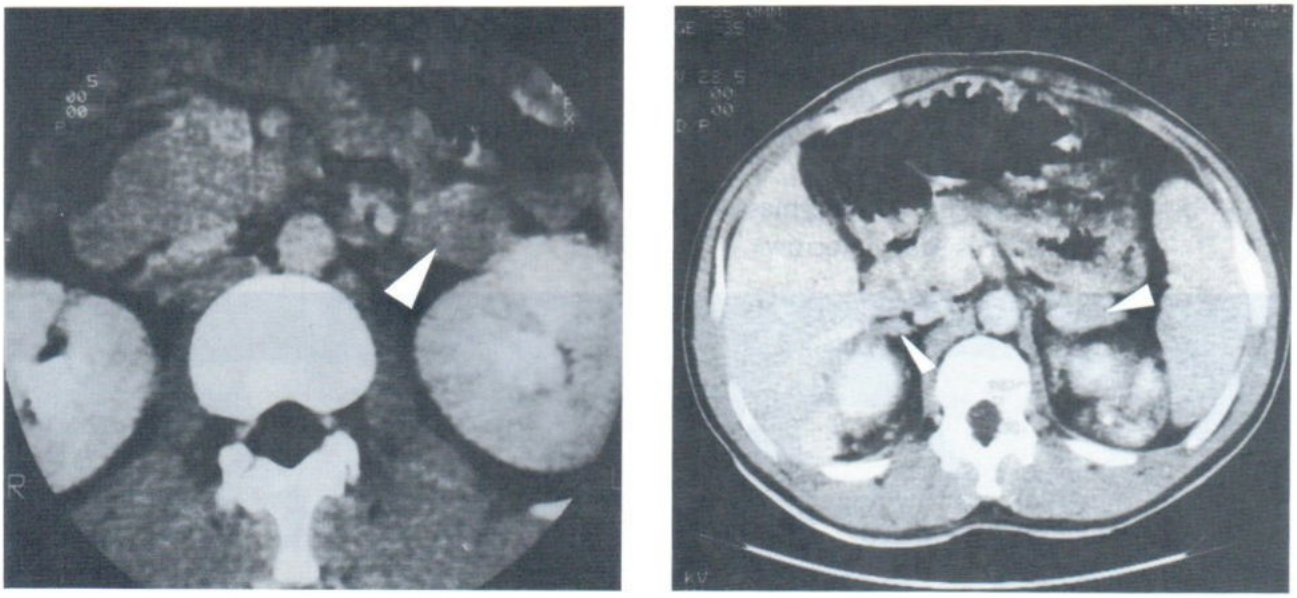

7A 7B

Fig. 7 Macronodular Hyperplasia

A. Magnification of LT.adrenal mass with slightly enhancement (arrow)
B. Thickening of adrenal limbs of both glands were shown. (arrow) More thickening on the LT. side is evident.

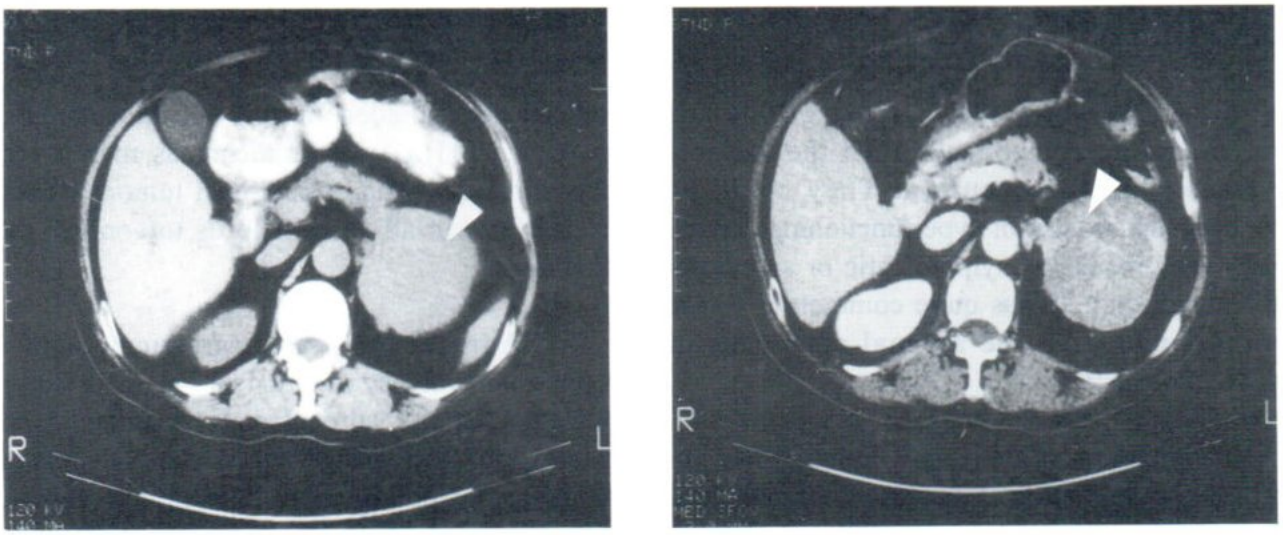

8A 8B

Fig. 8 Cortical Carcinoma
A. 6 cm. LT.adrenal mass with smooth contour, homogeneous density (arrow)
B. Post contrast image reveal mild degree of thin septal rim enhancement (arrow)

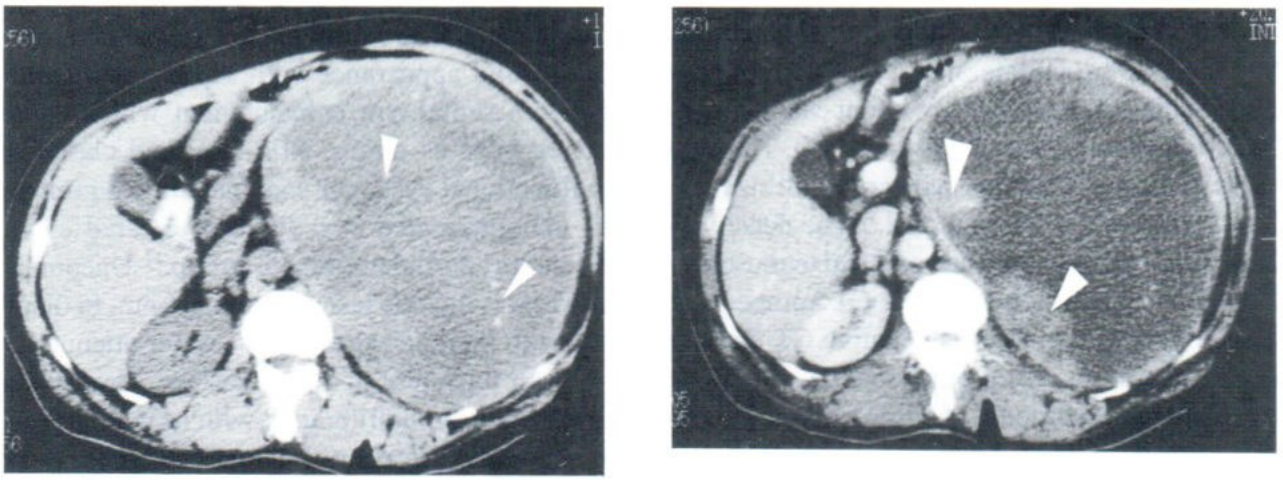

9A 9B

Fig. 9 Cortical Carcinoma
A. Huge LT.adrenal mass with heterogeneous density, punctate calcification (arrow)
B. Thick irregular rim enhancement with nodules (arrow) was shown on post – contrast images

DISCUSSION

As we know that adrenal glands had varied tissue components, then the variable masses could be occurred. They could be nonhyperfunctioning or hyperfunctioning masses. They may result in asymptomatic or symptomatic condition.[10] It was quite common to divide adrenal masses to be adrenal adenomas or nonadenomas.[13]

Although recently, MR imaging has improved the evaluation of masses of adrenal gland and several methods have been proposed. CT scan is still useful and widely accepted imaging techniques without longer time consuming or more expensive cost. It can detect the only tiny masses.

Our series had 13 adrenal masses in 13 patients who had pathologically proven from adrenalectomy in all cases.We found 4 cases of cortical adrenomas with all hyperfunction tumors. All masses were unilateral and had smooth contours, homogeneous density without calcification. Their diameter measured less than 5 cm. The only 1 case of Conn's adenoma had very small size,less than 2 cm.,as in previous report.[10] The density of adenomas was low (less than or equal to muscles), about 5 and 17 H.U.in available CT number of 2 cases. But no any mass has negative CT number of attenuation as many other reports, it may be explained by less amount of adipose tissue in both 2 cases of available CT number. Mild to moderate homogeneous enhancement are shown. For 4 cases of pheochromocytoma, all tumor masses are unilateral, smooth contour, size less than 5 cm. Without calcification. Almost of them (3 cases) had heterogeneous density due to small areas of necrosis. Moderate to marked inhomogeneous enhancement are shown. The remaining one case has homogeneous density mass which could mimic cortical adenoma except the attenuation number is higher. As H.Miyake et al had reported that adrenal mass with less attenuation (< 20 H.U.) indicate cortical adenomas, if the attenuation is more than 20 H.U. may be adenomas, metastases, pheochromocytoma, periadrenal tumor.[8] Rising urine VMA in all cases help us to confirm the diagnosis.

Adrenal cysts are infrequent, with a reported prevalence of 0.064 % - o.180% But in one recent study, adrenal cysts constitued 5.7% The apparent increasing frequency is likely related to incidental radiographic detection of adrenal masses[12] which like one case in our series.

Two cases of adrenal cysts in our series, one had round shape, homogeneous hypodensity mass but there's no enhancement at all which indicate the simple cyst and could distinguish from adenomas. Another one had no symptom and came to our hospital for check up.Ultrasound show an echoic mass. The following CT reveal heterogeneous solid appearance with septal calcification and thin septal rim enhancement which cause misdiagnose as tumor. Alla et al had classified nonfunctional cystic adrenal mass into 3 groups ; (a) uncomplicated cyst (b) complicated cystic lesions (c) an indeterminate group.[12] Uncomplicated cysts include lesions up to 5-6 cm. In diameter with homogeneous near – water attenuation and wall thickness of 3 mm. or less. These cysts may be uni- or multilocular, with or without wall or septal calcification. Lesions that meet these criteria can be safely observed as one case in our series. Complicated cystic lesions have at least one of the following features ; high attenuation value, nonhomogeneous texture, stippled central or thick peripheral calcification, or a thick wall (>, = 5 mm.). Such findings are likely caused by acute or chronic hemorrhage as in our case. Such lesions should be surgically explored, although most of them will prove to be hemorrhagic cysts. A short observation period with documentation of the evolution of intracystic hemorrhage may be

appropriate in some cases. Radiologically indetermine lesions include uncomplicated cysts larger than 5-6 cm.,with slightly higher-than-water attenuation (up to 30 HU), or with borderline wall thickness. Patients with these cysts may benefit from percutaneous cyst aspiration and otherwise conservative management.

Two types of adrenal hyperplasia have been described ; the common smooth hyperplasia and the less common nodular type, also known as cortical nodular hyperplasia. Nodular hyperplasia can be of (a) the micronodular variety in which the glands may appear normal and possess nodules of varying sizes (b) the macronodular variety, in which the gland are thickened and posesses nodules of varying size. The macronodular variety can at times be difficult to diagnose, as it can easily misdiagnosed as a hyperfunctioning cortical adenomas. Macronodular hyperplasia produce solitary mass with slightly enhancement. Our patient present with hypertension, precoccious puberty. Ultrasound and CT shows left adrenal mass .Then patient underwent unneccesary Lt. adrenalectomy after it was reported as adrenal tumor. If carefully evaluate, there's helpful finding to document adrenal hyperplasia by visible thickening of adrenal limbs of both glands. Finally, the patient is proven for congenital adrenal hyperplasia with salt retention by 11-? hydroxylase deficiency in adrenogenital syndrome.

ADRENAL CARCINOMA

Typical features are large mass bigger than 5 cm. with heterogeneous density and thick irregular rim enhancement accompanying with involvement to adjacent organs.[1,6,11] One of our 2 cases had these features as well. Another one had homogeneous density with slightly thin septal rim enhancement but there was large size,bigger than 5 cm.

CONCLUSION

Small homogeneous adrenal masses with less amount of attenuation number are likely to be cortical adrenomas. Heterogeneous masses with necrotic areas, moderate to marked enhancement indicate pheochromocytomas. Adrenal cysts had to be evaluated as uncomplicated or complicated cysts. Macronodular hyperplasia can mimic tumor, but carefully pay attention to the morphological features of the adrenal glands whether there are hyperplasia will allow radiologists to distinguish this condition from adrenal tumor and unnecessary adrenalectomy may be avoided. Then large size masses (more than 5 cm.) with thick irregular rim enhancement and invasion to adjacent organ are definitely to be adrenal carcinoma .

REFERENCES

1. Sarwat H., Arie B., Steven ES, et al. Differentiation of Malignant from Benign Adrenal Masses : Preductive indices on Computed Tomography AJR 1985 ; 144 : 61 – 65
2. John LD, Donald LM, Andrew JD, et al Macronodular Adrenal Hyperplasia in Cushing Disease Radiology 1988 ; 166 : 347 – 352
3. Lincoln LB, D.Bradley K, Philip JK, et al Differentiation Between Small Benign and Malignant Adrenal Masses with Dynamic Incremented CT AJR 1988 ; 151 : 95 – 101
4. Francesco M, Lorenzo ED, Franco Z, et al Myelolipoma of the Adrenal Gland : Sonographic and CT Features AJR 1988 ; 151 : 961 – 964
5. Hidetoshi M, Hirofumi M, Makoto T, et al CT of Adrenal Tumors, Frequency and Clinical Significance of Low – Attenuation lesions AJR 1989 ; 152 : 1005 – 1007
6. N. Reed Dunnick et al Adrenal Imaging : Current status AJR 1990 ; 154 : 927 - 936

7. N.Sato, Y.Watanabe, T. Saga, et al Adrenocortical adenoma containing a fat component : CT and MR Image evaluation Abdominal Imaging 1995 : 20 : 489-490
8. H. Miyake, H. Takaki, S.Matsumoto, et al Adrenal nonhyperfunctioning adenoma and nonadenoma : CT attenuation value as discriminative index : Abdominal Imaging 1995 : 20 : 559 - 562
9. Michael JL, Peter FH, Nicholas P, et al Benign and Malignant Adrenal Masses : CT Distinction with Attenuation Coefficients, Size and Observer Analysis Radiology 1991 ; 179 : 415 – 418
10. Isaac RF, Milton DG, Brahm S, et al Integrated Imaging of Adrenal Disease Radiology 1992 ; 184 : 1 – 13
11. McLoughlin RF, Bilbey JH. Tumors of the Adrenal Gland : Findings on CT and MR Imaging ; AJR 1994 ; 163 : 1413 - 1418
12. Alla R, Helen TM, E. Stephen A. Cystic Adrenal Lesions : CT features Radiology 1996 ; 201 : 541 – 548
13. Melvyn K, Frederick JB, Gerald Gy, Issac RF, et al. Differentiation of Adrenal Adenomas from nonadenomas Using CT Attenuation Values AJR 1996 ; 166:531 – 536
14. Randell R, Cynthia LD, Helene G, et al Adrenal and Extra – Adrenal Retroperitoneal Ganglioneuroma : Imaging Findings in 13 Adults Radiology 1997 ; 202:703 – 707
15. Gregory LJ, Ralph HH, Fray FM, Elliot KF Primary Adrenal Ganglioneuroma : CT Findings in Four Patients AJR 1997 ; 169: 169 - 171

CHONDROBLASTIC OSTEOSARCOMA OF THE RIGHT CLAVICLE: CASE REPORT AND LITERATURE REVIEW

Prathana CHOWCHUEN, M.D.[1] Jumphon MITRCHAI, M.D.[2]
Jiraporn SRINAGARIND, M.D.[1]

INTRODUCTION

Chondroblastic osteosarcoma is a rare, high-grade bone tumor in which a substantial volume(up to 90%) of tumor tissue is a chondrosarcomatous phenotype growing next to osteoid-forming areas.[1] Its prevalence ranges from 4.2[2] to 25[3] percent of all osteosarcomas. Primary tumors of this type of the clavicle represents only 1% of primary osteosarcoma.[4] Chondrosarcoma at this location is also infrequent.[2] In cartilaginous-forming tumor, the chondroid calcifications can be detected on plain radiographs. Well-differentiated tumor cartilage has also been identified by septal or septonodular enhancement pattern on gadolinium-DTPA enhanced MR images.[5,6] Differentiating chondroblastic osteosarcoma from chondrosarcoma is of clinical importance because of the substantial difference in treatment and prognosis, the former having a poorer prognosis and requiring resection and chemotherapy.[1,2]

Our aim is to report a rare case of chondroblastic osteosarcoma of the clavicle recognized on plain radiographs, computed tomography (CT) and magnetic resonance (MR) imaging.

CASE REPORT

CLINICAL INFORMATION

A 32-year-old man presented with a 6-month history of a gradually enlarging palpable mass on his right shoulder. His medical history was unremarkable and he did not recall any trauma to this area. Physical examination revealed a large, lobulated, firm mass over the right clavicle and shoulder area with superficial venous dilatation.

Laboratory findings were within normal limits, except for elevated level of serum alkaline phosphatase.

RADIOLOGICAL FINDINGS

The plain radiograph demonstrated a large soft tissue mass over the right clavicular region, containing chondroid calcifications. The entire clavicle was almost completely destroyed (figure 1). CT scans revealed the destruction and the broken through cortex at the medial end of the clavicle, osteoblastic lesions and a perpendicular type periosteal reaction (figure 2A). Discrete chondroid calcifications were detected through out the mass (figure 2B). MRI was performed and produced a heterogeneous, intermediate signal intensity indicating a mass surrounding the clavicle with high signal intensity within the medullary cavity and loss of cortical dark signal at the medial end of the clavicle (figure 3A and 3B). Septonodular enhancement of the mass was observed on post gadolinium enhanced T1-weighted MR images (figure 4).

[1] Department of Radiology
[2] Department of pathology, Faculty of Medicine, Khon Kaen University, Khon Kaen, 40002, Thailand.
E-mail: Pratha-c@medlib2.kku.ac.th.

*Presented at the10th Annual Scientific Meeting of the Singapore Radiological Society and the 3rd Annual Scientific Meeting of the Asian Musculoskeletal Society.

The differential diagnosis was chondrosarcoma .

THE PATHOLOGICAL DIAGNOSIS

The patient underwent open biopsy of the mass. The histopathological examination revealed large areas of low-grade chondrosarcoma showing atypical, multinucleated chondrocytes in a hyaline cartilaginous matrix. Areas of unequivocal osteoid production by neoplastic cells were presented elsewhere (figure 5A and 5B). The pathological diagnosis in this case was chondroblastic osteosarcoma .

Within the one month follow-up period, the mass had enlarged so rapidly that it was too large for resection. The surgeon advised neoadjuvant chemotherapy but the patient did not return for follow-up.

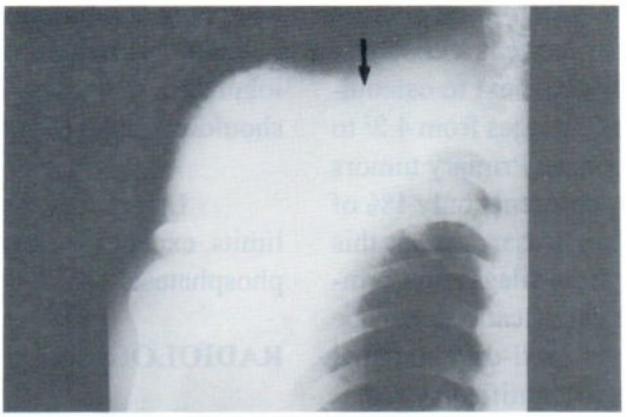

Fig. 1. Plain radiograph of the right clavicle demonstrated a large soft tissue mass containing chondroid calcifications. The entire clavicle was almost completely destroyed.

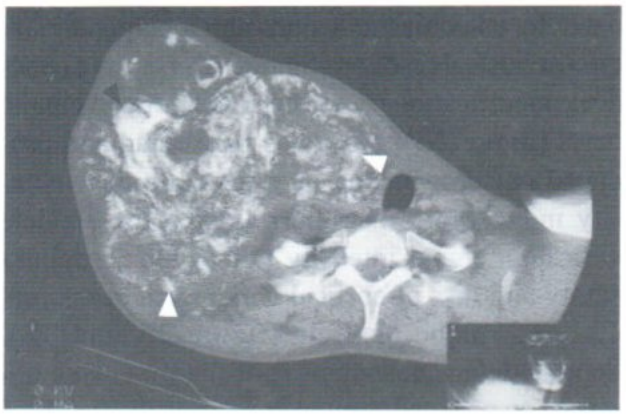

2A

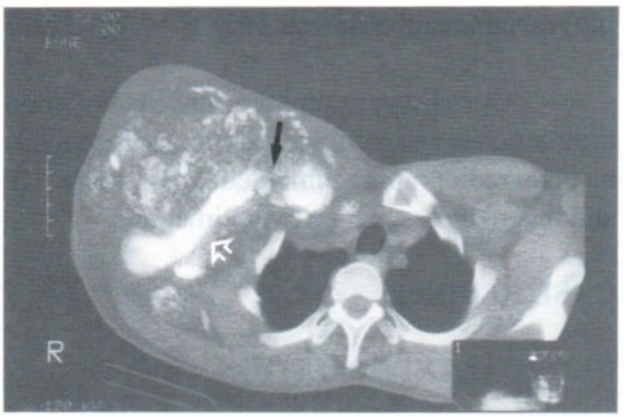

2B

Fig. 2A,B. Axial CT images demonstrated destruction and breaking through the cortex at the medial end of the clavicle (black arrow), osteoblastic lesion in the remainder, a perpendicular type periosteal reaction (open arrow) and discrete chondroid calcifications (arrowhead) through out the mass.

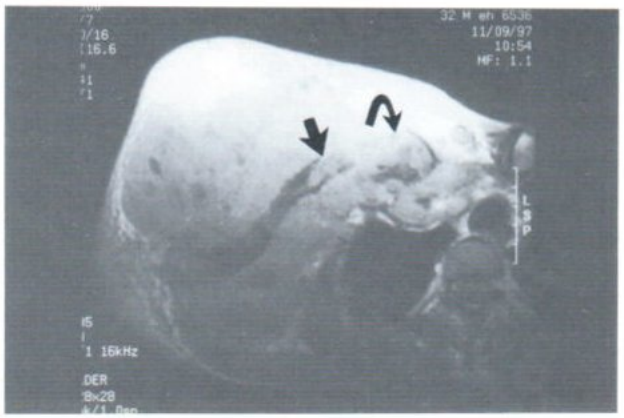

3A

Fig. 3A. Axial T1-weighted (TR/TE; 895/20) MR image revealed heterogeneous, intermediate signal intensity indicating a mass surrounding the clavicle and a hyperintense lesion (arrow) within the medullary cavity and loss of cortical dark signal (curve arrow) at the medial end of the clavicle.

3B

Fig. 3B. Coronal T2-weighted (TR/TE; 5454/96) MR image showed heterogeneous increased signal intensity of the mass.

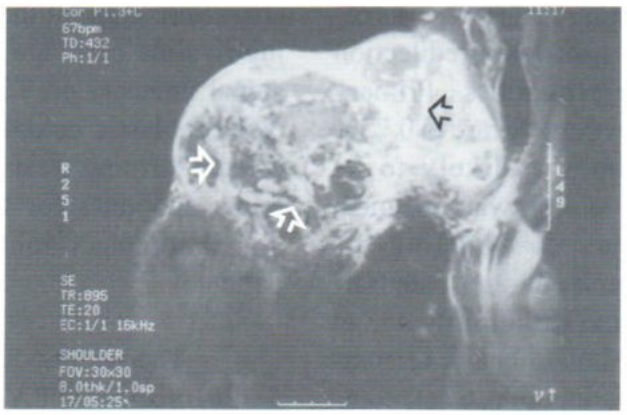

Fig. 4. Post gadolinium-enhanced coronal T1-weighted (TR/TE; 700/20) MR image revealed septonodular enhancement of the mass.

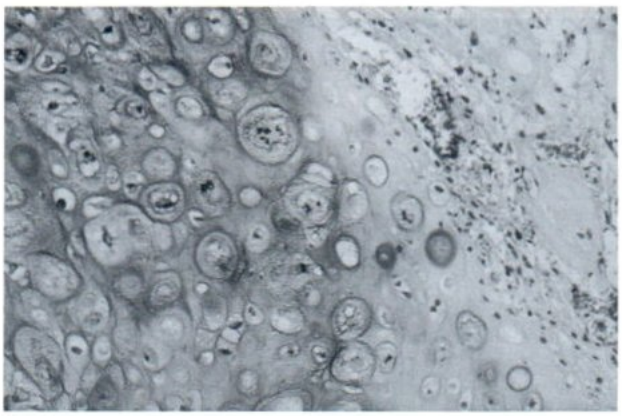

5A

Fig. 5A. A large area of low-grade chondrosarcoma showing atypical multinucleated chondrocytes in hyaline cartilaginous matrix.

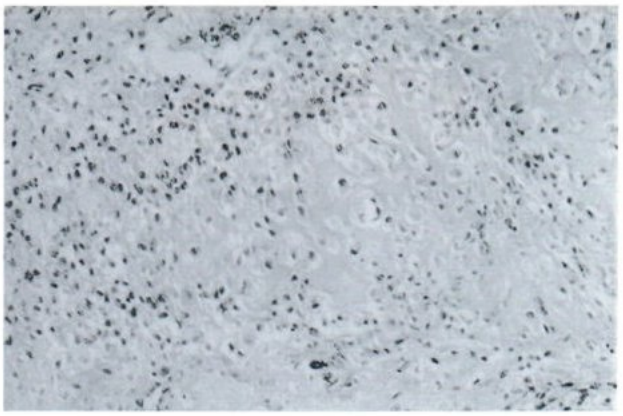

5B

Fig. 5B. Areas of unequivocal osteoid production by neoplastic cells.

DISCUSSION

Osteosarcoma is a relatively stereotypic entity, with some exceptions. This neoplasm is a disease of the young, affecting males twice as often as females and shows a marked predilection for the long bones of the extremities.[1] Primary tumors of the clavicle are extremely rare (a 0.73% frequency), and four times as likely to be malignant as benign.[2] Myeloma was the most common primary malignancy affecting the clavicle, followed by lymphoma and osteosarcoma; the clavicle being the site of only 1% of primary osteosarcomas.[1,2] Chondroblastic osteosarcoma is a relatively rare variant of osteosarcoma with a reported incidence of 4.2%.[3]

In our patient, the tumor produced a large calcified cartilaginous matrix, which was detectable using plain radiograph and CT scan, so we suspected a malignant cartilaginous-forming tumor. Among this group of tumors, chondrosarcoma is more common than chondroblastic osteosarcoma, however, the location of the tumor was uncommon and our patient was younger than average for a central chondrosarcoma.[1,5,9]

Non-enhanced and Gadolinium-DTPA-enhanced MR imaging provide increased tissue characterization of the tumor.[5-8] Tumors containing hyaline cartilage appear as lobules of high signal intensity on T2-weighted images as does chondroblastic osteosarcoma.[7] The presence of osteoid forming areas in chondroblastic osteosarcoma accounts for the absence of very high signal intensity lobules[6] as was seen in our patient.

The septonodular enhancement pattern in Gadolinium-DTPA-enhanced MR images observed, as in our patient, characterizes a tumor that has a substantial hyaline cartilaginous matrix.

In summary, a 32-year-old man was diagnosed with chondroblastic osteosarcoma of the right clavicle. The rarity of primary tumor at this site and the diagnostic problems of this tumor on conventional radiographs are discussed. The Gadolinium-DTPA-enhanced MR images supported the diagnosis of a cartilaginous-form-

ing tumor by revealing septonodular enhancement of the mass. The identification of osteoid-forming tumor tissue in the biopsied specimen was crucial to the diagnosis of chondroblastic osteosarcoma.

ACKNOWLEDGEMENTS

The authors thank Mr. Bryan Roderick Hamman for assistance with the English presentation of the manuscript.

REFERENCES

1. Mirra JM. Bone tumors: clinical, radiologic, and pathologic correlations, 2nd ed. Philadelphia: Lea & Febiger, 1989: 248-344, 440-589.
2. Unni KK. Dahlin's bone tumors: general aspects and data on 11,807 cases, 5th ed. Springfield: C Thomas, 1996: 6-7, 71-109, 143-85.
3. Darfman HD, Czerniak B. Bone cancers. Cancer 1995; 75: 203-10.
4. Greenspan A, Unni KK, Mann J. Case report 804: chondroblastic osteosarcoma grade 3 of the left clavicle. Skeletal Radiol 1993; 22: 469- 71.
5. Geirnaerdt MJA, Bloem JL, Eulderink F, et al. Cartilaginous tumors: correlation of gadolinium-enhanced MR imaging and histolopathologic findings. Radiology 1993; 186: 813-817.
6. Geirnaerdt MJA, Bloem JL, Woude HJ, et al. Chondroblastic osteosarcoma: characterization by gadolinium-enhanced MR imaging correlated with histopathology. Skeletal Radiol 1998; 27: 145-53.
7. Cohen EK, Kressel HY, Frank TS, et al. Hyaline-cartilage-origin bone and soft tissue neoplasm: MR appearance and histologic correlation. Radiology 1988; 167: 477-81.
8. Evans H, Ayala AG, Romsdahl MM. Prognostic factors in chondrosarcoma of bone: a clinicopathologic analysis with emphasis on histologic grading. Cancer 1977; 40: 818-31.

KEITHLEY

Model 6517
Electrometer/High Resistance Meter

- Measure resistance up to $10^{17}\ \Omega$
- Measure current with 100aA sensitivity
- Measure coulombs 10 fc – 2 mc
- Vottage Source f 1 kv

Nuclear Associates

WIPER™ SINGLE-WELL WIPE TEST COUNTER

- Meets all requirements for nuclear medicine wipe testing.
- Full-featured multichannel analyzer for high resolution detail.
- Automatic calibration for trouble-free compliance.

Model 35040

Advanced Therapy Dosimeter

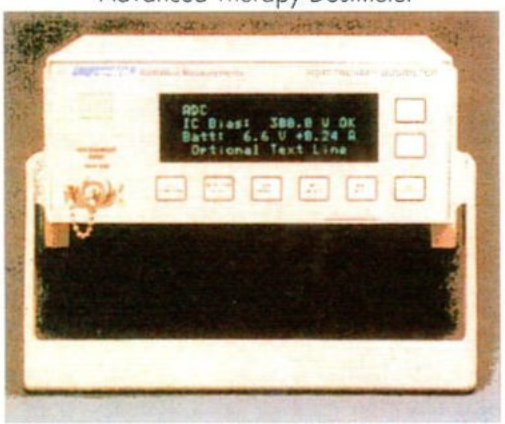

- Ultra long-term stability error of approximately 0.1% per five years
- Read out in C, A, R, Gy, Sv, Bq, and more
- Automatic reset and hold of measured values between exposures.
- Thirty-two (32) ion chamber calibration factors.

Victoreen Model 8000

NERO™mAx

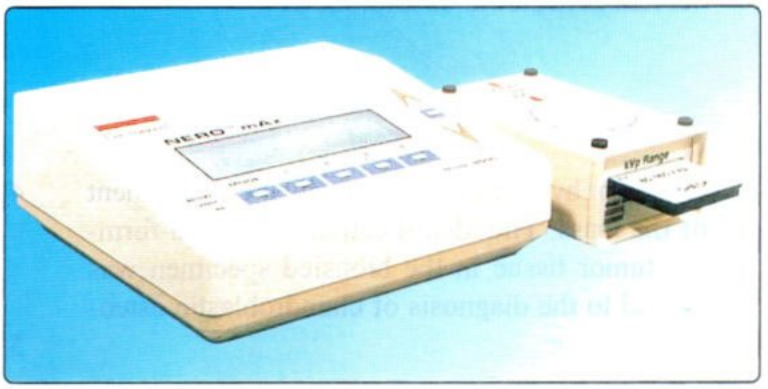

- 100 kHz sampling speed captures data from the most difficult machines
- 0.5 kV or 1% accuracy from 22 to 160 kV
- Measures kVp average, kV effective, kV peak, time, exposure or rate, mA or mAs, HVL, exposure/frame, and mAs/frame
- Displays R or Gy
- Convenient Excel Add-in with templates for Reproducibility, Accuracy, mAs Linearity, Beam Quality and Summary Reports
- RS-232 computer interface
- Enhanced dental capabilities

DDD DUAL-DIODE PATIENT DOSE MONITOR

- Provents the potential for misadministration.
- Provides instantaneous readings on the radiation dose being delivered to the patient.

2-Channel Unit!

Inovision Model 451P

Pressurized µR Ion Chamber Survey Meter

- High sensitivity µR measurements of exposure and exposure rate
- Available with dose equivalent energy response (SI units)
- Fast response to measure radiation from leakage, scatter beams and pinholes
- Ergonomic, anti-fatigue handle with replaceable grip and wrist strap
- Excel add-in for Windows® for data logging and selection of instrument operating parameters (optional)
- Low noise chamber bias supply for fast background reading
- Choice of bright, highly visible colors
- Easy touch keys

H.V.T. SUPPLY CO., LTD.

82/31 Moo 2 Kanchanapisek Road, Bangchuaknang, Talingchan, Bangkok 10170

Tel : (662) 447-9111-3, 887-5602, 887-7037 Fax : (662) 447-9114

E-mail : hvt@loxinfo.co.th

THE PREDICTIVE VALUE OF EARLY CT FINDINGS FOR SUBSEQUENT CEREBRAL INFARCTION IN HYPERACUTE ISCHEMIC STROKE

Parichad CHANPONG, M.D.[1] Patama NAKBUMRUNG, M.D.[2]

PURPOSE: To evaluate the relationship and the prediction of early CT signs of ischemic stroke and the location of subsequent infarction.

METHOD: We prospectively evaluated cranial CT signs of 75 consecutive patients with hyperacute ischemic stroke (within 6 hours of ictus) in the territory of the middle cerebral artery with evaluated at least 2 CTs (1 initial, within first 6 hours and 1 repeated CT within 48-72 hours of onset to confirm the infarct location) by one radiologist. On the first CT, early signs were hyperdenseMCA sign (HMCAS), early parenchymatous signs (attenuation of the lentiform nucleus [ALN], loss of the insular ribbon [LIR]), and early cortical edema are hemispheric sulcal effacement [HSE] and cortical hypodensity. Subsequent infarct locations were classified according to total, partial superficial, deep, or multiple MCA territories.

RESULT: Early CT abnormalities were found in 42 patients (56%). Isolated sign (HMCAS, isolated ALN and isolated LIR) 6 patients (14%), two signs (ALN/LIR) 7 patients (16%) and more than two signs 29 patients (70%). We found isolated HMCAS, two parenchymatous signs (ALN/LIR) and one or both parenchymatous signs (ALN or LIR) with cortical edema (HSE /cortical hypodensity) were strongly associated with subsequent large infarction and the positive predictive value of these signs for subsequent large infarctions were 100%, 85.7% and 86% respectively. The positive predictive value of isolated parenchymatous sign (isolated ALN or LIR) for deep infarction was 100% but the positive predictive value of negative early CT signs and isolated parenchymatous sign for subsequent large infarction were 0% and negative predictive value of these signs were 75% and 86.5% respectively.

CONCLUSION: Our findings suggested that positive early CT signs in first 6 hours allow the prediction of subsequent infarct locations. Early parencymatous signs associated with early cortical edema are strongly associated with subsequent large infarction but negative early CT signs and isolated parenchymatous sign are associated with subsequent deep infarction.

MCA = Middle Cerebral Artery
HMCAS = Hyperdense MCA sign.

[1] Division of neuroradiology Prasat Songkhla Neuropsychiatric Hospital Thailand
[2] Division of radiology Surathanee Hospital Thailand

INTRODUCTION

Cerebrovascular disease (CVD) or stroke is considered to be a national medical problem in Thailand.[1] In Thailand cerebral infarction was found about 70% of all stroke[2] lower than in America, ischemic stroke was found about 80-85%.

CT is widely used for early evaluation of acute strokes. Most importantly, CT excludes acute hemorrhage or other diseases mimicking ischemia (tumor, subdural hematoma). Therefore, CT is the main imaging examination in patients with brain ischemia and when antithrombotic agents are considered.[3,4] There are many early CT signs of ischemic stroke, hyperdense middle cerebral artery sign (HMCAS), early parenchymal abnormalites which are the attenuation of lentiform nucleus (ALN), loss of the insular ribbon (LIR), hemispheric sulcal effacement (HSE). Early parenchymal abnormalities might also predict subsequent infarct extension [5]and hemorrhagic transformation. [6]Finally, initial CT findings may help to predict response to therapy.[7] There are few previous studies about early CT signs and subsequent infarction. The purpose of this study is to evaluate the relationship and the prediction of the early CT signs in hyperacute period ischemic stroke in 6 hours of first ever stroke for each types of subsequent cerebral infarction.

METHOD

We prospectively evaluated cranial CT signs of 75 patients first ever episodic ischemic stroke in the MCA territories with clinically hemiparesis, from April 2001 to April 2002. All patients were evaluated neurological sign; Glasgow coma score and muscle power by the neurologist and taking CT scan before admitted in the stroke unit Prasat songkhla neuropsychiatric Hospital. The time from ictus to the time at the perfomed CT scan was not more than 6 hours. The all CT imagings were evaluated and analyzed by a radiologist, who did not know the clinical but aware the clinical stroke. The first CT scans were done in all 75 patients within 6 hours after onset. Repeated imaging studies (second CT scan) were performed in all cases within 48 –72 hours after stroke onset to confirm the size and location of infarction. Collected information included analysis cranial CT signs within 6 hours of onset (hyperacute period) of 1st CT scan and subsequent CT findings in second CT scan.

CT technique: All non-contrast CT brains were performed using a Toshiba spiral CT scanner - Auklet /FS with 512x512 metrix and 1 second scan time. The section thickness and increments were 5 mm., from the foramen magnum to the suprasellar region and 10 mm. contiguous slices above, the early CT signs were classified as:

1. HyperdenseMCA sign (HMCAS): spontaneous high contrast in the MCA. This definition required that the vessel appear not only brightly than adjacent brain tissue but also brighter than the other intracranial arteries, especially contralateral MCA and finally that it not be attributable to calcification.[8]
2. Attenuation of the lentiform nucleus (ALN): a decrease in density involving the lentiform nucleus area inducing the loss of the precise delineation of this area.[9]
3. Loss of insular ribbon sign (LIR): decreased precision in delineating the gray-white interface at the lateral margin of the insula.[10] The ALN and LIR signs are parenchymatous signs.
4. Hemispheric sulcal effacement (HSE)
5. Cortical hypodensity. HSE and cortical hypodensity are represent early cortical edema.

We analyzed CT findings in the first 6 hours after stroke

The results of CT finding were classified as:

1. No abnormality visible or negative findings.
2. Abnormality visible or positive findings, one or more than one signs in CT scan.

Second CT scans were performed in 48 hours after first CT scan in all cases. Using templates,[11] infarct locations were classified, as follow

1. Large MCA territory, if total superficial and deep MCA territories or the total superficial MCA territory were involved.
2. Multiple MCA infarct; if partial superficial MCA and deep territories were involved.
3. Deep MCA infarct, if the infarct was limited to the deep MCA territory.
4. Partial superficial MCA infarct, if the superficial (superior, insular, or inferior) MCA territory was Involved.

RESULT

The analyzed CT signs were

Table 1

First CT (within 6 hours of stroke)	Number of patients(%)
Negative finding	33 (44%)
Positive findings	42 (56%)

Table 2 Number and percentage of patients for each positive CT signs

ALN	LIR	HSE	Cortical hypodensity	HMCAS
34 (81%)	30 (71%)	29 (69%)	29 (69%)	2 (4.7%)

Table 3 Distribution of early CT signs (isolated and in association with each other)

	ALN (n= 34)	LIR (n=30)	HSE (n=29)	Cortical hypodensity (n=29)	HMCAS (n=2)
Isolated sign	2	2	-	-	2
2 signs					
ALN		7	-	-	-
LIR	7		-	-	-
3 signs	8	-	8	8	-
	-	4	4	4	-
4 signs					
(ALN/LIR/HSE/ cortical hypodensity)	17	17	17	17	-

ALN = Attenuation of lentiform nucleus, **LIR** = Loss of the insular ribbon
HSE = Hemispheric sulcal effacement

Table 4 Distribution between early CT signs and subsequent infarct lesions

2nd CT / 1st CT	Subsequent large Infarction	multiple Infarction	deep Infarction	partial superficial Infarct
Negative CT [n=33(44%)]	-	2	25	6
Positive CT [n = 42(56%)]				
-Isolated HMCAS (n = 2)	2 (2.6%)	-	-	-
-Isolated ALN (n = 2)	-	-	2	-
Isolated LIR (n = 2)	-	-	2	-
2 signs				
-ALN/LIR (n = 7)	6 (86%)	1 (25%)	-	-
3 signs				
-ALN/HSE/cortical Hypodensity (n = 8)	6 (75%)	2 (25%)	-	-

Table 4 (Continue) Distribution between early CT signs and subsequent infarct lesions

2nd CT / 1st CT	Subsequent large Infarction	multiple Infarction	deep Infarction	partial superficial Infarct
-LIR/HSE/cortical Hypodensity (n = 4)	3 (75%)	1	-	-
4 signs				
-ALN/LIR/HSE/ cortical Hypodensity (n = 17)	16 (94%)	1	-	-
Total	33 (44%)	7 (9%)	29 (39%)	6 (8%)

RESULT

There were 41 men and 34 women with a mean of 53 years old.

CT CHARACTERISTICS

The first CT was performed at a mean time of 5.4 hours .The first CT was normal in 33 cases. (44%), and it showed at least one abnormalities in 42 pts. (56%) (table 1). ALN was observed in 34 patients and the most common sign(table2), isolated in 2 of 34 pts. (6%), and was frequently found with LIR 32 patients (94%) and with HSE/

cortical hypodensity 25of 32 pts. (78%) (table 3). LIR was found in 30 patients, isolated sign 2 patients (6%), associated with HSE and cortical hypodensity was 21 of 30 pts. (70%)which was nearly ALN. HMCAS was observed in 2 patients (2.6%) and seen isolated sign, no associated with other signs. HSE and cortical hypodensity were not found in isolated sign but they are found associated with one or both parenchymatous signs, associated with one parenchymatous sign (ALN or LIR) 12 of 29 pts. (41%)(ALN 28%, LIR 14%)and both ALN/LIR 17 of 29 pts (59%).The second CT was performed on mean 57 hours after the first CT performed. Subsequent infarcts involved the large MCA territory in 33 pts (44%)of the patients, the multiple MCA territories in 7 pts (9%), the deep MCA territory in 29pts (39%) and partial superficial MCA territory in 6 cases (8%)(table 4)

NUMBER OF EARLY CT SIGNS AND SUBSEQUENT INFARCT TOPOGRAPHY (TABLE4)

In isolated sign, only 2 HMCAS patients developed subsequent large infarction, 2 in 6 patients (33%) but all isolated parenchymatous signs (ALN or LIR) patients developed subsequent deep infarction, no patients developed subsequent large infarction, subsequent multiple infarctions and partial superficial infarction.

In the patients with two positive signs (all were parenchymatous signs), subsequently developed large infarction , 6 in 7 cases (86%) and 1 case with multiple infarctions. In the patients with 3 CT signs positive are also associated with subsequent large infarction 9 in 12 cases or 75% with 3 patients developed multiple infarctions. In patients with 4 signs positive 16 of 17 patients developed large infarction (94%). No association between two or more than two signs with deep partial superficial infarcts (0%). Deep infarction and superficial infarction were found in 25 of 33 patients (75%), 6 of 33 patients (18%) respectively in cases of no abnormalities of early signs. We found hemorhagic transformation 12 of 33 patients (36%) in subsequent large infarction and 10 of these 12 hemorrhagic transformation had midline shift and mass effect affecting lateral ventricle.

EARLY CT FINDINGS AND SUBSEQUENT INFARCT TOPOGRAPHY.

In cases with negative early signs (33 pts), developed subsequent infarcts involving the deep MCA territory in 25 patients, partial superficial territory in 6 patients, multiple MCA territories in 2 patients but never develope infarction in large MCA territory. (table 4)

In case positive early CT signs (42 cases), all 2 isolated HMCAS patients developed large MCA territories infarct (100%) equally to isolated parenchymatous signs (isolated ALN or isolated LIR) which all were associated with deep infarction (100%). Two parenchymatous signs were found association, ALN/LIR in 7 patients, 6 of 7 patients developed subsequent large MCA territory (86%). One parenchymatous sign with early cortical edema (ALN/ HSE/ and cortical hypodensity or LIR/ HSE/ and cortical hypodensity) developed subsequent large infarction 6 in 8 cases and 3 in 4 cases respectively or equal to 75%. Two parenchymatous signs with early cortical edema (ALN/LIR/ HSE/ and cortical hypodensity) was seen in 17 patients and 16 of 17 developed subsequent large MCA territory infarction (94%) and multiple infarctions only 1 case.

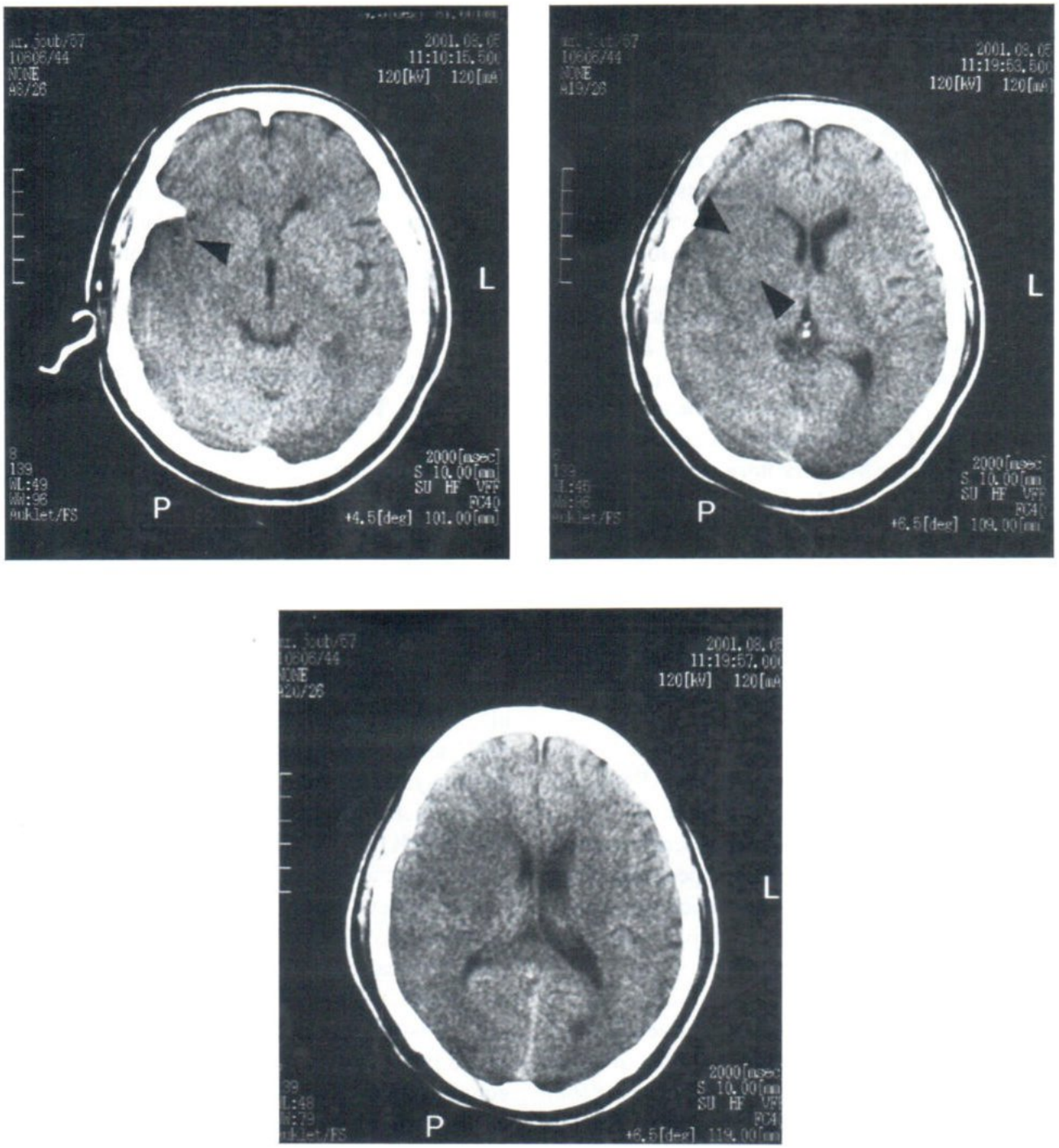

Fig. 1-3 Patient presented with acute stroke about 6 hours of onset. CT scan shows loss of the insular ribbon sign (LIR) (arrow head in figure 1), Attenuation of the lentiform nucleus (ALN) sign; (between arrows heads in figure 2) and Rt. hemispheric cortical effacement (HCE) compare to normal Lt. side in figure 3.

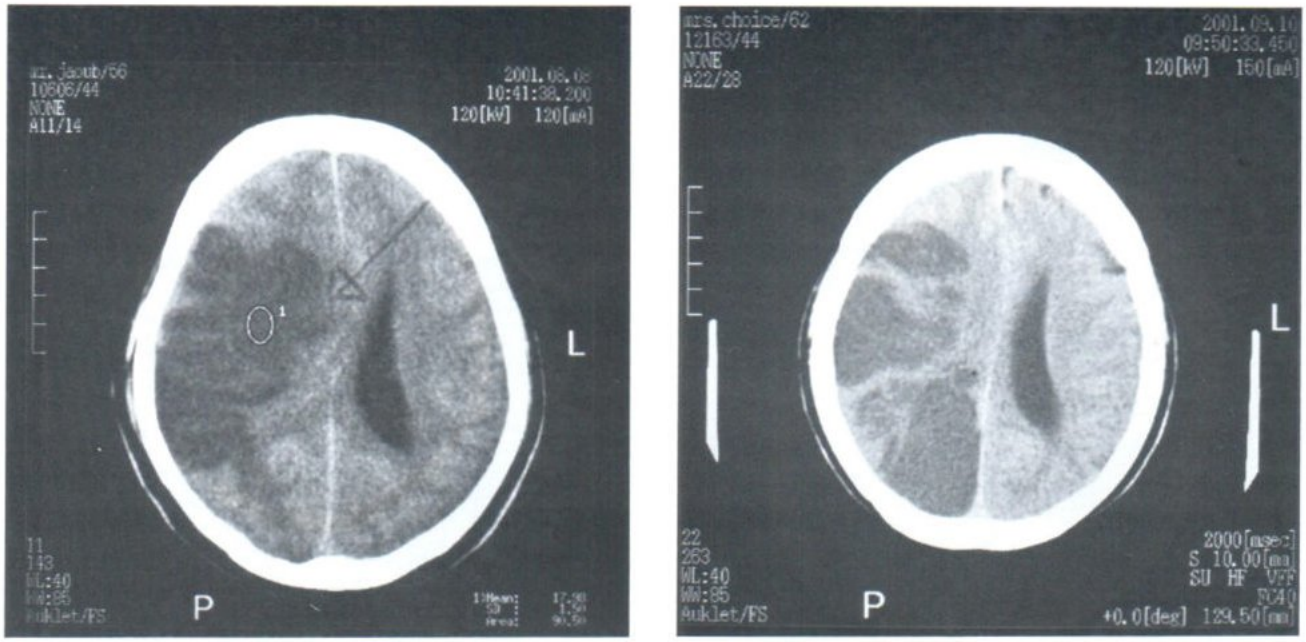

Fig. 4-5 The same patient followed up CT at 48 hours developed subsequent large infarction

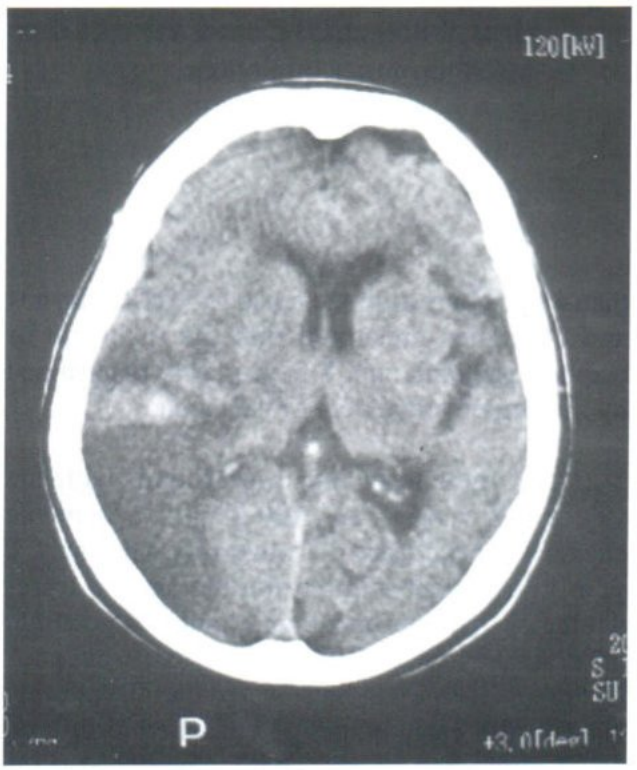

Fig. 6 Another patient with positive early CT signs showed subsequent large infarction with hemorrhagic transformation.

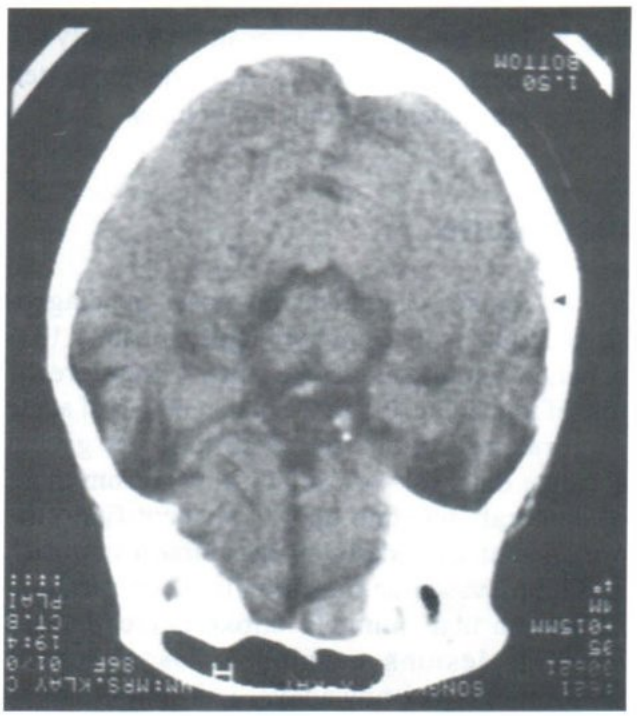

Fig. 7 Hyperdense Middle Cerebral Artery Sign (HMCAS). The patient unenhanced CT showing left hyperdense sign (HMCAS), this patient developed subsequent large infarction.

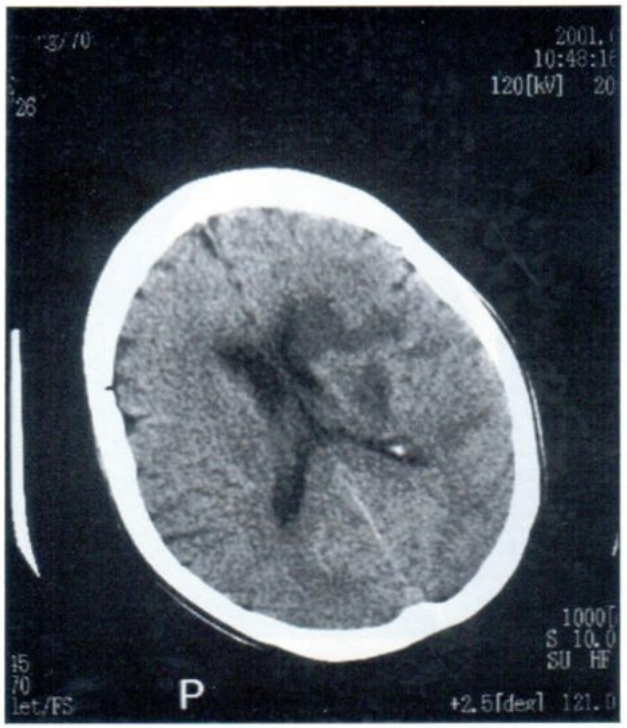

Fig. 8 This patient showed positive for early CT signs, followed up CT demonstrated subsequent multiple infarctions.

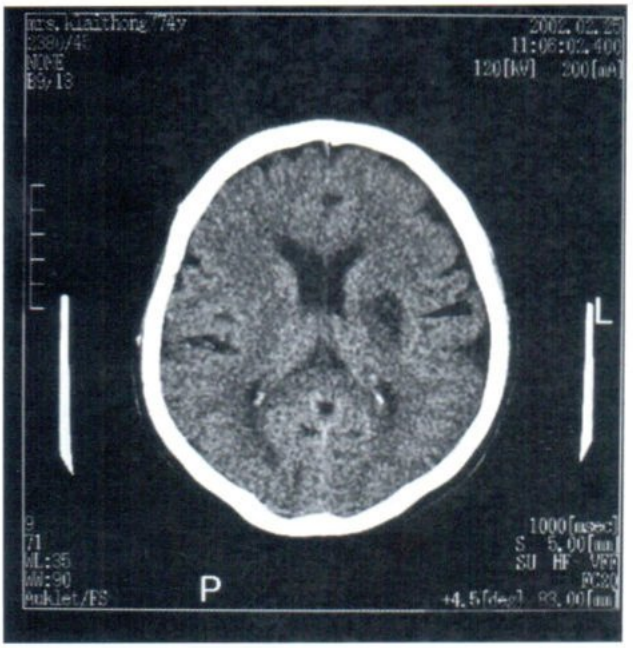

Fig. 9 This patient showed negative early CT signs, follow up CT demonstrated Lt. deep MCA territories infarctions.

DISCUSSION

Stroke is a clinical diagnosis, the diagnosis of stroke is inaccurate in approximately 13% of patient admitted to stroke units.[12] Therefore the role of immediate CT in the management of acute cerebral infarction is two fold: 1. In giving accurate diagnosis or excluding ICH from those of cerebral ischemia and 2. In identifying the presence of an underlying structural lesion such as tumor, vascular malformation, or subdural hematoma that mimick stroke clinically, non vascular lesions causing 1-2% of stroke syndromes[13] and nowadays, it is important to select patients for given thrombolytic therapy. The CT findings in acute cerebral infarction evolve with time. Although almost 60% of CT scans obtained within the first few hours after cerebral infarction are normal,[14] but several early signs of acute stroke can often be identified in stroke less than 4 to 6 hours after the episode. Von Kummer R and collagues presumed that the visibility of cerebral ischemia in CT is primarily determined by the degree and extent of ischemia.

If hypoperfusion is profound, with the values below 10-15 mL. 100 g^{-1}. min^{-1}, ischemic edema will occur early.[15] Conversely, a normal CT scan in a patient with stroke indicates a lesser degree of hypoperfusion and indicates potential reversibility of the functional disturbance.[16] Cytotoxic edema can be detected by CT scanning even in the early stages after ischemic infarct, which presented as early parenchymatous signs (ALN and LIR).

The x-ray attenuation seen with CT is directly proportional to tissue water content. A 1%

increase in tissue water content results in a 3 % to 5% decrease in x-ray attenuation, which translates into a decrease of approximately 2.5 Housfield units (HU).[17 - 18] In the past decade, a number of authors have identified CT findings which are based on the detection of early cytotoxic edema.[19-21] In our series, early CT abnormalities in the first 6 hours were usually found in all patients(56%). Our result were similar to those previously reported which vary from 31 to 92 %, depending on the time on which the CT was performed (4 to 8 hours).[9- 10, 22 - 26]

Previous studies evaluated early prenchymatous signs including ALN and LIR.[27] Many previous studies demonstrated that ALN was the earliest and the most common sign. More than 70% of cases (range from 60-92%) which CT were performed within 6 hours of onset. Our study shows ALN is the most common sign (81%) in agreement with the previous studies.[28 - 31]

HSE is the reflection of extracellular vasogenic edema, which is subsequent to intracellular cytotoxic edema. This is the superficial MCA territories sign and usually seen in early 3 hours or more after the onset of ischemia and rarely found isolation.[32 - 33] Our study found that HSE always associated with cortical hypodensity (100%) and frequently seen with one or both parenchymatous signs. Both HSE and cortical hypodensity represent cortical edema.[31]

HSE = Hemispheric sulcal effacement

The positive predictive value of isolated parenchymatous sign for subsequent large infarction and for deep infarction were 0% and 67% respectively and the negative predictive value of these signs were 87% and 0 % respectively. The positive predictive value of two parenchymatous signs (ALN/LIR) for subsequent large infarction was 85.7%, higher than one parenchymatous sign associated with early cortical edma (one parenchymatous sign with HSE/cortical hypodensity) which is 75% but less than the combination of two parenchymatous signs with cortical edema (both parenchymatous signs with HSE/cortical hypodensity) which is 94%. The negative predictive value for subsequent large infarction of two parenchymatous signs, three signs and four signs were 75%, 80% and 63% respectively. Our results confirmed an association between the number of early CT signs and subsequent large cerebral infarction corresponding to previous study[31] but bilateral parenchymatous signs should be more reliable signs than only one parenchymatous sign with sign of early cortical edema which has not been in the previous study. Therefore, we believe that both parenchymatous signs associated with signs of early cortical edema may be the most reliable predictive factor the for subsequent large cerebral infarction.

On the whole, hemorrhagic transformation (HT) seems to be correlated to both the intensity of ischemia and the extension of delayed infarcted rather than to the presence of early CT signs.[25,34] However, previous studies demonstrated a close relationship between hemorrhagic transformation and early CT signs[6,35] and another study found that hypodensity of the lentiform nuclei on early CT studied was strongly associated with later hemorrhagic transformation of the initially ischemic infarction.[36] Our study demonstrated that hemorrhagic transformation in 12 of 33 patients (36%) with subsequent large MCA infarct and 10 of these 12 patients had midline shift which is lower than in the previous study[31] which HT (Haemorhagic transformation) were found in about 50 % of the patients.

Hyperdense MCA sign is caused by acute intraluminal thrombus. The hyperdense MCA sign has been reported in 25% of all unselected acute infarcts and is seen in 35-50% of patients who have stroke symptoms in the MCA territory.[37 - 39] The hyperdense MCA sign typically occurs with cortical and large, deep MCA infarcts.[38] HMCAS in our results was found in 2 patients or 2.6% and had never been seen associated with other signs which was different from the previous studies (26-50%).[5, 25 - 26, 40] The specificity of HMCAS is very good, ranging from 85 to 100% in most series.[22,25–27,40]

However, some patients with clinical MCA ischemia do not exhibit HMCAS despite of an angiographic proven MCA occlusion, illustrating a lower sensitivity that varies from 29 to 69 %.[24-26,41] Our standard CT procedure did not include specific scan (less than 5mm.in thickness) on the perisylvian fissure, which may provide a higher positive rate. On the other hand. Although HMCAS usually occurs very early in time course of MCA occlusion, the MCA occlusion is often a transient phenomenon, as suggested by serial CT studies [24] and the value of isolated HMCAS as a predictor of outcome remains controversial.[27,40,42] Our study found the HMCAS only in 2 patients due to only a few patients had been studying.

In case of negative CT or no abnormalities visible with subsequent infarction, no studies have previously been reported, we found the positive predictive value of large infarction was 0% and negative predictive value was 78% but the positive predictive value for deep infarction and partial superficial infarction were 75%and 19% respectively. So our study confirm the clinician to avoid repeating CT in cases with negative early signs in hyperacute ischemic stroke patients because the chance of developing subsequent large infarction is low but it may associated with subsequent deep infarction and partial superficial infarction. The number of cases we studied is rather small. It needs further study in future. The association between each early CT signs, times related and subsequent infarct extension could be substantiated in further studies.

In summary, CT is still the first choice in the differential diagnosis of acute stroke and when elected thrombolytic therapy, has to be given within the first 3-6 hours after the onset of symptoms. Early CT signs of ischemia are frequently present, even during the first few hours of ischemic stroke. Early CT signs may allow the prediction of further infarct size and location. We mentioned on large infarction because there are many complications of large infarction such as hemorrhagic transformation, brain edema and most severely, brain herniation. Our study confirmed that the number and types of early CT signs may also indicate and predict the types of subsequent infarction, especially large infarction. The cases with negative early CT signs may develope deep infarction with few partial superficial infarction without developing large or multiple infarction. So repeated CT in cases with negative early sign in clinically ischemic stroke may be unnecessary. Finally, the presence or absence of early CT sign have implications in the diagnosis, prognosis, choice of supplementary examination and the choice of treatment.

ACKNOWLEDGEMENTS

We thank Professor R von Kummer for his helpful advices together with some reprints and Dr.Pitchaya Tantiseranee for many good comments.

REFERENCES

1. Hanchaiphiboolkul S. Cerebral infarction in the young at Prasat Neurological Institute, The journal of Prasat Neurological Institute ; 2 : 8-15
2. Poungvarin N. Stroke in the developing world. Lancet 1998;352 : (suppl3) 19-22
3. Moulin T, Cattin F, Crepin-Leblond, et al. Early CT signs in acute middle cerebral artery infarction. Neurology, 1996; 47: 366-375.
4. Adams HP, Brott TG, Crowell RM, et al. Guidelines for the management of patients with acute ischemic stroke. A statement for healthcare professionals from a special writing group of the Stroke Council American Heart Association. Stroke 1994; 25:1901-1914.
5. Horowitz SH, Sito JL, Donnarumma R, Patel M,Alvir J. Computed tomographic–angiographic findings within the first five hours of cerebral infarction. Stroke 1991; 22: 1245-53

6. Bazzo L, Angeloni U, Bastianello S, Fantozzi LM, Pierallin A, Fieschi C. Early angiographic and CT findings in patients with hemorrhagic infarction in the distribution of the middle cerebral artery. AJNR Am J Neuroradiol 1991; 12:1115-1121.
7. Okada Y, Sadoshima S, Nakane H, Utsunomiya H. Fujishima M. Early computed tomographic findings for thrombolytic therapy in patients with acute brain embolism. Stroke 1992; 23: 20-3
8. Granstrom P. CT visualization of thrombus in cerebral artery J Comput Assist Tomogr 1986; 10: 541-2
9. Tumura N, Uemura K, Inugami A, Fujita H, Hiagno S, Shishido F. Early CT finding in acute cerebral infarction: obscuration of the lentiform nucleus. Radiology 1992; 168:463-467.
10. Truwit CL.Barkovich AJ. Gean-Martin A, Hibfi N, Normal D. Loss of the insular ribbon: another early CT sign of acute middle cerebral artery infarction. Radiology 1990; 176:801-806.
11. Damasio H. A computed tomographic guide to the idenfification of cerebral vascular territories. Arch Neurol 1983 ; 40: 138-42
12. Shuaiab A, Lee D. Pelz D et al: The impact of magnetic resonance imaging on the management of acute ischemic stroke, Neurol 1992; 42:816-18
13. Hankey GJ. Warlow CP: The role of imaging in the management of cerebral and ocular ischaemia, Neuroradiol 1990; 33: 381-90
14. Bryan RN, Lery LM. Whitlow WD et al: Diagnosis of acute cerebral infarction : comparison of CT and MR imaging, AJNR Am J Neuroradiol 1991;12:611-20
15. Hossmann KA. Viability thresholds and the prenumbra of focal ischemia. Ann Neurol 1994; 36: 557-65
16. von Kummer R, Allen KL, Hole R, et al: Usefulness of early CT finding before Thrombolytic therapy, Neuroradiol 1997; 205:327-33
17. Torack RM, Alcala H, Gado M, et al: Correlative assay of computerized crdanial tomography (CT) water content and specific gravity in normal and pathological postmoretm brain. J Neuropathol Exp Neurol 1976; 35:385-92
18. Unger E, Littlefield J, Gado M: eater content and water structure in CT and MR signal changes: possible influence in detection of early stroke. AJNR Am J Neuroradiol AJNR l9: 687-91, 1988
19. Bozzao L, Bastianello S, Fantozzi LM,et al : Correlation pf angiographic and sequential CT findings in patients with evolving cerebral infarction. AJNR Am J Neuroradiol AJNR 1989;10:1215-22
20. Barkovich AJ. Gean-Martin A, Hibfi N, Normal D. Loss of the insular ribbon: another early CT sign of acute middle cerebral artery infarction. Radiology 1990; 176:801-806.
21. Tumura N, Uemura K, Inugami A, et al: Early CT finding in cerebral infarction. Radiology 1988; 168:463 - 7
22. European Cooperative Acute Stroke Study (ECASS): Intravenous thrombolysis with recombinant tissue plasminogen activator for acute hemispheric stroke. JAMA 1995; 274:1017-59
23. Bryan RN. Levy LN. Whitelow WD, Killian JM, Preziosi TJ. Rosario JA. Diagnosis of acute cerebral infarction: comparision of CT and MR imaging. AJNR Am J Neuroradiol 1994; 2: 611-620.
24. Bastianello S, Pierallini A, Colonnese C et al. Hyperdense middle cerebral artery sign. Comparison with angiography in the acute phase of ischemic supratentorial infarction. Neuroradiology 1996; 33:207-211.

25. Wolpert SM, Bruchmann H, Greenlee R, et al. Neuroradiologic evaluation of patients with acute stroke treated with recombinant tissue plasminogen activator. AJNR Am J Neuroradiol 1993; 14:3-13.
26. von Kummer R, Meyding-Lamade U, Forsting M, et al. Sensitivity and prognostic value of early CT in occlusion of the middle cerebral artery trunk. AJNR Am J Neuroradiol 1994; 15:9-15
27. Tomsick TA, Brott T, Barsan W, et al: Thrombus localization with emergency cerebral computed tomography. AJNR Am J Neuroradiol 1992; 13:257-64
28. Bell BA, Symon L, Branston NM: CBF and time thresholds for the formation of ischemic cerebral edema, and effect of reperfusion in baboons. J Neurosurg 1985; 62: 31-41
29. Bozzao L, Angeloni U, Bastianello S, et al : Early angioghraphic and CT findings in patient with hemorrhagic infarction in the distribution of the middle cerebral artery. AJNR Am J Neuroradiol 1991; 12: 1115-21
30. Beauchanmp, N. J. Jr, Barker, P. B., Wang L, et al. Imaging of acute cerebral Ischemia. Radiology 1999; 212: 307-24
31. Marks MP. : CT in ischemic stroke. In: CT in neuroimaging revised, Neuroimaging clinics of North America 1998; 8 :515-23 infarction.
32. Culebras A, Kase CS, Masdeu JC, Fox AJ et al. Practice guidelines for the Use of Imaging in Transient Ischemic Attacks and Acute Stroke. A report of the Stroke Council, American Heart Association. Stroke. 1997; 28: 1480-1497.
33. Truwit CL.Barkovich AJ. Gean-Martin A, Hibfi N, Normal D. Loss of the insular ribbon: another early CT sign of acute middle cerebral artery infarction. Radiology 1990; 176: 801-806.
34. Lodder J. CT-detection hemorrhagic infarction: relation with the size of the infarct, and the presence of midline shift. Acta Neurol Scand 1984; 70: 328-45
35. Toni D, Fiorelli M, Bastianello S, Sacchetti ML, et al. Hemorrhagic transformation of brain infarct: Predictability in the first 5 hours from stroke onset and influence on clinical outcome. Neuroradiol 1996; 46: 341-345.
36. Elster AD, Moody DM: Early cerebral infarction, Radiology 1990; 17: 627-32
37. Bastianello S, Pierallini A, Colonnese C et al: Hyperdense middle cerebral artery CT sign. Neuroradiol 1991; 33: 207-11
38. Leys D, Pruvo JP, Godefroy O et al, Prevalence and significance of hyperdense middel cerebral artery in acute stroke, Stroke 1992; 23: 317-24
39. Rauch RA, Nazan C, Jarsson E-M, Hyperdense middle cerebral arteries as identified on CT as a false sign of vascular occlusion, AJNR Am J Neuroradiol 1993; 14: 669-74
40. Pressman BD, Tourje EJ, Thompson JR. An early CT signs of ischemic infarction: increase density in the cerebral artery AJNR Am J Neuroradiol 1987; 8:645-8
41. Tomsick T, Brott TG, Chamber AA, et al. Hyperdense middle cerebral artery sign on CT: efficacy in detecting middle cerebral artery thrombosis. AJNR Am J Neuroradiol 1990; 11:473-7
42. Launes J, Ketonen L, Dense middle cerebral artery sign: an indicator of poor outcome in middle cerebral artery area infarction. J Neurol Neurosurg Psychiatry 1987; 50:1550-2

MAGNETIC RESONANCE IMAGING OF SKIN-COVERED BACK MASSES IN CHILDREN

Pannee VISRUTARATNA[1], Punjama POOPAT[1], Jesda SINGHAVECHSAKUL[2], Kriengsak LIMPASTAN[2]

ABSTRACT

Purpose: To evaluate role of magnetic resonance imaging (MRI) in children with skin-covered back masses.

Materials and methods: MR studies of fourteen children with skin-covered back masses were compared with surgical findings, histopathological reports, or clinical history. The greatest diameters of the palpable masses were compared with the greatest diameters of the masses on MR images. MRI findings important for treatment planning were noted.

Results: The masses in five children were histologically proven; they were sacrococcygeal mature teratoma,[2] sacrococcygeal endodermal sinus tumor,[2] and Ewing sarcoma.[1] Three children with lipomyelomeningocele, three with posterior meningocele, one with lipomyelocele, and one with anterior sacral meningocele had their masses surgically confirmed. The clinical history and MRI of the mass of one child were consistent with hemangioma. In the child with an anterior sacral meningocele, the greatest diameter of the mass on MR images was three times as big as that of the palpable mass. In three children (two with endodermal sinus tumor and one with Ewing sarcoma), the greatest diameters of the masses on MR images were twice as big as those of the palpable masses. Two children with endodermal sinus tumor and one with Ewing sarcoma had intraspinal invasion; one with a mature sacrococcygeal teratoma had a retrorectal extension; and one with an anterior sacral meningocele had a connection of the mass with the spinal canal. MRI findings of a child with hemangioma obviated biopsy.

Conclusion: MRI had an important role in diagnosing these children and their treatment planning.

Key Words: Lumbosacral Region, Sacrococcygeal Region, Magnetic Resonance Imaging, Meningocele, Teratoma.

INTRODUCTION

Masses without skin over the caudal spine in children are usually myelomeningoceles, which can be diagnosed clinically without difficulty.[1] Imaging studies are rarely performed in the newborn with a myelocele or myelomeningocele.[2] However, back masses with skin cover in

[1]Department of Radiology and
[2]Department of Surgery, Faculty of Medicine, Chiang Mai University, Chiang Mai 50200, Thailand

children are difficult to diagnose clinically. In the past, correct diagnoses were made only at the time of operation.[1] Skin-covered back masses in children have included lumbosacral lipoma, teratoma, meningocele, hemangioma, and terminal myelocystocele.[1,3,4] The purpose of this study was to evaluate the role of magnetic resonance imaging (MRI) in children with skin -covered back masses.

MATERIALS AND METHODS

Between December 1998 and November 2001, fifteen children with skin-covered back masses were examined using MRI. One child was excluded from this study because she died before surgery. The children, ten girls and four boys, ranged in age from 2 days to 12 years (median, 7 months).

MR studies were performed with a 1.5-Tesla system (Signa Horizon, GE Medical Systems, Milwaukee, USA). All children underwent sagittal and axial T1-weighted imaging, and sagittal and axial fast spin-echo (FSE) T2-weighted imaging with fat suppression. Contrast-enhanced T1-weighted imaging was performed in four children (cases 3, 4, 13, and 14). The T1-weighted imaging (440-640/8-20/2-4 [TR/TE/excitations]) and FSET2-weighted imaging (2500-3200/60-150/2-4[TR/TE/excitations]) were obtained with sections 2-4 mm thick and 0-0.5 mm interslice spacing. A spine-phased array coil was used for eleven children and a head coil was used for three children.

The diagnoses from the MRI reports were compared to the surgical reports, histopathological reports, or clinical history. The greatest diameters of the palpable masses were compared with the greatest diameters of the masses on MR images. MRI findings important for treatment planning were also noted.

RESULTS

The MR diagnoses, final diagnoses, and important MRI findings are summarized in Table 1. The masses in five children were histologically proven; they were sacrococcygeal mature teratoma,[2] sacrococcygeal endodermal sinus tumor,[2] and Ewing sarcoma.[1] Three children with lipomyelomeningocele, three children with posterior meningocele, one child with lipomyelocele, and one child with anterior sacral meningocele had their masses surgically confirmed. One year and nine months after an MRI, the mass of one child was decreased in size; this child had a bluish discoloration of the skin. The clinical history and MRI of this child were consistent with hemangioma.

The greatest diameters of the palpable masses varied from 3-15 cm, average 7.8 cm. In case 2, leakage of fluid from the mass had occurred before the MRI examination. The masses of twelve children were at the midline, one mass was left of the midline (case 5), and one mass was right of the midline (case 14). In ten children the greatest diameters of the palpable masses were the same as those on MR images. In the child with an anterior sacral meningocele, the greatest diameter of the mass on MR images was three times as big as that of the palpable mass. In three children (two children with endodermal sinus tumor and one child with Ewing sarcoma), the greatest diameters of the masses on MR images were twice as big as those of the palpable masses. According to Altman's classification, two children with mature teratoma had type 1 tumors and two children with endodermal sinus tumor had type 2 tumors.[5]

The MRI diagnoses were correct in 13 patients (92.9%). In case 9, a posterior meningocele had been misdiagnosed as a lipomyelomeningocele. MRI provided information which was important in the treatment planning in five children (35.7%). Two children with endodermal

sinus tumor and one child with Ewing sarcoma had intraspinal invasion (Figs. 1 and 2), one child with mature sacrococcygeal teratoma had a retrorectal extension, and one child with an anterior sacral meningocele had a connection of the mass with the spinal canal (Fig. 3). The MRI findings in case 13 obviated biopsy of the mass, which was finally diagnosed as a hemangioma (Fig. 4).

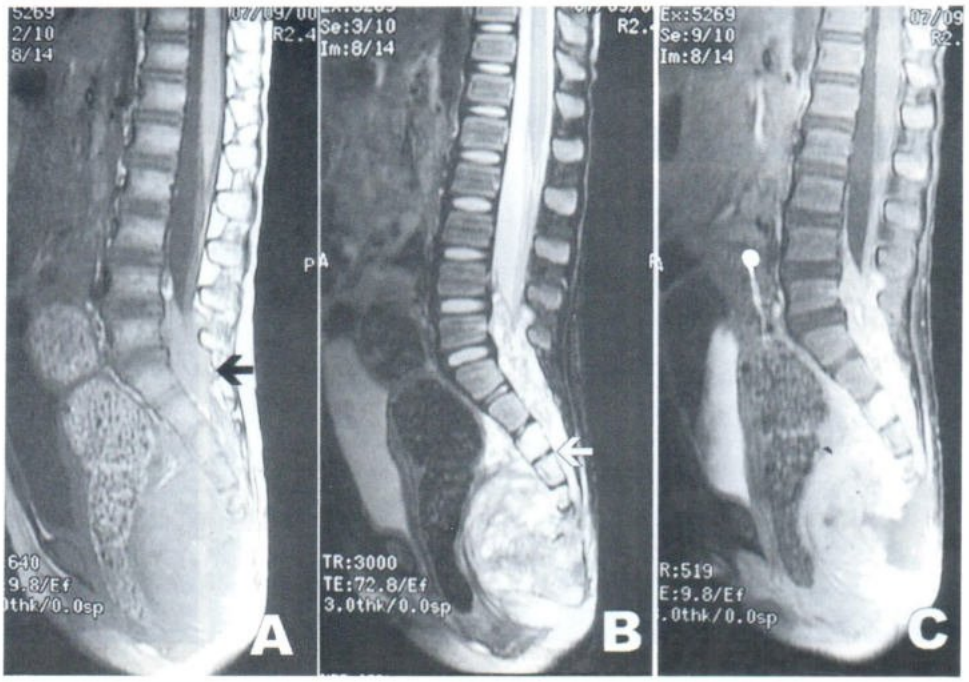

Fig. 1. Endodermal sinus tumor. Sagittal T1-weighted image (A) shows a slightly hyperintense mass compared to muscle in the retrorectal space with invasion of the spinal canal (black arrow). On sagittal FSET2-weighted image with fat suppression (B), the mass is mixed hyper- and hypointense. Abnormal hyperintensity of the S3-S5 (white arrow) and destruction of S5 and coccyx are seen. Postcontrast sagittal T1-weighted image with fat suppression (C) shows heterogeneous enhancement of the mass and abnormal enhancement of S3-5.

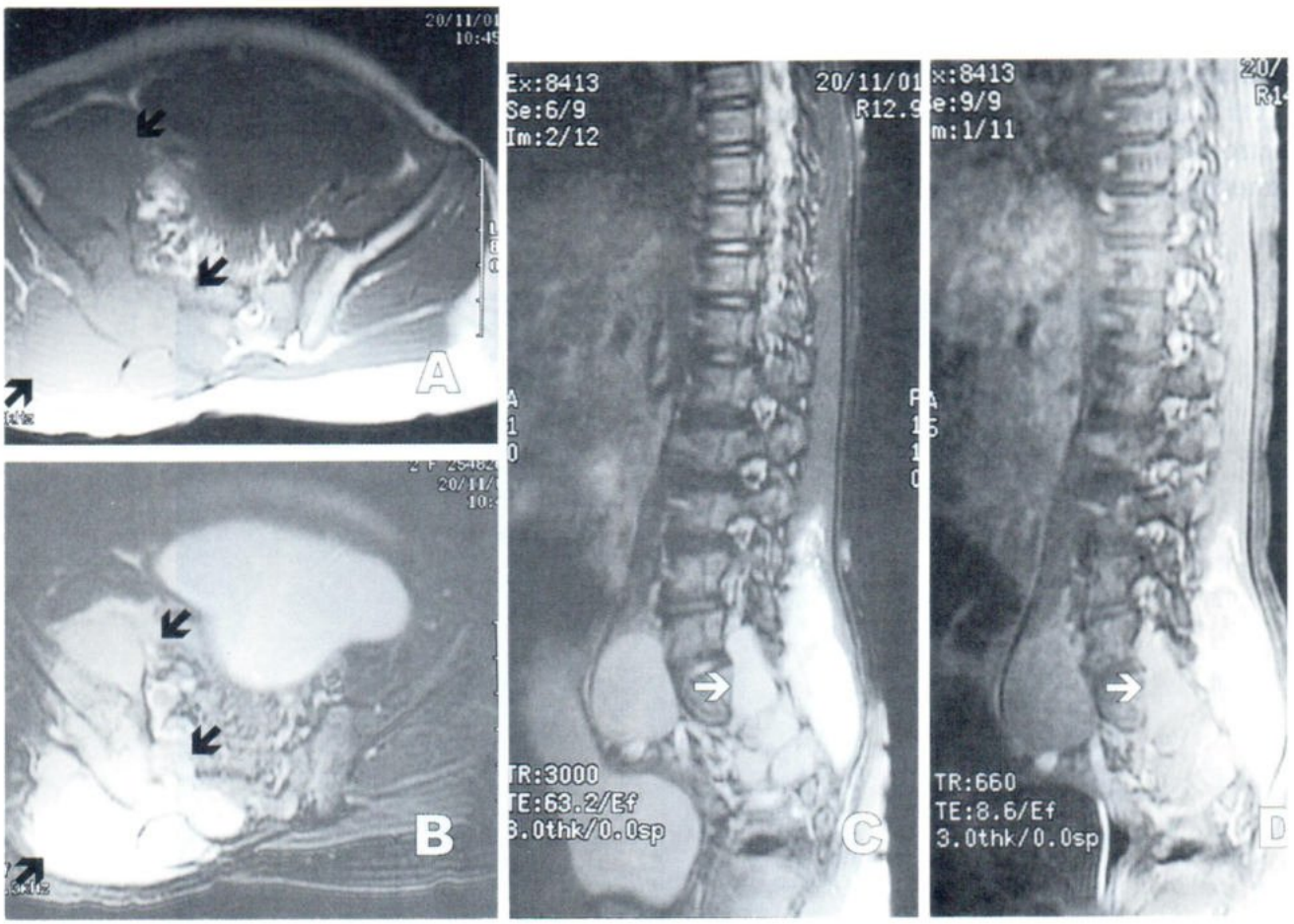

Fig. 2. Ewing sarcoma. Axial T1-weighted image (A) shows a slightly hyperintense mass (black arrows) compared to muscle surrounding the right ilium. On axial and sagittal FSET2-weighted image with fat suppression (B and C), the mass (black arrows) is hyperintense. Invasion of the right ilium, invasion of the right side of the sacrum, and invasion into the sacral foramina (white arrow) and spinal canal are seen. Postcontrast sagittal T1-weighted image with fat suppression (D) shows heterogeneous enhancement of the mass.

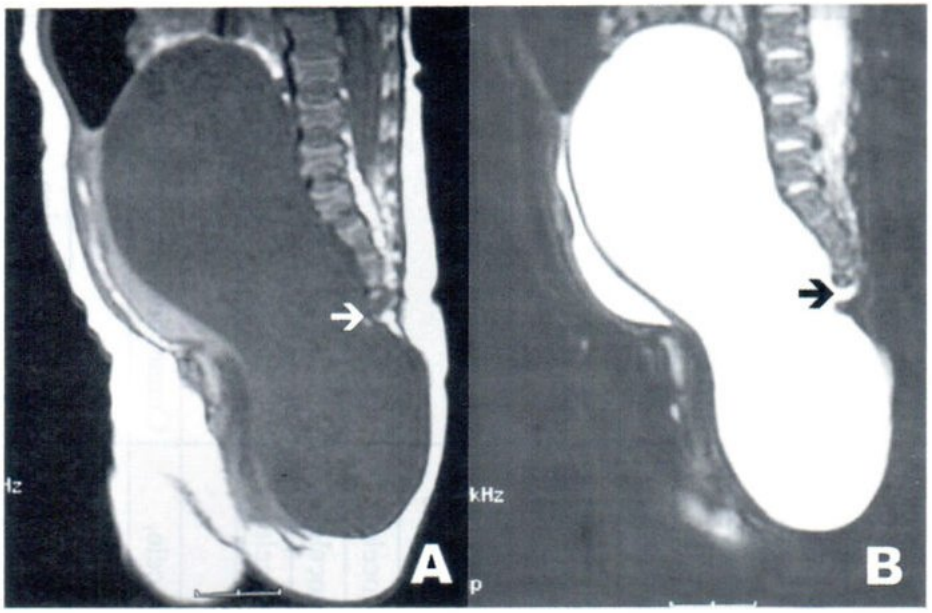

Fig. 3. Anterior sacral meningocele. Sagittal T1-weighted image (A) and sagittal FSET2-weighted image with fat suppression (B) show a large cyst in the pelvic cavity and lower abdomen. Note a small connection between the cyst and the spinal canal (arrows) and pressure erosion of the anterior aspect of the sacrum.

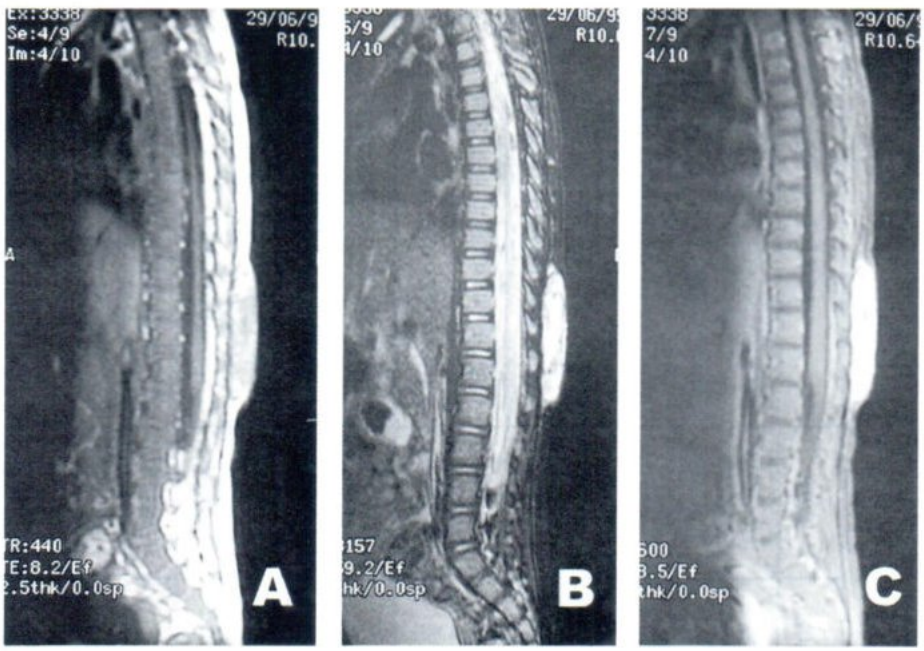

Fig. 4. Subcutaneous hemangioma. Sagittal T1-weighted image (A) shows a mass with heterogeneous intensity in the subcutaneous tissue of the back. On sagittal FSET2-weighted image with fat suppression (B), the mass is mixed hyper- and hypointense. On postcontrast sagittal T1-weighted image with fat suppression (C), the mass is markedly enhanced.

Table 1. MRI diagnoses, final diagnoses, and important MRI findings

Case No.	Sex	Age	MRI diagnosis	Final diagnosis	Important MRI findings
1	M	14 days	Benign germ cell tumor	Mature teratoma	Retrorectal extension
2	F	6 days	Benign germ cell tumor	Mature teratoma	Intraspinal invasion
3	F	3 years	Mailgnant germ cell tumor	Endodermal sinus tumor	Intraspinal invasion
4	M	2 years	Mailgnant germ cell tumor	Endodermal sinus tumor	
5	M	4 years	Lipomycelomeningocele	Lipomycelomeningocele	
6	F	2 months	Lipomycelomeningocele	Lipomycelomeningocele	
7	M	12 years	Lipomycelomeningocele	Lipomycelomeningocele	
8	F	4 days	Posterior meningocele	Posterior meningocele	
9	F	1 year	Lipomycelomeningocele	Posterior meningocele	
10	F	2 days	Posterior meningocele	Posterior meningocele	
11	M	2days	Lipomyelocele	Lipomyelocele	
12	F	1 month	Anterior meningocele	Anterior meningocele	Connection with spinal canal
13	F	1 year	Hemangioma	Hemangioma	
14	F	2years	Sarcoma	Ewing sarcoma	Intraspinal invasion

DISCUSSION

In this study the three most common skin-covered back masses in children were teratoma, lipoma (lipomyelomeningocele or lipomyelocele), and meningocele, which differs slightly from the study of Lemire et al.[1] They found that the three most common ones were teratoma, lipoma, and mixed neural lesions.

The sacrococcygeal region is the most common location for teratoma in children. CT or MRI is an excellent method for determining the extent of the sacrococcygeal teratomas;[6,7] however MRI is better for the detection of spinal canal invasion. In general, benign teratomas are more likely to be predominantly cystic and malignant teratomas are more likely to be solid.[6] Sacral destruction, invasion of surrounding structures, and metastatic disease are sign of malignancy. Extension of sacrococcygeal teratoma into the spinal canal is rare; it has been described as occurring in association with malignant or recurrent tumor.[8] The two endodermal sinus tumors in this study were solid masses and had invaded the spinal canal. Abnormal signal intensity of the bone marrow of the sacrum and destruction of sacrum were also seen in one child with endodermal sinus tumor. However, a few cases of benign sacrococcygeal teratomas with intradural extension have been reported.[8,9] It has been reported that the MRI finding in a neonate who had a benign sacrococcygeal teratoma with intradural extension was a huge heterogeneous mass with solid and fluid-filled components extending into the spinal canal.[8] This MRI finding differs from our cases.

MRI is the method of choice for imaging the pediatric spine, particularly in patients with myelopathy or suspicion of developmental malformations.[2] Two of the three most common skin-covered back masses in children in our study were developmental malformations, lipoma and meningocele. In these cases, CT can be used to study the mass, but it requires the injection of an intrathecal contrast medium. Spinal ultrasonography has been recommended as the primary imaging method in infants with suspected congenital spinal anomalies of the lower spine.[10,11] However, in case of any pathologic finding, especially if surgical intervention is considered, MR imaging should be done. This gives more anatomic details of the pathology.[10]

MRI is superior to ultrasonography in demonstrating the entire spinal canal, the extent of the lesions, and their anatomic relationship to surrounding structures.[10] In this study MRI provided information which was important in the treatment planning in five children. MRI also made diagnosis possible, which obviated biopsy of the mass in one child with hemangioma.

The limitation of this study is that it is retrospective. The MRI diagnoses were made by single reader before surgery. However, this study confirms the role of MRI in the evaluation of children with skin-covered back masses.

REFERENCES

1. Lemire RJ, Graham CB, Beckwith JB. Skin-covered sacrococcygeal masses in infants and children. J Pediatr 1971;79: 948-54.
2. Barkovich AJ. Pediatric neuroimaging. 3rd ed. Philadelphia: Lippincott Williams & Wilkins, 2000.
3. Byrd SE, Darling CF, McLone DG. Developmental disorders of the pediatric spine. Radiol Clin North Am. 1991;29: 711-52.
4. Byrd SE, Harvey C, Darling CF. MR of terminal myelocystoceles. Eur J Radiol 1995;20:215-20.

5. Altman RP, Randolph JG, Lilly JR. Sacrococcygeal teratoma: American Academy of Pediatrics Surgical Section Survey-1973. J Pediatr Surg 1974; 9:389-98.
6. Keslar PJ, Buck JL, Suarez ES. Germ cell tumors of the sacrococcygeal region: radiologic-pathologic correlation. Radiographics 1994 ;14:607-20.
7. Feldman M, Byrne P, Johnson MA, Fischer J, Lees G. Neonatal sacrococcygeal teratoma: multiimaging modality assessment. J Pediatr Surg 1990;25:675-8.
8. Ribeiro PR, Guys JM, Lena G. Sacrococcygeal teratoma with an intradural and extramedullary extension in a neonate: case report. Neurosurgery 1999;44:398-400.
9. Powell RW, Weber ED, Manci EA. Intradural extension of a sacrococcygeal teratoma. J Pediatr Surg 1993;28:770-2.
10. Rohrschneider WK, Frosting M, Darge K, Tr?ger J. Diagnostic value of spinal US: comparative study with MR imaging in pediatric patients. Radiology 1996; 200: 383-8.
11. Unsinn KM, Geley T, Freund MC, Gassner I. US of the spinal cord in newborns: spectrum of normal findings, variants, congenital anomalies, and acquired diseases. Radiographics 2000;20:923-38.

DISCORDANCE IN THE DIAGNOSIS OF OSTEOPOROSIS DUE TO PEAK BONE MINERAL DENSITY FROM DIFFERENT REFERENCES: JAPANESE AND NORTHEASTERN THAI WOMEN

Charoonsak SOMBOONPORN, M.D.[1], Woraluk SOMBOONPORN, M.D.[2], Sukree SOONTRAPA, M.D.[2], Suppasin SOONTRAPA, M.D.[3]

ABSTRACT

According to the WHO guideline in the diagnosis of osteoporosis, use of inappropriate reference can result in the inappropriate bone mineral classification. This study aimed to explore the difference between the prevalence of abnormally low bone mass diagnosed by using the Japanese and the northeastern Thai reference. The subjects were retrospectively recruited from women, aged 20-90 years, residing in the northeast Thailand who underwent bone mineral density (BMD) measurement at the lumbar spines and proximal femur from May 1998 to August 2000 at Srinagarind Hospital. Concordant and discordant rate in the interpretation between both criteria were reported. There were 653 subjects with 779 studies included. Higher prevalence of osteopenia and osteoporosis was observed by using T-score of the northeastern Thai population, compared with that diagnosed by the Japanese reference at almost all sites except Ward's triangle. Concordant diagnoses were found in 73.6% of all sites. Significant diagnostic agreement between both criteria was noted at all sites (Kappa = 0.18-0.80, $p < 0.001$). Although resulting in some discordant classification, using the northeastern Thai reference classified the same BMD status in almost three-fourths of all sites. This study stressed the limitation of the WHO diagnostic guideline regarding the effect of different reference range used.

INTRODUCTION

It has been widely recognized that a low peak bone mass in adults is a significant risk factor for osteoporotic fractures later in life.[1-3] Various factors influence the level of peak bone mass including genetic and environmental factors such as calcium intake, exercise and smoking.[4-7]

The World Health Organization (WHO) proposed diagnostic categories to define normal, osteopenic and osteoporotic individuals accord-

[1] Department of Radiology,
[2] Department of Obstetrics and Gynecology,
[3] Department of Orthopaedics, Faculty of Medicine, Khon Kaen University, Khon Kaen 40002, Thailand

For correspondence:
Assistant Professor Charoonsak Somboonporn, M.D.
Nuclear Medicine Division, Department of Radiology, Faculty of Medicine, Khon Kaen University, Khon Kaen 40002, Thailand
E-mail address: chasom@kku.ac.th

This study was presented at the 39th Annual Scientific Meeting of the Royal College of Radiologists of Thailand and the Radiological Society of Thailand, 27-29 March 2002.

ing to the standard deviation (SD) in bone mineral density (BMD) measured by dual-energy X-ray absorptiometry (DEXA) below the average value in the normal young adults as the reference, or T-score.[8] Although the BMD is peak at the young adult age, the age at which peak bone mass is attained has continued to be debated and estimates range widely in cross-sectional investigations from late adolescence [9-10] and the third decade,[11] into the fourth decade of life [12] and beyond.[13] These certainly affect the reference T-score and also have an impact on the diagnosis of low bone mass or osteoporosis.[14-15] Accordingly, to obtain an appropriate T-score for BMD interpretation, the local reference BMD database should be carried out to provide the appropriate BMD cut-off level for the diagnosis of osteopenia or osteoporosis in that specific group of population. Our group had studied the BMD at the lumbar spines and proximal femur in the normal northeastern Thai women and reported the BMD cut-off value for the diagnosis of osteopenia and osteoporosis for this group of population.[16] However, in the routine service, we have used the T-score from the Japanese reference database, an Asian ethnicity close to Thai, provided by manufacturer's software of our bone densitometer. This can give different diagnostic results from using the northeastern Thai reference database.

We therefore conducted this study to explore the difference between the prevalence of osteopenia and osteoporosis diagnosed by using the Japanese and the northeastern Thai reference range applied to the northeastern Thai women. This study was approved by the Ethics Committee, Faculty of Medicine, Khon Kaen University.

MATERIALS AND METHODS

SUBJECTS

Retrospective review of the medical records and results of BMD measurement of subjects performed at the Division of Nuclear Medicine, Department of Radiology, Srinagarind Hospital, Faculty of Medicine, Khon Kaen University from May 1998 to August 2000 was conducted. The inclusion criteria were women, aged 20-90 years, undertaking the BMD study both at the lumbar spines and proximal femur at the same time. The exclusion criteria were those who had the history of fracture and who did not reside in the northeast Thailand.

BMD MEASUREMENT

BMD values (g/cm^2) at the lumbar spines (L_{2-4}) and non-dominant proximal femur including femoral neck, Ward's triangle, trochanteric region and total proximal part were measured using DEXA technique of EXPERT-XL bone densitometer of Lunar Corp., USA, by the standardized well-trained technician. Quality control of the instrument was undertaken daily, using the standard phantom with automatic software program by technicians under the supervision of an experienced nuclear medicine physician. The precision error of BMD measurement at all sites was less than 1.5% measured on phantom.

BMD INTERPRETATION

Both the Japanese and northeastern Thai criteria were used in the interpretation of a measured BMD in each subject. A T-score acquired from the normal Japanese reference was calculated by the manufacturer's software on the process of data analysis of each measurement and was then interpreted as normal bone mineral status, osteopenia or osteoporosis according to the WHO guideline.

In the interpretation of BMD by using the northeastern Thai reference, the BMD cut-off values previously reported by our group were used.[16] From that study, we prospectively recruited

350 subjects aged 20-70 years from the Obstetrics and Gynecology Out-patient Clinic, Srinagarind Hospital, Faculty of Medicine, Khon Kaen University from May 1998 to August 2000. The inclusion criteria were healthy women residing in the provinces of northeastern part of Thailand who had body mass index (BMI) in the range of 19-25 kg/m^2. The exclusion criteria were pregnancy, smoking, alcohol drinking, chronic back pain or other skeletal diseases, having prior ovarian surgery, having concurrent diseases such as hyperthyroidism, chronic illnesses, history of hospitalization for more than 2 weeks, taking medications affecting BMD such as corticosteroid, hormonal contraception, calcium, vitamin D, diuretics, anti-convulsant, and having prior radioisotope or radiocontrast study within a week before the BMD study. All subjects were measured for BMD at the antero-posterior lumbar spines and non-dominant proximal femur by the same machine used in the present study. The group of peak bone mass of each skeletal site was identified and the mean BMD with SD of this group were used to define the BMD cut-off level for determining the bone mineral status of that site. According to the WHO criteria, the individuals were classified into three categories with respect to their BMD status as follows: normal (T-score $\geq$ -1), osteopenic (-2.5 < T-score < -1), osteoporotic (T-score $\leq$ -2.5). Accordingly, it was found that osteopenia of the L_{2-4} spines, femoral neck, Ward's triangle, trochanteric region and total proximal femur was diagnosed when the BMD was lower than 1.091, 0.854, 0.734, 0.728 and 0.935 g/cm^2 respectively, whereas BMD of equal or lower than 0.889, 0.678, 0.483, 0.594 and 0.785 g/cm^2 was used for the diagnosis of osteoporosis of these sites respectively. These BMD thresholds were used for the diagnostic classification by the northeastern Thai reference range in the present study.

STATISTICAL ANALYSIS

The recorded data included age, weight, height, BMI, BMD of the antero-posterior lumbar spines (L_{2-4}), femoral neck, Ward's triangle, trochanteric region, total proximal part of the non-dominant femur and its interpretation by the criteria of both reference ranges.

The continuous data were expressed as mean $\pm$ SD. Concordance and discordance in the diagnosis of normal bone mineral status, osteopenia or osteoporosis using the two criteria were presented as the percentage. Statistical test for agreement of the classification was performed by Kappa analysis. P-value less than 0.05 was considered significant.

RESULTS

Of all subjects referred for BMD measurement during the study period, 653 cases meeting our criteria were studied. From all 653 cases, most subjects were studied once, whereas 88 were studied for 2 times and 19 were studied for 3 times resulting in total 779 studies enrolled for analysis. Four hundred and sixty-nine studies (60.2%) were performed in women who were sent from the Menopause Clinic, Srinagarind Hospital, for baseline BMD measurement, to find evidence of low bone mass or osteoporosis, or to follow up BMD after a period of hormone replacement therapy, whereas 310 studies (39.8%) were performed in those sent from various other units in order to find the evidence of osteopenia or osteoporosis.

Baseline characteristics and BMD values of the subjects were shown in Table 1. By using T-score criteria from the two references, the prevalence of osteopenia and osteoporosis in each skeletal site was demonstrated (Table 2). Higher prevalence of both osteopenia and osteoporosis was observed by using T-score reference range of

the northeastern Thai population, compared with those diagnosed by the Japanese reference range at almost all sites of the skeleton measured except lower prevalence of osteoporosis at the Ward's triangle diagnosed by the northeastern Thai reference.

Concordant diagnoses-normal, osteopenic or osteoporotic-between criteria from the two references were observed in about three-fourths of all skeletal sites (73.6%), while the diagnoses of the remaining about one-fourth (26.4%) were found to be discordant (Table 3). Ward's triangle was the skeletal site that had the highest percentage of concordant diagnoses (88.1%). Significant agreement in the diagnosis between the two reference criteria was noted at all skeletal sites with the Kappa values ranging from 0.18 to 0.80 (p-value < 0.001).

Regarding the discordant diagnoses, it was noted that of all 1,030 discordant interpretations, mostly at the total proximal femoral part, shown in Table 3, only 4 out of 937 skeletal sites at the non-Ward's region-L_{2-4}, femoral neck, trochanteric region and total proximal femur-were more severe when diagnosed by the northeastern Thai criterion compared with those diagnosed by the Japanese criterion. On the contrary, all 93 discordant interpretations at the Ward's region were found to be more severe when diagnosed by the Japanese criterion compared with those diagnosed by the northeastern Thai criterion.

Table 1. Baseline characteristics and BMD values of the subjects.

Characteristic	Value
Age (year)	
mean ± SD	51.9 ± 8.7
range	21 - 88
Weight (kg)	
mean ± SD	57.1 ± 8.4
range	33 - 85
Height (cm)	
mean ± SD	154.9 ± 5.6
range	133 - 175
BMI (kg/m^2)	
mean ± SD	23.8 ± 3.3
range	15.4 - 38.3
BMI (g/cm^2)	
mean ± SD	
L_{2-4}	1.062 ± 0.169
Femoral neck	0.874 ± 0.135
Ward's triangle	0.721 ± 0.153
Trochanter	0.750 ± 0.122
Total proximal femur	0.946 ± 0.133

Table 2. Comparison between the prevalence of osteopenia and osteoporosis in each skeletal site diagnosed by using criteria from the Japanese and the northeast Thai database (N=779 studies).

Skeletal site	Prevalence			
	Osteopenia		Osteoporosis	
	Japanese	Northeastern Thai	Japanese	Northeastern Thai
L_{2-4}	220 (28.2%)	310 (39.8%)	61 (7.8%)	117 (15.0%)
Femoral neck	174 (22.3%)	269 (34.5%)	24 (3.1%)	59 (7.6%)
Ward's triangle	340 (43.6%)	383 (49.2%)	109 (14.0%)	41 (5.3%)
Trochanter	112 (14.4%)	255 (32.7%)	16 (2.1%)	68 (8.7%)
Total proximal femur	101 (13.0%)	279 (35.8%)	15 (1.9%)	84 (10.8%)

Table 3. Comparison of the BMD interpretation classified as concordant or discordant diagnosis between the two reference criteria at each skeletal site.

Skeletal site	Concordance		Discordance
	Number (%)	Kappa[a]	Number (%)
L_{2-4}	575 (73.8%)	0.55	204 (26.2%)
Femoral neck	610 (78.3%)	0.56	169 (21.7%)
Ward's triangle	686 (88.1%)	0.80	93 (11.9%)
Trochanter	532 (68.3%)	0.31	247 (31.7%)
Total proximal femur	462 (59.3%)	0.18	317 (40.7%)
Total	2,865 (73.6%)	-	1,030 (26.4%)

DISCUSSION

According to the WHO diagnostic guideline, T-score values of < -1 and ≤ -2.5 are used to classify a subject's skeletal status at each site as osteopenia or osteoporosis respectively. Although has been widely accepted, this guideline remains have several problems regarding the optimal site for assessment, thresholds for diagnosis in men and the diagnostic inaccuracies at different sites.[17] Several studies from USA,[18] European[19-22] and Asian countries[23] have been conducted to establish the reference BMD values at different skeletal sites for their own population to aid correct diagnosis of osteoporosis, to screen individuals at the higher risk of fractures and to make international or interracial comparisons of bone mass.

Although the local Thai BMD reference ranges are now available, many institutes in Thailand still use their manufacturer's reference criteria, especially from Japanese or Korean population, in the interpretation of BMD results since they are recognized as the database from the Asian races close to that of Thai. This may, in part, be due to some limitations such as different bone densitometer instruments used among the institutes. The mean absolute difference in L_1-L_3 BMD between Hologic and Lunar devices might be up to 18.5%.[24] If this is the case, a cross-calibration for BMD values from one instrument to another is crucial and has to be performed before applying reference database from one instrument to another.[25-26]

Applying T-score from the two reference criteria studied by Lunar bone densitometer to our study population yielded higher prevalence of osteopenia and osteoporosis diagnosed by the northeastern Thai reference criterion at L_{2-4}, femoral neck, trochanteric region and total proximal femur. This could be attributable to the difference in the BMD cut-off levels between the two reference ranges. Although the BMD cut-off values from the Japanese reference range in our study could not be exactly defined, we could calculate them approximately by determining the average BMD values that corresponded to the T-score of -1 for the cut-off level of osteopenia and -2.5 for the cut-off level of osteoporosis in our study population. By this method, it was found that the BMD cut-off levels of the Japanese reference range for osteopenia at L_{2-4}, femoral neck, trochanteric region and total proximal femur were 1.012, 0.799, 0.642 and 0.825 g/cm^2 respectively whereas those for osteoporosis were 0.831, 0.626, 0.516 and 0.625 g/cm^2 respectively. These cut-off levels were clearly lower than those of the northeastern Thai reference range. On the contrary, we found by the same way that the higher prevalence of osteoporosis at Ward's triangle diagnosed by the Japanese reference criteria was due to the higher BMD cut-off level than that of the northeastern Thai (0.561 versus 0.483 g/cm^2).

In choosing a cut-off value of -2.5 SD, the intention of the WHO group was to make osteoporosis a rarity in healthy women before menopause. Assuming a normal distribution of BMD, about 0.7% of the young adult population would be characterized as having osteoporosis.[17] Some problems have been found in applying these concepts in practice. The normal young adults used to calculate mean BMD and SD values may or may not include population that are randomly selected, giving bias results. Moreover, the reference data may exclude individuals with risk factors for osteoporosis and, therefore, artificially increase the mean BMD value and reduce the SD used to compute the cut-off values. Therefore, the choice of a reference range is important for an accurate bone mineral categorization of subjects. This is clearly supported by the study of Chen et al., which showed a reduction of about 40% prevalence of osteoporosis at the spines and/or the total hip when the old Hologic normal reference was replaced by the new Hologic hip normal reference.[27]

In determining the agreement in the diagnosis between the two reference criteria of our study, concordant diagnoses were found in about three-fourths of the subjects with the high strength of agreement at Ward's triangle (Kappa 0.80), moderate strength at L_{2-4} (Kappa 0.55) and femoral neck (Kappa 0.56), fair strength at the trochanteric region (Kappa 0.31) and poor strength at the total proximal femoral part (Kappa 0.18). However, discordant diagnoses were found in about one-fourth of our BMD studies especially at the total proximal femur and, therefore, could have an influence on the decision in giving management of patients. This was evident by the recent study of Pressman et al., which showed that the result of BMD test showing evidence of osteoporosis had a higher influence on the

initiation of osteoporosis treatment than other factors including age or gender of the patients, history of recent fracture, history of corticosteroid exposure, or even the specialty of health care practitioners taking care of patients.[28]

To our knowledge, this is the first study reporting the magnitude of difference in the diagnostic classification between using the manufacturer' s and local references applied in the northeastern Thai women so far.

The study, however, had some limitations. The northeastern Thai reference range applied in this study was derived from the peak bone mass of 5-year age band of 35 normal northeastern Thai women. This number of sample size in determining the average peak bone mass and also the SD might be too small to represent the actual peak bone mass in the general population. Moreover, the exclusion criteria used to extract our normal database were selected because they are widely quoted as risk factors for osteoporotic fracture rather than because of their inherent validity, and may have led to a bias in our northeastern Thai reference population. Applying this reference, even being the same race and ethnicity of the observed population, to the northeastern women might over-diagnose abnormally low bone mass and, therefore, cause over-treatment in these subjects. Furthermore, it should also be stressed that the data presented in our study dealt with the hospital-based subjects. Extrapolation of these findings to the community-based subjects must be viewed with caution.

In conclusion, this study reported the discordance in the diagnosis of low bone mass in the northeastern Thai women between using the peak BMD range from the Japanese reference and the northeastern Thai reference and stressed the limitation of the WHO diagnostic guideline regarding potentially varying diagnostic classifications of the BMD status in the same individual.

REFERENCES

1. Hui SL, Slemenda CW, Johnston CC Jr. The contribution of bone loss to postmenopausal osteoporosis. Osteoporos Int 1990; 1: 30-4.
2. Matkovic V. Calcium and peak bone mass. J Intern Med 1992; 231: 151-60.
3. Newton-John HF, Morgan DB. The loss of bone with age, osteoporosis, fractures. Clin Orthop 1970; 71: 229-52.
4. Pollitzer WS, Anderson JJ. Ethnic and genetic differences in bone mass: a review with a hereditary vs environmental perspective. Am J Clin Nutr 1989; 1244-59.
5. Johnston CC Jr, Miller JZ, Slemenda CW, et al. Calcium supplementation and increases in bone mineral density in children. N Engl J Med 1992; 327: 82-7.
6. Valimaki MJ, Karkkainen M, Lamberg-Allardt C, et al. Exercise, smoking and calcium intake during adolescence and early adulthood as determinants of peak bone mass. Cardiovascular Risk in Young Finns Study Group. BMJ 1994; 309: 230-5.
7. Welten DC, Kemper HC, Post GB, et al. Weight-bearing activity during youth is a more important factor for peak bone mass than calcium intake. J Bone Miner Res 1994; 9: 1089-96.
8. Kanis JA. Assessment of fracture risk and its application to screening for postmenopausal osteoporosis: synopsis of a WHO report. WHO Study Group. Osteoporos Int 1994; 4: 368-81.
9. Theintz G, Buchs B, Rizzoli R, et al. Longitudinal monitoring of bone mass accumulation in healthy adolescents: evidence for a marked reduction after 16 years of age at the levels of lumbar spine and femoral neck in female subjects. J Clin Endocrinol Metab 1992; 75: 1060-5.
10. Lu PW, Briody JN, Ogle GD, et al. Bone mineral density of total body, spine, and femoral neck in children and young adults: a cross-sectional and longitudinal study. J Bone Miner Res 1994; 9: 1451-8.

11. Teegarden D, Proulx WR, Martin BR, et al. Peak bone mass in young women. J Bone Miner Res 1995; 10: 711-5.
12. Rodin A, Murby B, Smith MA, et al. Premenopausal bone loss in the lumbar spine and neck of femur: a study of 225 Caucasian women. Bone 1990; 11: 1-5.
13. Arlot ME, Sornay-Rendu E, Garnero P, Vey-Marty B, Delmas PD. Apparent pre- and postmenopausal bone loss evaluated by DXA at different skeletal sites in women: the OFELY cohort. J Bone Miner Res 1997; 12: 683-90.
14. Ahmed AI, Blake GM, Rymer JM, Fogelman I. Screening for osteopenia and osteoporosis: do the accepted normal ranges lead to overdiagnosis? Osteoporosis Int 1997; 7: 432-8.
15. Melton LJ III. The prevalence of osteoporosis. J Bone Miner Res 1997; 12: 1769-71.
16. Somboonporn W, Somboonporn C, Soontrapa S, Lumbiganon P. Bone mineral density of lumbar spines and proximal femur in the normal Northeastern Thai women. J Med Assoc Thai 2001; 84 (Suppl 2): S593-98.
17. Kanis JA, Gluer CC. An update on the diagnosis and assessment of osteoporosis with densitometry. Committee of Scientific Advisors, International Osteoporosis Foundation. Osteoporos Int 2000; 11: 192-202.
18. Looker AC, Wahner HW, Dunn WL, et al. Updated data on proximal femur bone mineral levels of US adults. Osteoporos Int 1998; 8: 468-89.
19. Ryan PJ, Spector TP, Blake GM, Doyle DV, Fogelman I. A comparison of reference bone mineral density measurements derived from two sources: referred and population based. Br J Radiol 1993; 66: 1138-41.
20. Lehmann R, Wapniarz M, Randerath O, et al. Dual-energy X-ray absorptiometry at the lumbar spine in German men and women: a cross-sectional study. Cacif Tissue Int 1995; 56: 350-4.
21. Smeets-Goevaers CG, Lesusink GL, Papapoulos SE, et al. The prevalence of low bone mineral density in Dutch perimenopausal women: the Eindhoven perimenopausal osteoporosis study. Osteoporos Int 1998; 8: 404-9.
22. Shipman AJ, Guy GW, Smith I, Ostlere S, Greer W, Smith R. Vertebral bone mineral density, content and area in 8789 normal women aged 33-73 years who have never had hormone replacement therapy. Osteoporos Int 1999; 9: 420-6.
23. Iki M, Kagamimori S, Kagawa Y, Matsuzaki T, Yoneshima H, Marumo F. Bone mineral density of the spine, hip and distal forearm in representative samples of the Japanese female population: Japanese Population-Based Osteoporosis (JPOS) Study. Osteoporos Int 2001; 12: 529-37.
24. Kolta S, Ravaud P, Fechtenbaum J, Dougados M, Roux C. Accuracy and precision of 62 bone densitometers using a European Spine Phantom. Osteoporos Int 1999; 10: 14-9.
25. Genant HK, Grampp S, Gluer CC, et al. Universal standardization for dual x-ray absorptiometry: patient and phantom cross-calibration results. J Bone Miner Res 1994; 9: 1503-14.
26. Kalender WA, Felsenberg D, Genant HK, Fischer M, Dequeker J, Reeve J. The European Spine Phantom—a tool for standardization and quality control in spinal bone mineral measurements by DXA and QCT. Eur J Radiol 1995; 20: 83-92.
27. Chen Z, Maricic M, Lund P, Tesser J, Gluck O. How the new Hologic hip normal reference values affect the densitometric diagnosis of osteoporosis. Osteoporos Int 1998; 8: 423-7.
28. Pressman A, Forsyth B, Ettinger B, Tosteson AN. Initiation of osteoporosis treatment after bone mineral density testing. Osteoporos Int 2001; 12: 337-42.

RAPID TURNOVER PATTERN OF RADIOIODINE UPTAKE IN GRAVES' DISEASE: CLINICAL CORRELATION AND THERAPY OUTCOME

Charoonsak SOMBOONPORN, M.D.,
Krisana ROYSRI, M.D.

ABSTRACT

The retrospective study was designed to explore the prevalence of rapid turnover pattern (RTP) of radioiodine (^{131}I) uptake in the patient with Graves' disease, to find the possible clinical factors associated with this kind of uptake pattern and to compare the successful rate of ^{131}I treatment between RTP and non-rapid turnover pattern (NRTP). The subjects were Graves' disease patients referred for the first ^{131}I therapy. The 3-hour uptake value > 24-hour uptake value was classified as RTP, whereas 3-hour value < 24-hour value was classified as NRTP. Of all 938 study subjects, 252 cases (26.9%) had RTP. The successful rate of RTP group was significantly lower than that of NRTP group (17.1% versus 42.7%, $p < 0.001$). In univariate analyses, significant associations were found between the RTP and age ($p = 0.021$), prior >24-month antithyroid drug treatment ($p = 0.011$), thyroid gland size, 3-hour and 24-hour uptake values ($p < 0.001$). However, multiple logistic regression analyses showed only 3- and 24-hour uptake values were the independent predictors of RTP ($p < 0.001$). RTP, even found in only about one-fourth of Graves' disease patients, affects the outcome of ^{131}I treatment. No clinical history is reliable to predict the possibility of RTP, except the 3- and 24-hour uptake values.

INTRODUCTION

It has been accepted that treatment of Graves' hyperthyroidism by ^{131}I is a convenient, safe and rather inexpensive method and can effectively control hyperthyroidism with a single dose.[1] A variety of factors have been reported to affect the success of ^{131}I therapy including size of thyroid gland, homogeneity of radioiodine uptake in the thyroid gland, pretreatment with antithyroid drug (ATD) and ^{131}I administered dose regimen.[1-4] The radiation dose to the thyroid gland depends on the amount of administered ^{131}I per gram of thyroid gland weight and the duration of ^{131}I retaining in the gland. About 15% of Graves' disease patients was reported to have the unusual radioiodine uptake called the rapid turnover pattern in which the radioiodine was discharged more rapidly from the gland than usual.[5-7] Radiation dose to the thyroid in this uptake pattern, therefore, is lower than expected resulting in a higher incidence of treatment failure. Moreover, an in-

Nuclear Medicine Division, Department of Radiology, Faculty of Medicine,Khon Kaen University, Khon Kaen 40002, Thailand

For correspondence:
Assistant Professor Charoonsak Somboonporn, M.D.
Nuclear Medicine Division, Department of Radiology, Faculty of Medicine, Khon Kaen University, Khon Kaen 40002, Thailand
E-mail address: chasom@kku.ac.th

This study was presented at the 39th Annual Scientific Meeting of the Royal College of Radiologists of Thailand and the Radiological Society of Thailand, 27-29 March 2002.

creased total body radiation is acquired from the release of protein-bound ^{131}I into the blood circulation.[6]

An easy and practical method in measuring the retaining time of radioiodine in the thyroid gland was the measurement of an early to late radioiodine thyroid uptake ratio proposed by Aktay et al.[5] Generally in Graves' disease, the early uptake value at 3 or 4 hours after oral ^{131}I administration should be lower than the late uptake value at 24 hours or determined as the uptake ratio less than 1. In the patient with rapid turnover pattern of uptake, the uptake ratio was equal or more than 1. The study of Aktay et al. found that besides male gender, prior ATD treatment and non-Graves' hyperthyroidism, the high early uptake value and high uptake ratio were other two additional factors associated with the unfavorable outcome of ^{131}I therapy in hyperthyroid patients, whereas size of thyroid gland, late uptake value and amount of radioiodine dose per gram of thyroid tissue were not significantly associated with the outcome. We thus would like to find the prevalence of Graves' disease with rapid turnover pattern of radioiodine uptake and compare the successful rate of ^{131}I therapy in both rapid and non-rapid turnover uptake groups. Any possible associated clinical factors to predict the rapid turnover uptake pattern was also explored.

MATERIALS AND METHODS

SUBJECTS

We retrospectively studied medical records of consecutive Graves' disease patients residing in the northeast Thailand and referred for the first ^{131}I treatment at the Division of Nuclear Medicine, Department of Radiology, Srinagarind Hospital, Faculty of Medicine, Khon Kaen University from June 1994 to August 2000. Clinical diagnosis of Graves' disease, later confirmed by the nuclear medicine physician, was determined by referring physicians and was supported by the elevation of serum thyroxine and/or serum triiodothyronine, with or without serum thyroid stimulating hormone. The exclusion criteria were patients who had history of ^{131}I therapy or had any type of thyroid surgery and received lithium administration before or after ^{131}I uptake and treatment. Data regarding age at the time of ^{131}I treatment, gender, indication for ^{131}I treatment, weight of thyroid gland estimated by palpation, date of ^{131}I treatment, result of ^{131}I thyroid uptake test, date of established euthyroidism and permanent hypothyroidism following ^{131}I therapy and date of the last follow-up were recorded. The last evaluation was at the end of July 2001. This study was approved by the Ethics Committee of the Faculty of Medicine, Khon Kaen University.

^{131}I THYROID UPTAKE TEST AND ^{131}I TREATMENT

In performing radioiodine thyroid uptake test, contraindications of ^{131}I treatment, women during pregnancy and breast-feeding, were firstly excluded before for the test. ATD, if taken, was discontinued at least 7 days before the study. Other drugs and foods known to affect iodine uptake by the thyroid gland were refrained for their appropriate periods of time. At least 4-hour fasting before ^{131}I administration was recommended in all subjects to make sure that radioiodine could be properly absorbed by gastrointestinal tract.

Radioactivity of 20 microCuries (?Ci) of the standard ^{131}I solution, supplied by the Office of Atomic Energy for Peace, Bangkok, Thailand was counted before and after ingestion by the patient, and then radioactivity at 10-cm distance from the patient's neck extended by a pillow under the shoulders was measured at 3 and 24 hours later. Background radioactivity was corrected by measuring radioactivity at 10-cm distance from patient's thigh at the level of 10-cm

above the knee. Time-decay correction was also computed. All radioactivity measurements were performed by the external counter probe system of the Elscint Company, model DTR-4A. Thyroid uptake value was calculated according to the following equation:

$$\% \text{ uptake of } {}^{131}\text{I by the thyroid} = \frac{\text{neck counts - background counts}}{\text{standard counts - background counts}} \times 100$$

In determining the ^{131}I dose for individual patients, 24-hour thyroid uptake value and weight of thyroid gland were used for calculation to achieve 100 ?Ci of ^{131}I per gram of thyroid tissue. A few patients with history of cardiac failure or cardiac arrhythmia were treated with a higher dose regimen of 150 ?Ci per gram. There were two nuclear medicine physicians involving in the ^{131}I treatment during the study period.

ATD and/or beta-blocker were prescribed as needed after ^{131}I treatment to the individual case according to the justification of physician. Although there was no exact follow-up schedule after ^{131}I treatment, each follow-up time was usually between 3 months and one year, mostly according to the severity of hyperthyroidism. Retreatment with ^{131}I was considered in persistent hyperthyroid cases in no shorter than 3 months after the previous dose.

CLASSIFICATION OF THE UPTAKE PATTERN AND THE SUCCESS OF ^{131}I TREATMENT

The rapid turnover pattern of uptake was indirectly classified when the 24-hour uptake value was equal or less than the 3-hour uptake value, otherwise classified as the non-rapid turnover uptake pattern.

In determining the success of ^{131}I therapy, the subjects were classified into one of the three outcomes including success, failure or undetermined. The success was considered at 6 months after treatment with patients having no symptoms and signs of hyperthyroidism even not taking ATD. The failure was defined as the patients still had symptoms and signs of hyperthyroidism at least 6 months after treatment or retreatment with ^{131}I was administered. The undetermined outcome was defined if the follow-up time was less than 6 months and the subjects were not retreated during this time.

DATA HANDLING AND STATISTICAL ANALYSIS

For descriptive analysis of patient's characteristics, continuous variables including age, thyroid gland weight, radioiodine uptake value were reported as mean $\pm$ standard deviation (SD) together with range. Ratio or percentage was used to present categorical variables including gender and indication for ^{131}I therapy. Univariate and multivariate analyses were used to determine that which factors contributed to the prediction of pattern of radioiodine thyroid uptake. The data analysis was performed using STATA, version 6. Statistical significance was defined as $p < 0.05$.

RESULTS

Of all 1,029 Graves' disease patients treated by radioiodine during the time of study, 91 subjects were excluded; 46 cases because of having a previous history of thyroid surgery and 45 cases due to an incomplete data obtained. The rest 938 cases, therefore, were enrolled for analysis. All subjects lived in the province of the northeast Thailand. Characteristics of subjects including age, gender, estimated thyroid gland weight, indication for ^{131}I treatment (new cases without prior ATD treatment, medical failure within 6-month ATD treatment, failure between 6-month and 24-month ATD treatment, failure after 24-month ATD treatment, relapse of hyperthyroidism within 2 years after ATD cessation and

relapse beyond 2 years after ATD cessation), 3-hour and 24-hour thyroid uptake values were shown (Table 1).

Of all 938 subjects, 252 (26.87%) had the uptake of rapid turnover type while the uptake of the remaining 686 (73.13%) were non-rapid turnover. In comparison of the outcome of ^{131}I therapy between the two groups of uptake pattern, 275 subjects –53 cases (19.27%) of rapid turnover group and 222 cases (80.73%) of non-rapid turnover group–were excluded since their treatment outcome was undetermined. The rest 663 cases included 199 (30.00%) and 464 (70.00%) subjects with rapid and non-rapid turnover uptake pattern, respectively. It was found that the successful treatment was significantly lower in the rapid turnover group (34 cases, 17.1%) as compared with that in the non-rapid turnover group (198 cases, 42.7%), $p < 0.001$.

The relevant clinical data of both rapid and non-rapid turnover groups in all subjects enrolled were shown in Table 2. By the univariate analysis, significant association was found between the rapid turnover pattern and the younger age subjects ($p = 0.021$), subjects with pretreatment with ATD for more than 24 months ($p = 0.011$), the larger thyroid gland size ($p < 0.001$), the higher 3-hour ($p < 0.001$) and the lower 24-hour uptake values ($p < 0.001$). However, the multivariate analysis showed that only 3-hour and 24-hour uptake values were the independent predictors of the rapid turnover pattern ($p < 0.001$).

Table 1. Characteristics of subjects. (N = 938)

Characteristic	Value
Gender (female: male)	
Number	751 : 187
Ratio	4 : 1
Age (year)	
mean ± SD	40.8 ± 11.6
range	14 - 75
Thyroid gland (g)	
mean ± SD	44.5 ± 23.6
range	20 - 200
Indications: number (%)	
no previous ATD	19 (2.0%)
ATD < 6 months	144 (15.4%)
ATD 6 > 24 months	278 (29.6%)
ATD >2 years	382 (40.7%)
relapse < 2 years	80 (8.5%)
relapse >2 years	35 (3.7%)
3-hour uptake (%)	
mean ± SD	68.8 ± 20.7
range	11.1 - 98.7
24-hour uptake (%)	
mean ± SD	79.8 ± 11.2
range	33.5 - 98.8

Table 2. Comparative characteristics of subjects with rapid and non-rapid turnover patterns.

Characteristic	Rapid turnover (N = 252)	Non-rapid turnover (N = 686)	Significance
Gender (female: male)			
Number	211 : 41	540 : 146	NS
Ratio	5.2 : 1	3.7 : 1	
Age (year)			
mean ± SD	39.3 ± 11.5	41.4 ± 11.6	p = 0.021
range	16 - 70	14 - 75	
Thyroid gland (g)			
mean ± SD	56.6 ± 27.9	40.1 ± 20.2	p < 0.001
range	20 - 200	20 - 150	
Indications: number (%)			
no previous ATD	1 (0.4%)	18 (2.6%)	NS
ATD < 6 months	37 (14.7%)	107 (15.6%)	NS
ATD 6 > 24 months	76 (30.2%)	202 (29.5%)	MS
ATD >2 years	120 (47.6%)	262 (38.2%)	p = 0.011
relapse < 2 years	14 (5.6%)	66 (9.6%)	NS
relapse >2 years	4 (1.6%)	31 (4.5%)	NS
3-hour uptake (%)			
mean ± SD	86.2 ± 6.9	62.4 ± 20.4	p < 0.001
range	61.6 - 98.7	11.1 - 97.3	
24-hour uptake (%)			
mean ± SD	77.9 ± 9.7	80.6 ± 11.6	p < 0.001
range	45.5 - 96.4	33.5 - 98.8	

DISCUSSION

Calculation of the absorbed radioiodine dose in the thyroid gland is a very important factor in ^{131}I therapy for Graves' disease. It can be performed by measurement of the effective half-life of radioiodine in the gland. However, the effective half-life cannot be practically calculated since repeated measurements of thyroid uptake cannot be done in every patient. Generally, two-day radioiodine thyroid uptake measurements are used to show the pattern of iodine retention in the gland and to calculate the appropriate treatment dose of ^{131}I to Graves' disease patients. Aktay et al. used a 4- to 24-hour ^{131}I uptake ratio as an index of thyroidal ^{131}I retention and proposed it as a practical means to determine the effective half-life without the need for extended thyroid uptake measurements.[5]

The prevalence of rapid turnover pattern of radioiodine uptake has been rarely reported in the literature. This study showed that the prevalence of this kind of uptake pattern, based on the early to late uptake ratio ≥ 1, was about a quarter (26.9%) in our study population. This figure was slightly higher than that found in the study of Aktay et al., which was 15%.[5]

The successful rate of ^{131}I therapy in the rapid turnover pattern group (17.1%) was significantly lower than that in the non-rapid turnover pattern group (42.7%), $p < 0.001$). This finding was in accordance with the study of Aktay et al., which reported 52% and 89% successful rate in the rapid and non-rapid turnover group respectively. Higher failure rate of treatment in the rapid turnover pattern was directly explained as a shorter retention time for ^{131}I to irradiate thyroid gland and consequently less biological damage occurred in the gland. Furthermore, it could give rise to the increased amount of radiolabeled thyroid hormones or protein-bound ^{131}I circulating in the blood and irradiating normal tissue, causing undesirable and probably hazardous radiation exposure to various organs especially the bone marrow.[6]

Although the rapid turnover pattern gives an unfavorable ^{131}I treatment outcome, the effectiveness of treatment can be enhanced by the adjunct treatment with lithium. Its action is by the blockage of organic iodine and thyroid hormone release from the thyroid gland [8], so a longer retention of ^{131}I in the gland can be achieved, resulting in a longer biological effect of radiation to the thyroid. It is beneficial particularly in young patients where the total body radiation dose must be kept to a minimum.[9-10]

To the best of our knowledge, clinical factors possibly associated with the rapid ^{131}I turnover pattern have never been clearly stated. We therefore try to find the clinical variables likely to predict this type of uptake pattern. In univariate analysis, age, history of pretreatment with ATD for more than 24 months, thyroid gland size, 3-hour uptake value and 24-hour uptake value were found to significantly associate with the rapid turnover pattern ($p < 0.05$), whereas sex predilection, no previous ATD treatment and other periods of pretreatment with ATD were not the associated factors. However, by the multivariate analysis only 3-hour and 4-hour thyroid uptake values were found to be the independent variables to predict this type of uptake pattern. This meant that practically the type of uptake pattern could be known only by performing the actual measurement of at least two-day radioiodine uptake.

Another significance addressing the issue about the rapid turnover pattern is about the calculation of late radioiodine uptake by using early uptake value. Some institutes undertook the study to acquire the formula in order to calculate the late 24-hour uptake value by the early 3- to 6-hour uptake value without actual measurement of the late uptake and found that the calculated late uptake value correlated in the moderate to high degrees with the actual measured late uptake value.[11-13] Moreover, it was also showed that the administered doses of ^{131}I derived from the calculated and the actual measured late uptake were very close. By this method, ^{131}I therapy could be completed within one single visit. Morris et al.[14] reported that the prediction of late uptake value by this method might not be used in Graves' disease patients who were likely to have rapid turnover uptake. Eliminating these patients before developing the regression equation to predict the late uptake value yielded an accurate calculation of the predicted late uptake. The authors suggest that the separate regression equations should be acquired from both groups of uptake pattern to get the suitable formula to predict the late uptake value in each specific group of patients.

As with most retrospective studies, this

study had certain shortcomings. Some degree of error regarding the estimation of thyroid gland weight by palpation was expected in particular with the larger gland size. Among the experienced clinicians, the interobserver variability for the estimate of thyroid gland was could be significant. In eliminating this subjectivity of the manual estimation, the use of ultrasonography to measure the thyroid volume was reported to be significantly correlate with the manual estimation by the endocrinologists and was recommended as a safe and precise way to determine the actual thyroid size when calculating the treatment dose.[15-16] Another drawback of this study, since the subjects without pretreatment with ATD in our study population was only 2%, association between presence or absence of ATD pretreatment and the type of turnover pattern was not reliably determined. Berg et al. found that ATD could cause a significantly faster turnover of radioioidine from the gland [6] so it was possible to be another factor associated with the rapid turnover pattern. This issue remains to be determined in further studies.

In conclusion, our study revealed the uncommon but significant proportion of patients with rapid turnover pattern and its negative effect on ^{131}I treatment outcome. Moreover, it was shown that none of the clinical characteristics could be used to predict this kind of uptake pattern.

ACKNOWLEDGEMENT

The authors wish to thank Ms Kaewjai Cumsook of the Clinical Epidemiology Unit, Faculty of Medicine, Khon Kaen University for her kind assistance in statistical analysis of the data.

REFERENCES

1. Shapiro B. Optimization of radioiodine therapy of thyrotoxicosis: what have we learned after 50 yr? J Nucl Med 1993; 34: 1638-41.
2. Nordyke RA, Gilbert FI Jr. Optimal iodine -131 dose for eliminating hyperthyroidism in Graves' disease. J Nucl Med 1991; 32: 411-6.
3. Allahabadia A, Daykin J, Sheppard MC, Gough SC, Franklyn JA. Radioiodine treatment of hyperthyroidism-prognostic factors for outcome. J Clin Endocrinol Metab 2001; 86: 3611-7.
4. Bajnok L, Mezosi E, Nagy E, et al. Calculation of the radioiodine dose for the treatment of Graves' hyperthyrodism: is more than seven-thousand rad target dose necessary? Thyroid 1999; 9: 865-9.
5. Aktay R, Rezai K, Seabold JE, Bar RS, Kirchner PT. Four-to twenty-four-hour uptake ratio: an index of rapid iodine-131 turnover in hyperthyroidism. J Nucl Med 1996; 37: 1815-9.
6. Berg GE, Michanek AM, Holmberg EC, Fink M. Iodine-131 treatment of hyperthyroidism: significance of effective half-life measurements. J Nucl Med 1996; 37: 228-32.
7. Clerc J, Izembart M, Dagousset F, et al. Influence of dose selection on absorbed dose profiles in radioiodine treatment of diffuse toxic goiters in patients receiving or not receiving carbimazole. J Nucl Med 1993; 34: 387-93.
8. Temple R, Berman M, Robbins J, Wolff J. The use of lithium in the treatment of thyrotoxicosis. J Clin Invest 1972; 51: 2746-56.
9. Turner JG, Brownlie BE, Rogers TG. Lithium as an adjunct to radioiodine therapy for thyrotoxicosis. Lancet 1976; 20: 614-5.

10. Bogazzi F, Bartalena L, Brogioni S, et al. Comparison of radioiodine with radioiodine plus lithium in the treatment of Graves' hyperthyroidism. J Clin Endocrinol Metab 1999; 84: 499-503.
11. Hayes AA, Akre CM, Gorman CA. Iodine -131 treatment of Graves' disease using modified early iodine-131 uptake measurements in therapy dose calculations. J Nucl Med 1990; 31: 519-22.
12. Hennessey JV, Berg LA, Ibrahim MA, Markert RJ. Evaluation of early (5 to 6 hours) iodine 123 uptake for diagnosis and treatment planning in Graves' disease. Arch Intern Med 1995; 27: 621-4.
13. Vemulakonda US, Atkins FB, Ziessman HA. Therapy dose calculation in Graves' disease using early I-123 uptake measurements. Clin Nucl Med 1996; 21: 102-5.
14. Morris LF, Waxman AD. Braunstein GD. Accuracy considerations when using early (four- or six- hour) radioactive iodine uptake to predict twenty-four-hour values for radioactive iodine dosage in the treatment of Graves' disease. Thyroid 2000; 10: 779-87.
15. Lucas KJ. Use of thyroid ultrasound volume in calculating radioactive iodine dose in hyperthyroidism. Thyroid 2000; 10: 151-5.
16. Crawford DC, Flower MA, Pratt BE, et al. Thyroid volume measurements in thyrotoxic patients: comparison between ultrasonography and iodine-124 positron emission tomography. Eur J Nucl Med 1997; 24: 1470-8.

CORRELATION BETWEEN IHA ANTIBODY TITER AND IMAGING FINDINGS AMONG THAI HOSPITALIZED PATIENTS WITH AMEBIC LIVER ABCESS

Viroj WIWANITKIT[1]

ABSTRACT

Amebic hepatic abcess is a tropical disease with wide spectrum of clinical presentations. The retrospective case review was made on 39 Thai hospitalized patients who had diagnosis of amoebic liver abcess. In our series, there were 23 men (59 %) and 16 women (41 %), with a mean age of 44.56 ± 21.81 years (range, 10 to 88 years). Concerning the imaging presentations, most cases had single abcess at right lobe of liver. Concerning the serological study, average IHA titer of the cases was 1: 1190.35 ± 895.42 (range, 1:256 to 2048). Concerning the multiple logistic regression analysis, no significant correlation was found between antibody titer and the other parameters

INTRODUCTION

Amebiasis is a widespread parasitic disease caused by Entamoeba histolytica. This protozoan organism is the third leading parasitic cause of death in the developing world and is an important health risk to travelers in endemic areas.[1] Amebiasis most commonly results in asymptomatic colonization of the gastrointestinal tract, but some patients may develop intestinal invasive disease or extraintestinal disease. The most common extraintestinal manifestation of is a hepatic abscess.[1] This infection is common throughout the world and can be associated with life-threatening consequences.[1-4]

Concerning hepatic amebiasis, the nfection starts from ingestion of amoebic cysts, which after excystation form trophozoits in the small intestine, colonize the bowel lumen and invade the intestinal epithelium resulting in amoebic colitis. Spread to the liver and formation of amoebic liver abscesses occurs in one third of the cases.[1-4] This infection can demonstrate a wide spectrum of clinical presentations from no complaints to arrest.[5-9] Given the often nonspecific nature of the complaints related to an amebic abscess, a retrospective review of patients with confirmed disease to recognize the most common patterns of presentation is useful.[5-9]

Since amoebic liver abscess have a good prognosis when treated with metronidazole,[1-4] therefore, an early diagnosis and treatment is therefore important. The diagnosis is made by demonstration of E. histolytica cysts in the pus or positive serology.[1-4] Essentially, all patients with invasive amoebiasis have E. histolytica- specific IgG;[10] presence of these antibodies is indicative of current or previous infection.[10] The serological titers are elevated in 100% of patients with amebic liver abscess, 98% with amebic dysentery and 66% of asymptomatic carriers.[11]

Here, we retrospectively study the serological titer from Entamoeba histolytica indirect hemagglutination (IHA) test among hospitalized 39 Thai patients with amebic liver abcess. The

[1] Department of Laboratory Medicine, Faculty of Medicine, Chulalongkorn University Bangkok Thailand 10330

correlation between the titer and the other laboratory results of the patients is also studied as well.

MATERIALS AND METHODS

CASES RECRUITMENT

The retrospective case review was made on hospitalized patients who had diagnosis of amoebic liver abcess at the King Chulalongkorn Memorial Hospital, Bangkok, Thailand. This study focused on a ten-year period, from January 1992 to December 2001.

The inclusion criteria are 1) the cases with amebic liver abcess and 2) the cases with complete medical records for further analysis. Concerning the operative definitions, the liver abscess was diagnosed according to both the presentation of the abscess cavity on hepatic US and/ or CT scans, and according to pus drained from the cavity during needle aspiration or surgery. The confirmation of amoebic liver abcess was according to the identification of Entamoeba histolytica by microscopic examination of the pus or serological titer by ntamoeba histolytica indirect hemagglutination (IHA) test was 1:256 or greater.[12] The exclusion criteria are 1) the cases with liver cirrhosis, 2) the cases with malnutrition and 3) the cases with Anti HIV seropositive. Since these cases are mentioned to have impaired immune response and is reported to be risk for aberrant clinical and laboratory presentations.[13]

According to this study, there were 39 cases included. The review of these patients' medical records for further analysis was performed. The data from the discharge summary of these patients were then recorded including their age and sex, as well as the final diagnosis. Imaging information collected, included size, location and number of abscesses.

STATISTICAL ANALYSIS

Descriptive statistics were used in analyzing the demographic and laboratory parameters for each group. The multiple logistic regression analysis was used in determination of the correlation between the titer and the patients' characteristics. The statistical significant level was accepted at p value = 0.05. All the statistical analyses in this study were made using SPSS 7.0 for Windows Program.

RESULTS

Thirty-nine cases of liver cirrhosis patients with liver abcess were diagnosed. There were 23 men (59 %) and 16 women (41 %), with a mean age of 44.56 ± 21.81 years (range, 10 to 88 years). Concerning the imaging presentations, the abscesses were in the right lobe in 29 patients (74.4 %) in the left lobe in 3 patients (7.7 %), and in both lobes in 7 patients (17.9 %). In our series, 30 had single abscess (76. 9 %) and 9 patients had multiple abscesses (23.1 %). All of single abcesses were larger than 5 cm and all of multiple abcess were smaller than 5 cm. Concerning the serological study, average IHA titer of the cases was 1: 1190.35 ± 895.42 (range, 1:256 to 2048).

Concerning the multiple logistic regression analysis, no significant correlation was found between antibody titer and the other parameters (Table 1).

Table 1. Correlation coefficient between antibody titer and the imaging characteristic

Imaging characteristics	Correlation coefficient (r)	P value
Size of abcess	0.42	0.09
Location of abcess	0.12	0.16
Number of abcess	0.11	0.14

DISCUSSION

Amebic liver abcess is one of the two most common causes of liver abcess. Of interest, patients may or may not have symptoms of intestinal infection concurrently with amebicliver abscess.[2-4] This infection is present worldwide, but is most common in tropical areas where crowded living conditions and poor sanitation exist. Transmission occurs through ingestion of cysts in fecally contaminated food or water, use of human excrement as fertilizer, and person-to-person contact. The incidence is about 1 out of 100,000 people for amebic liver abscess.[2-4]

According to our series, the clinical and laboratory presentations in our patients were similar to those in the previous reports.[1, 4-5] The abcess usually present as a single abcess on the right lobe of liver. Nevertheless, these clinical manifestations are similar to those in pyogenic liver abcess patients.[13]

Of interest, we cannot find any correlation between the antibody titer to any imaging characteristic. However, since the total case in our study is rather few, the larger study to answer this question is necessary.

COMPETING INTERESTS

Not declared.

REFERENCES

1. Hughe MA, Petri WA Jr. Amebic liver abscess. Infect Dis Clin North Am 2000; 14:565-82.
2. Falaiye JM, Okeke GC, Fregene AO. Amoebic abscess in the cirrhotic liver. Gut 1980;21:161-3.
3. Rustgi AK, Richter JM. Pyogenic and amebic liver abscess. Med Clin North Am 1989;73:847–58.
4. Nunes A, Varela MG, Carvalho L, Ranchhod R, Saavedra JA. Hepatic amebiasis. Acta Med Port 2000;13:337-43.
5. Hoffner RJ, Kilaghbian T, Esekogwu VI, Henderson SO. Common presentations of amebic liver abscess. Ann Emerg Med 1999;34:351-5.
6. Kuo CM, Kuo CH, Changchien CS. Liver abscess in patients with cirrhosis of the liver: a 12-year experience. J Gastroenterol 2001;36:552-6.

7. Bissada AA, Bateman J. Pyogenic liver abscess: a 7-year experience in a large community hospital. Hepatogastroenterology 1991;38:317-20.
8. Branum GD, Tyson GS, Branum MA, Meyers WC. 1990. Hepatic abscess: changes in etiology, diagnosis, and management. Ann Surg 212:655-62.
9. Chiu CT, Lin DY, Wu CS, Chang-Chien CS, Sheen IS, Liaw YF. A clinical study on pyogenic liver abscess. J Formos Med Assoc 1987;86:405-12.
10. Arvind AS, Shetty N, Farthing MJG. Serodiagnosis of amoebiasis. Serodiagn Immunother Infect Dis 1988;2:79-84.
11. Kessel JF, Lewis WP, Paquel CM, Turner JA. Indirect hemagglutination and complement fixation tests in amebiasis. Am J Trop Med Hyg 1965;14:540-50.
12. Khan MH, Qamar R, Shaikh Z. 1Serodiagnosis of amoebic liver abscess by IHA method. J Pak Med Assoc 1989;39:262-4.
13. Branum G.B., G.S. Tyson, M.A. Branum, W.C. Meyers. Hepatic abscess: changes in etiology, diagnosis, and management. Ann Surg 1990;212:655-62.

MATHEMATICAL MODEL FOR VITAMIN B12 AND FOLATE FROM RIA CORRELATION CURVE, A SHORT REPORT

Viroj WIWANITKIT

ABSTRACT

Good nutrition is an important aspect of healthy living. Blood levels of vitamin B12 and folate are key markers of an individual's nutritional status. Laboratory support for the diagnosis and management of these multiple clinical entities is controversial and somewhat problematic. Although, the radioimmunoassay can be a useful reliable tool to perform these two tests but it is not easily available. Nevertheless, it is very expensive and seems not cost effective for the present situation of economic crisis. Here, we developed a new mathematical model to be an alternative for determination of estimated level of vitamin B12 and folate. The first model for vitamin B12 can be shown as the equation plot hemoglobin (x) versus vitamin B12 (Y): $Y = 1.7X + 252$. The second model for folate can be shown as the equation plot hemoglobin (x) versus folate (Y): $Y = 1.4X - 6.2$. The reference range for vitamin B12 and folate from our method are similar to the reference range by RIA in the text. However, before the conclusion to state that this model is an effective model, an in depth analysis of this new method as the comparative study including to the cost effectiveness analysis is recommended.

INTRODUCTION

Good nutrition is an important aspect of healthy living. Choosing foods that supply essential nutrients and limiting intake of certain fats and salts can help promote good health. Blood levels of vitamin B12 and folate are key markers of an individual's nutritional status. Vitamin B12 is important in maintaining heart health and minimizing the risk of anemia. In conjunction with folic acid, it helps regulate the use of iron and the formation of red blood cells. While, folate (folic acid) is a B vitamin that is essential to fetal development; adequate intake of folate during pregnancy can prevent certain types of birth defects. There is evidence that increased intake of folate and other B vitamins can lower levels of homocysteine, a risk factor for heart disease.[1]

However, these two tests are difficult to perform. Although, the radioimmunoassay can be a useful reliable tool to perform these two tests but it is not easily available.[2] Nevertheless, it is very expensive and seems not cost effective for the present situation of economic crisis. Here, we tried to develop the new method to determine the value of vitamin B12 and folate to be a simple crude tool for determination of these two hematologic parameters by means of mathematical model.

MATERIALS AND METHODS

REVIEW OF THE LITERATURE OF RIA ASSAYS FOR VITAMIN B12 AND FOLATE

We perform a literature review to find the relevance publications on the RIA assays for vitamin B12 and folate. We used the main search engine as the PubMed, Medscape, Science

Department of Laboratory Medicine, Faculty of Medicine, Chulalongkorn University, Bangkok Thailand 10330

Citation index and Thai Index Medicus to find the most proper paper for the further analysis. According to the searching, the most proper papers for the further analysis was the paper of Supawan et al.[3] Although this work did not present the correlation among haemoglobin, folic acid and vitamin B12. The trend as the correlation curves was presented.

DEVELOPMENT OF THE MATHEMATICAL MODEL FOR VITAMIN B12 AND FOLATE

The development of the mathematical model was performed as the three step procedures:

1. We randomly collected the laboratory results of hemoglobin from different 300 healthy patients of both sex from routine hematology test at Out-Patient Division, King Chulalongkorn Memorial Hospital.

2. We used the reported correlation curves for Vitamin B12 VS hemoglobin and folate VS hemoglobin to find the vitamin B12 and folate level according to the hemoglobin result for each subject.

3. Since the correlation curves were non-linear, we developed a new linear model by regression analysis of the determined vitamin B12 and folate to the hemoglobin. Then the least square equation was calculated.

TRIAL OF THE MATHEMATICAL MODEL FOR REFERENCE RANGE SETTINGS

We performed a trial of the new developed mathematical model by

1. Collection of the hemoglobin results from the other 200 non anemic healthy subjects

2. Finding the reference range for serum vitamin B12 and folate for these subjects using the new mathematical model. The reference range was calculated as the expected range (95% Confidence Interval). The statistical level was p value = 0.05.

3. The new reference range was compared to the previous reference range.

RESULTS

NEW MATHEMATICAL MODEL DEVELOPING

The average hemoglobin level for our subjects was 13.2 ± 2.4 g/dL. The average serum vitamin B12 and folate level using the correlation curve was and 354.2 ± 82.4 pg/mL, 5.1 ± 3.6 ng/mL, respectively. The least square equation plot hemoglobin (x) versus vitamin B12 (Y) was $Y = 1.7X + 252$. The least square equation plot hemoglobin (x) versus folate (Y) was $Y = 1.4X - 6.2$.

REFERENCE RANGE SETTINGS

Using the two new mathematical models, the reference ranges for vitamin B12 and folate are 326.3 - 641.6 pg/mL and 3.4 - 5.2 ng/mL, respectively.

DISCUSSION

Vitamin B(12) and folate are two vitamins that have interdependent roles in nucleic acid synthesis. Deficiencies of either vitamin can cause megaloblastic anemia; however, inappropriate treatment of B(12) deficiency with folate can cause irreversible nerve degeneration.[4] Inadequate folate nutrition during early pregnancy can cause neural tube defects in the developing fetus. In addition, folate and vitamin B(12) deficiency and the compensatory increase in homocysteine are a significant risk factor for cardiovascular disease. Laboratory support for the diagnosis and management of these multiple clinical entities is controversial and somewhat problematic. Automated ligand binding measurements of vitamin B(12) and folate are easiest to perform and widely used.[1-2] Nevertheless, the costs of these tests are high and may not suitable for the developing countries including to Thailand.

Presently, healthcare strategies that consider the impact of laboratory tests on the overall costs and quality of care should consider the advantages of all tests in use. The RIA test for vitamin B12 and folate seem not fit for the Era of Universal Coverage, therefore, finding for the simple crude method for the primary use of the physician is necessary. Here, we developed a new mathematical model to be an alternative for determination of estimated level of vitamin B12 and folate. Of interest, our developed model can provide the similar result comparing to the standard RIA method. The reference range for vitamin B12 and folate from our method are similar to the reference range by RIA in the text (vitamin B12: 243 - 894 pg/mL, folate: > 4.1 ng/mL). However, before the conclusion to state that this model is an effective model, an in depth analysis of this new method as the comparative study including to the cost effectiveness analysis is recommended.

References

1. Klee GG. Cobalamin and folate evaluation: measurement of methylmalonic acid and homocysteine vs vitamin B(12) and folate. Clin Chem. 2000;46:1277-83
2. Carmel R. Requesting vitamin B12 and folate assays. Lancet 1995;346:973
3. Prayurahong B, Tungtrongchitr R, Chanjanakijskul S, et al. Vitamin B12, folic acid and haematological status in elderly Thais. J Med Assoc Thai 1993;76: 71-8
4. Hoffbrand AV, Herbert V. Nutritional anemias. Semin Hematol 1999;36:13-23

nesco®

Innovation for Minimally Invasive Surgery

AZWELL

Microtaze®

Microwave surgical device – Microtaze **AZM-520**

Microwave Coagulation of Liver Cancer

Percutaneous, laparotomic and laparoscopic coagulation methods can be used in cases of liver cancer.

- Examples

Percutaneous coagulation

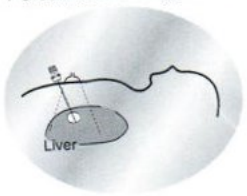

Laparotomic coagulation

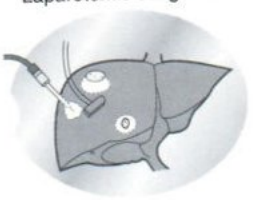

Subthoracic or abdominal laparoscopy

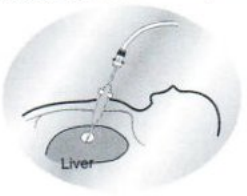

- Electrodes
  - Percutaneous monopolar electrode (deep-coagulation probe)
  - Laparoscopic monopolar electrode
  - Monopolar surgical electrode
  - Others

AZWELL Inc.

3-2-6 Nihonbashi - Honcho

Chuo - Ku, Tokyo 103-0023, Japan

Ozu - Honkan Bldg. 4F

Tel: 81-3-5695-4192 Fax: 81-3-5695-4193

E-mail nsktokyo@mx7.mesh.ne.jp

MAHACHAK INTERNATIONAL CO.,LTD.

159/12 Soi Vibhavadi Rangsit 64, Moo 3,

Vibhavadi Rangsit Road, Laksi, Bangkok

10210 Thailand.

Tel: (662) 973-5522-30 Fax: (662) 973-5533

E-mail: mahachak@ksc.th.com

THAILAND DISTRIBUTOR

SERUM FERRITIN LEVEL BY RIA AMONG ANEMIC AND NON ANEMIC PEDIATRIC SUBJECTS

Viroj WIWANITKIT[1], Paungpayom PREECHAKAS[2], Nara PARITPOKEE[1], Chiayaporn BOONCHALERMVICHIAN[1]

ABSTRACT

Ferritin is a family of iron-storage proteins that are found in animals, plants, fungi and bacteria. Presently, serum ferritin is used as a laboratory test for monitoring of iron status of the patient. It is recommended as a tool for monitoring of patient with hematological diseases. Here, we reported our study concerning serum ferritin at different hemoglobin level. Thirty subjects were included in this study. The ferritin in this study was performed by radioimmunoassay method (RIA) at the Nuclear Medicine Division, Department of Radiology, Faculty of Medicine, Chulalongkorn University. According to our study, 8 subjects were classified as anemic group and 22 subjects were classified as non anemic group. The average serum ferritin level for the whole subjects, the anemic group and non anemic group were 1912. 47 $\pm$ 1734.97 ng/ml, 1559.81 $\pm$ 1557.33 ng/ml, and 2040.71 $\pm$ 1812.15 ng/ml, respectively. Of interest, there was a significant different between the average serum ferritin between anemic and non anemic group ($p = 0.46$). Therefore, we can repeatedly state the importance of serum ferritin determination in hematology study.

INTRODUCTION

Ferritin is a family of iron-storage proteins that are found in animals, plants, fungi and bacteria. As far as we know, ferritin does not contribute to the magnetization of sediments, but it does provide an excellent example of the biomimetic approach to synthesizing small magnetic particles. Natural ferritin is produced by a BOB process and consists of a spherical protein shell with a external diameter of 12 nm surrounding a cavity with an internal diameter of 9 nm containing an iron oxy-hydroxide core.[1]

They form hollow, spherical particles in which 2000 to 4500 iron atoms can be stored as iron(III) (i.e. Fe^{3+} ions). Depending on the organism, ferritin particles are roughtly 8-12 nm in diameter, with several channels that appear to mediate iron transport to and from the interior. All ferritins are composed of 24 apoferritin monomers which associate to form a spherical particle. In mammalian cells, two types of ferritin monomers have been characterized (H and L types), which differ in the presence of certain residues that function to reduce ferric iron or facilitate mineralization of the particle with iron. Bacteria, including eubacteria and archaebacteria, have two types of ferritins: heme-containing bacterioferritins and heme-free ferritins. The structure of these molecules is very similar to those of animals and plants.

Presently, serum ferritin is used as a

1 Department of Laboratory Medicine, Faculty of Medicine, Chulalongkorn University, Bangkok 10330
2 Nuclear Medicine Division, Department of Radiology, Faculty of Medicine, Chulalongkorn University, Bangkok 10330

laboratory test for monitoring of iron status of the patient. It is recommended as a tool for monitoring of patient with hematological diseases. Here, we reported our study concerning serum ferritin of pediatric subjects at different hemoglobin level.

MATERIALS AND METHODS

SUBJECTS

Thirty subjects were included in this study. All subjects were asked to supply their informed consent before the study. All research protocols followed in this study are in accordance with the guideline of the local Ethical Committee (Faculty of Medicine, Chulalongkorn University).

Non - fasting blood specimens were collected from pediatric subjects by the antecubital venipuncture. 5 ml of clotted blood was collected from each subject and sent to the Central Laboratory, King Chulalongkorn Memorial Hospital, Bangkok, Thailand. Collection of sample was performed between 8.00 - 10.00 a.m.. Sera were used for the laboratory analysis. No hemolytic, icteric and lipemic specimen was included.

LABORATORY ANALYSIS

The ferritin in this study was performed by radioimmunoassay method (RIA) at the Nuclear Medicine Division, Department of Radiology, Faculty of Medicine, Chulalongkorn University. All analysis was performed according to the routine quality control at room temperature.

STATISTICAL ANALYSIS

The ferritin results were divided into two groups. The first group was the anemic group (Hb < 10 g/dL or Hct < 30 %). The second group was the non-anemic group (Hb ≥ 10 g/dL or Hct ≥ 30 %). The correlation between ferritin and hemoglobin for the whole case and for each group was then studied. Comparing between group was performed by Unpaired T-test at statistical significant level $p = 0.05$. Expected range was calculated by 95 % confidence interval analysis. SPSS for Window was used for statistical calculation in this study.

RESULTS

According to our study, 8 subjects (26.67%) were classified as anemic group and 22 subjects (73.33 %) were classified as non anemic group. The average serum ferritin level for the whole subjects, the anemic group and non anemic group were 1912. 47 $\pm$ 1734.97 ng/ml, 1559.81 $\pm$ 1557.33 ng/ml, and 2040.71 $\pm$ 1812.15 ng/ml, respectively (Table 1). Of interest, there was a significant different between the average serum ferritin between anemic and non anemic group ($p = 0.46$).

Table 1 Serum ferritin among our subjects.

Group	Average (ng/ml)	SD (ng/ml)
The whole subjects	1912.47	1734.97
● Non anemic (n = 22)	2040.71	1812.15
● Anemic (n = 8)	1559.81	1557.33

DISCUSSION

Ferritin is a widely used test in the present day. This test is measured to assess the amount of iron, which is important for red blood cell production, in the body. Ferritin is an iron binding protein that stores iron intracellularly in the liver. Translation of ferritin mRNA is regulated so that ferritin is only made when free iron is present, needing sequestration.[1-3] As ferritin is the major iron storage protein, the serum ferritin level is directly proportional to the amount of iron stored in the body. It can be an indicator of total body iron stores and the most reliable indicator other than bone marrow. Nevertheless, it can be an acute phase reactant.[4]

Generally, the normal range of serum ferritin among pediatric subject was 0 - 2000 ng/ml. According to this study, the average serum ferritin level among the healthy non anemic group was 2040.71 $\pm$ 1812.15 ng/ml. The expected range of our pediatric subjects was 0 – 1962.52 ng/ml. This range was similar to the reference value of general population in the text.[4] Concerning the average serum ferritin level in each group, the (Figure 1). Therefore, we can repeatedly state the importance of serum ferritin determination in hematology study. However, some problems due to the few subjects in this preliminary report can be the limitation in generalization of this study.

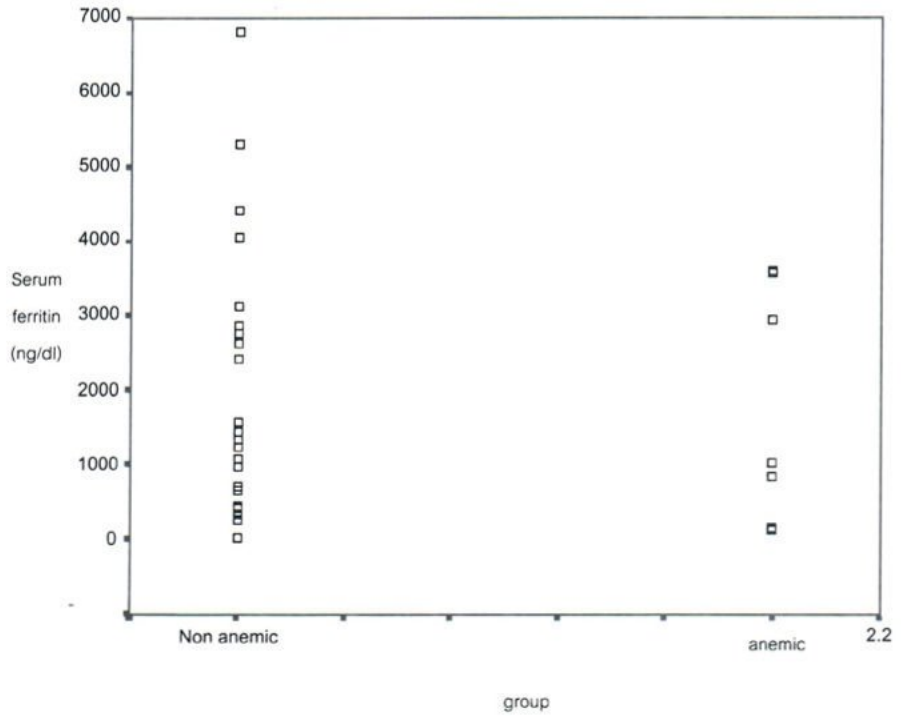

Fig. 1. Serum ferritin of the subjects

REFERENCES

1. Mann S. Molecular tectonics in biomineralization and biomimetic materials chemistry. Nature 1993;365,499-505
2. Chasteen ND, Harrison PM: Mineralization of ferritin: an efficient means of iron storage. J Struct Biol 1999;126:182-194
3. Harrison PM, Arosio P. The ferritins: molecular properties, iron storage function and cellular regulation. Biochimica et Biophysica Acta 1996;1275:161-203
4. Wiwanitkit V. Electrochemiluminescence immunoassay for ferritin analysis. Buddhachinaraj Med J 2000;17:151-7

STEREOTACTIC RADIOTHERAPY FOR BASE OF SKULL PARAGANGLIOMA: CASE REPORT

Nantakan IEUMWANANONTHACHAI,M.D., Yaowalak CHANSILPA, M.D., Pittayapoom PATTARANUTAPORN,M.D.

Summary: We present a case of atypical skull base paraganglioma involving intrasellar, suprasellar, sphenoid sinus and nasopharyngeal area. The patient presented with right-sided headache and tinnitus. Stereotactic Radiotherapy was selected to be the method of treatment for this patient because of the site of the tumor and the critical normal surrounding structures. The result showed satisfactory symptomatic improvement even if complete tumor involution did not occur.

INTRODUCTION

Paragangliomas are tumors that arise from widely distributed paraganglionic tissue, cell of neural crest tissue. The common locations of paragangliomas in head and neck are the carotid bifurcation, along the vagus nerve and the jugulotympanic area. The main treatments are surgery in resectable area and radiation for the area that is difficult to approach surgically. Stereotactic radiosurgery has been reported in a few series recently as effective treatment with minimal complication for these glomus tumors.[1-4]

Paraganglioma at intrasellar and suprasellar areas are rare locations with less than 10 cases reported.[5-7] They are classified as paraganglioma of uncertain origin because normally there is no paraganglionic cell in this area. There are some hypothesis that try to explain this; Khamlichi A.[8] proposed that it originated from the neural crest following the trigeminal nerve particularly the opthalmic division, Bibao JM.[9] proposed that it originated from abnormal migration of the neural crest in the development of the pituitary gland.

Treatment for the tumor in this area has to be considered about many important factors:
1) This tumor is mostly benign and slow growing so it takes many years before the patient can detect the symptoms. So the tumor is usually huge in size when it is detected.
2) Paraganglioma is highly vascularized tumor. Excessive bleeding from the tumor during surgery was founded in case report.[2] Preoperative embolization may give benefit.
3) Optic chiasm, optic nerve, cranial nerve 3,4,5,6 and the major vessel in sellar area are frequently involved or close to the tumor. Surgery and conventional radiation therapy are limited.

From these reasons; Stereotactic Radiosurgery (SRS) and Stereotactic Radiotherapy (SRT) which was reported to be the treatment of other diseases in this area such as pituitary adenoma, meningioma and AVM seems to be useful for the treatment of paraganglioma in this area. For that it helps to avoid complication from surgery and preserves the structure nearby.

Radiation Oncology Division Siriraj Hospital Medical School, Mahidol University Bangkok, Thailand

Send Correspondence and Reprint Requests to:
Nantakan Ieumwananonthachai, M.D.

Radiation Oncology Division Faculty of Medicine, Siriraj Hospital 2 Prannok Rd., Bangkok-noi District Bangkok 10700 Thailand.
Telephone: 02-4197082-3 Fax: 02-4197084 E-Mail address: nantakan_i@yahoo.com

CASE REPORT

A 47-year-old woman presented with off and on right-sided headache for 3-4 years. She had been diagnosed migraine and sinusitis and had got treatment for these diseases for years but the symptoms seemed to get worse. When she first came to our department, she had severe right-sided headache for twice to three times a day. From the retrospective review, we found that she also had right ear tinnitus for about 2 years. No eyes or other cranial nerve symptoms or endocrinologic disturbance were detected. On physical examination once, she was found to have a vascular mass with smooth surface at right middle turbinate of the nasal cavity. Then the patient was referred to our institute for additional evaluation and treatment.

A computed tomographic (CT) scan was obtained, it showed extensive enhancing mass, 5x5x5.5 cm. in maximal diameter, occupying in the midline from base of skull to suprasellar region superiorly and nasopharynx inferiorly. There were destruction of base of skull, sphenoid bone, sellar turcica and planum sphenoidale (figure 1). The tumor mass involved both parasellar area, more prominent on right side. A biopsy of the mass from right nasal cavity was done and the pathological report was paraganglioma. Agyrophilia, a feature of this site of tumor, was demonstrated in Grimelius stain.

She was treated by Stereotactic Radiotherapy with doses of 685 cGy x 5, daily fractions in 5 days in October 1997. The treatment was planned with 7 photon beams. After the treatment, her symptoms still persisted and the CT scan 1 month after treatment showed slightly decrease in size especially the intracranial part (figure 2). Then she got the second course of Stereotactic radiotherapy with dose 440 cGy. x 5 daily fractions equivalent to those in December 1997 (figure 3). The treatment interval was 80 days between the first and the second course. After the second course of SRT right-sided headache was almost completely disappeared. The CT scan 2 months after the treatment showed significant decrease in size of the suprasella lesion but there was still large residual tumor in the nasopharynx, sphenoid and ethmoid sinuses (figure 4). The patient was close follow up with good quality of life, no visual defect was detected. One year after the treatment the patient began to have repeated epistaxis, the CT scan showed persistent large lesion in the nasopharynx and sphenoid sinus (figure 5). The repeated biopsy from anterior rhinoscope showed residual paraganglioma. This time the patient was treated by 3 beams nasal irradiation, doses of 404 cGy x 10 fractions in 2 weeks in January 1999 (figure 6). The epistaxis was stopped. The CT and MRI studies 7 months after the treatment showed inhomogeneous enhancing mass occupied right parasella, pituitary fossa and right sphenoid sinus about 3x2 cm. in diameter (figure 7). The perfusion study of MRI showed only marginal perfusion of the tumor. The patient has best quality of life and no visual or any other complication is detected. Her last followed up was in September 2000.

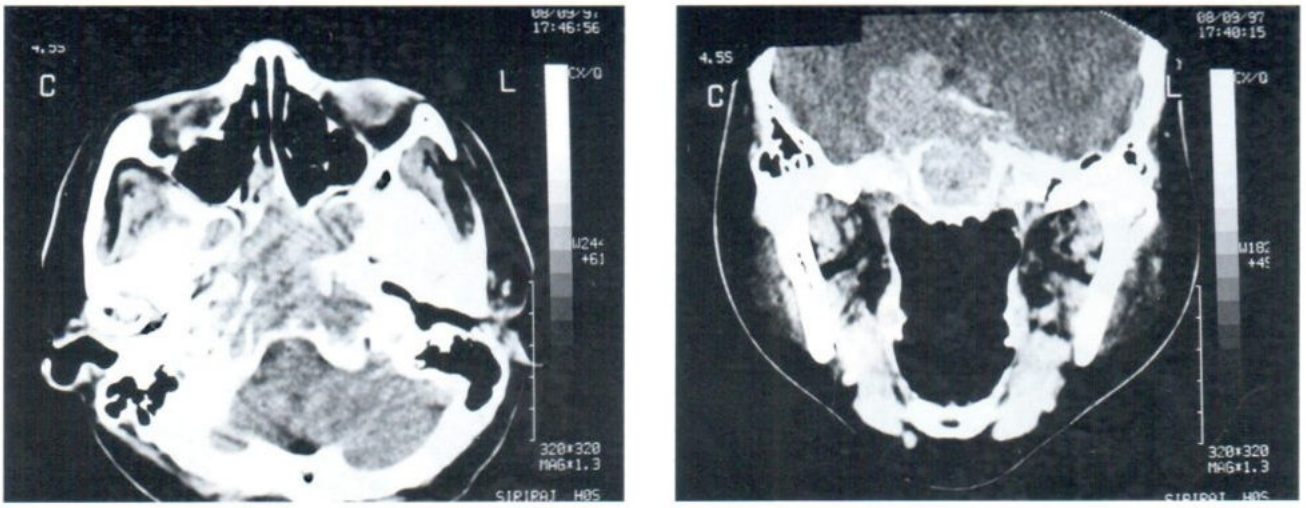

Fig. 1 Axial and sagittal CT images showed extensive enhancing mass, 5x5x5.5 cm. in maximal diameter, occupying in the midline from base of skull to suprasellar region superiorly and nasopharynx inferiorly with destruction of base of skull, sphenoid bone, sellar turcica and planum sphenoidale

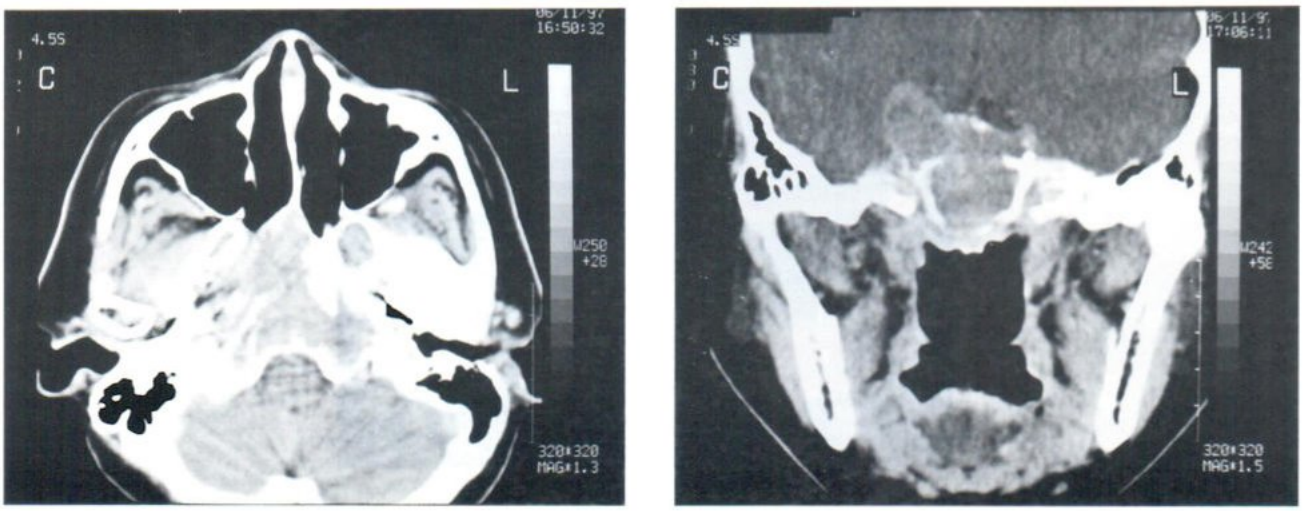

Fig. 2 Axial and sagittal CT images 1 month after the treatment showed slightly decrease in size especially the intracranial part

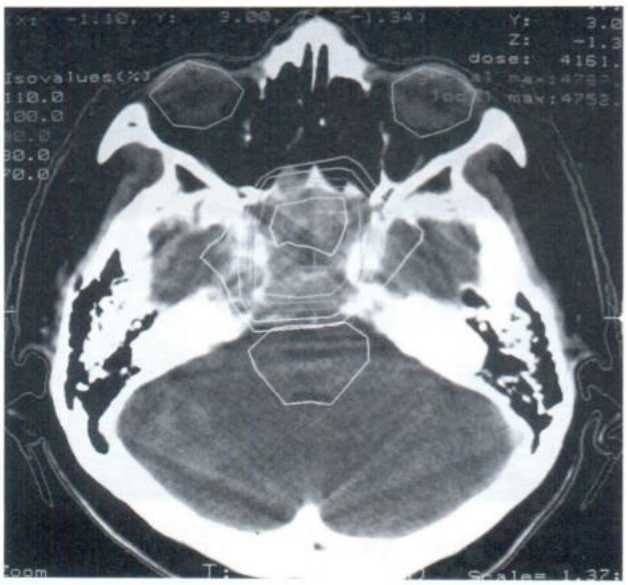

3A

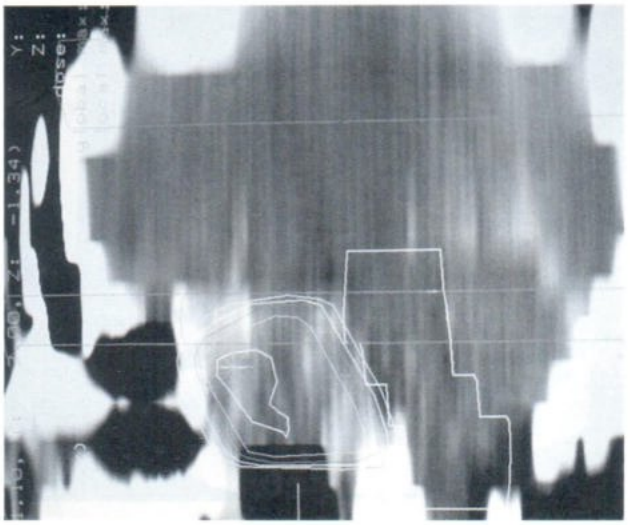

3B

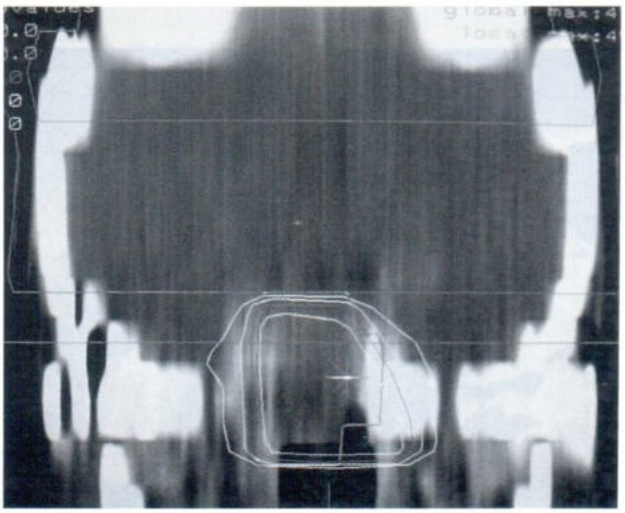

3C

Fig. 3 Isodose distribution of second SRT treatment planning White line represents tumor border
INNERMOST line shows 100% isodose
INNER line shows 90% isodose
OUTER line shows 80% isodose
OUTERMOST line shows 70% isodose
A. Axial view
B. Sagittal view
C. Coronal view

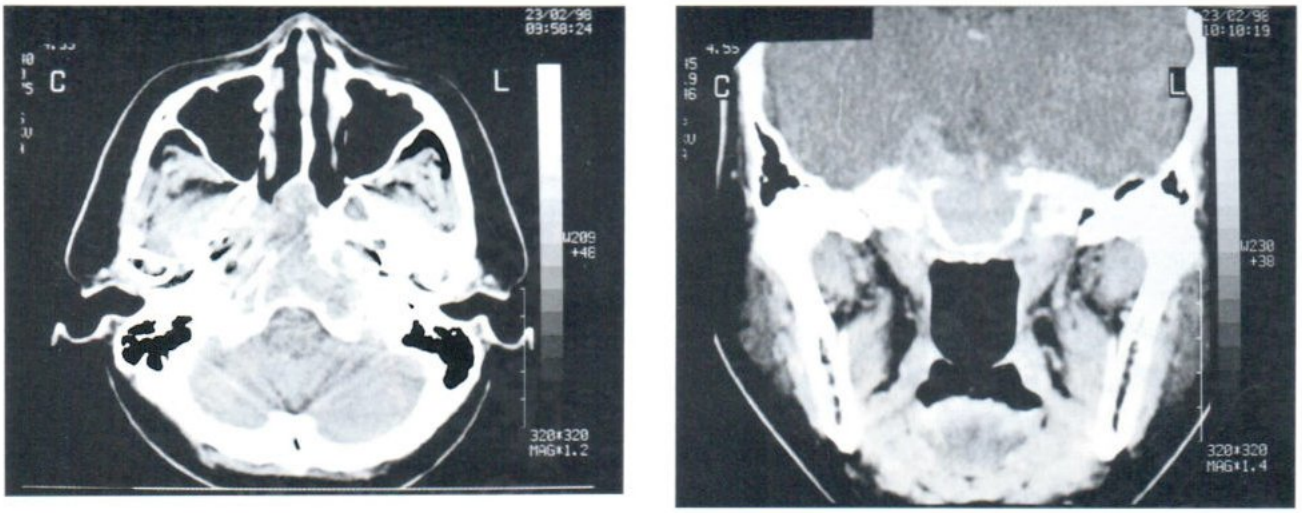

Fig. 4 Axial and sagittal CT images 2 months after the second SRT treatment showed significant decrease in size of the suprasella lesion but there was still large residual tumor in the nasopharynx, sphenoid and ethmoid sinuses

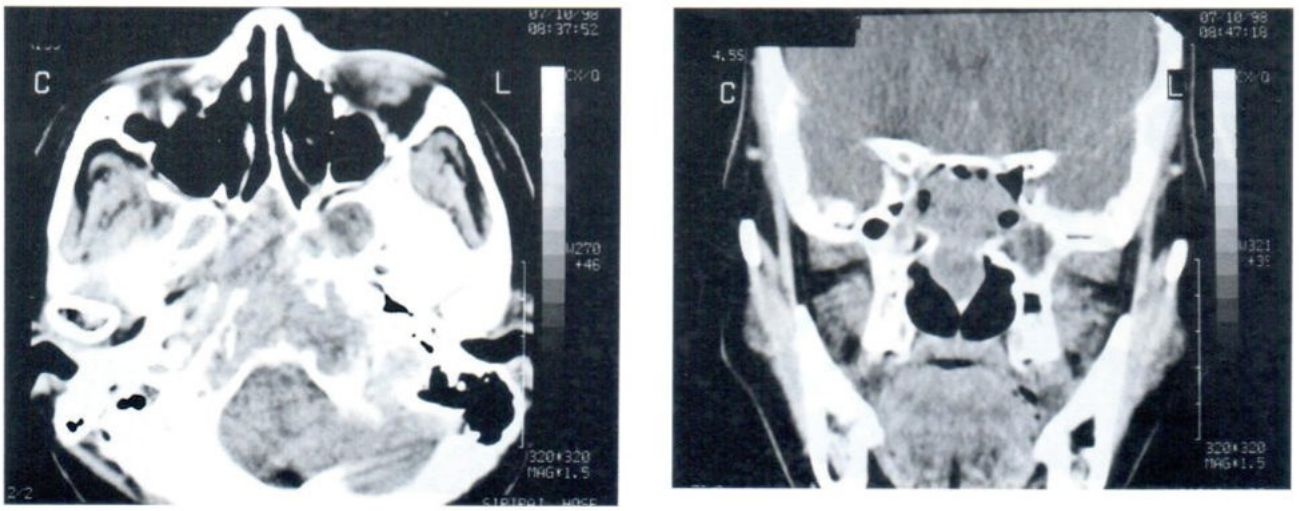

Fig. 5 Axial and sagittal CT images 1 year after the second SRT treatment showed persistent large lesion in the nasopharynx and sphenoid sinus which caused epistaxis

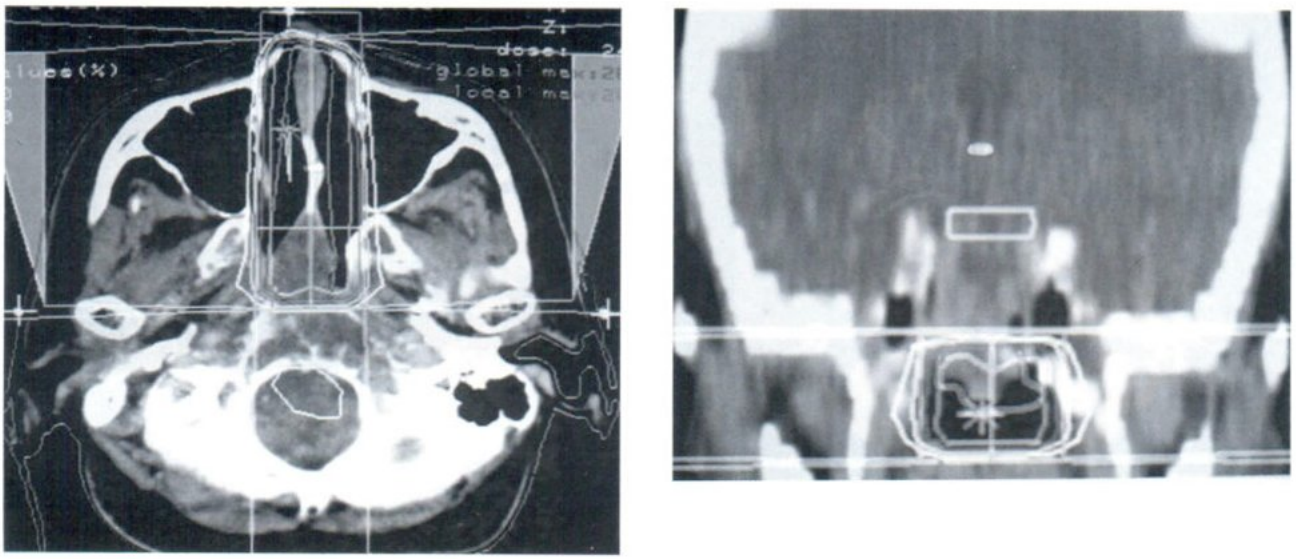

Fig. 6 Isodose distribution of the third SRT treatment with 3 photon beams aiming to stop epistaxis

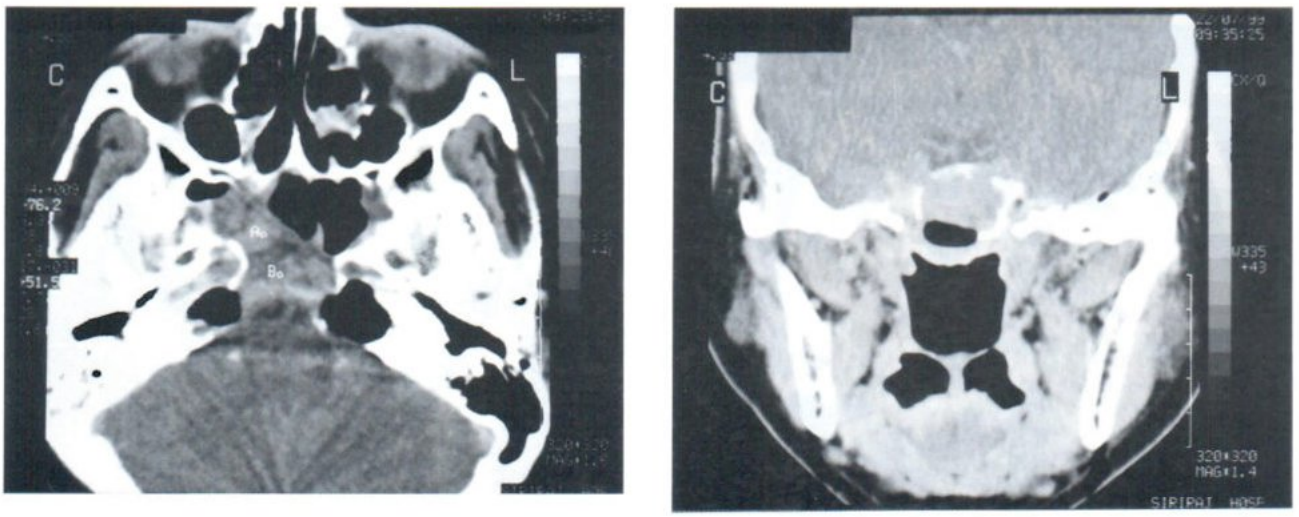

Fig.7 Axial and sagittal CT images 7 months after the third SRT treatment showed inhomogeneous enhancing mass occupied right parasella, pituitary fossa and right sphenoid sinus about 3x2 cm. in diameter

DISCUSSION

There had been reports [10-13] showing good results of the patients with paraganglioma in other areas treated by megavoltage radiotherapy alone (3500-5200 cGy conventional dose). The 10-year control rate is more than 90%. Series from 6 European centers[3-4] using SRS as the treatment for glomus jugulare tumors in 52 patients with 24 months median follow up time showed good control rate with 40% decrease in tumor size and 60% no change. The other series from Austria[1-2] using SRS for skull-base glomus tumor showed similar result with 36% decreased in tumor size and 64% had symptomatic improvement after mean follow-up time of 42 months.

Stereotactic radiotherapy gives the same benefit as radiosurgery with higher doses to the tumor and less side effect to the surrounding structures. Even there was no literature so far using hypofractionation SRT for the treatment of this type of tumor, we selected SRT to be the treatment for this patient because of the location which is close to cranial nerve and hypofractionation for the reason of cost-effectiveness. The result showed satisfactory symptomatic relief even if the image still showed residual tumor, it was smaller in size and less vascularized. This is considered to be successful treatment. However paraganglioma is a slow growing tumor and we need up to 10 year follow-up time to evaluate the result of the treatment.

Radiation of paraganglioma and other slow growing tumors mainly affects in proliferative and perivascular fibrosis with minimal alterations in the chief epithelial cells.[14] In this case angiography or perfusion MRI scan may be useful to evaluate the result of the treatment than using the imaging to see the tumor size alone. Liscak R, et al[4] compared pre and post treatment angiography in 6 patients, pathological vascularisation was completely disappeared in one patient, reduction in size in 2 and no change in 3 patients. The risk for cranial nerve complication in this patient is also high and needs to be closely followed.

REFERENCES

1. Leber KA, Eustacchio S, Pendl G. Radiosurgery of glomus tumors: midterm results. Stereotact Funct Neurosurg. 72 (suppl 1): 53-9, 1999.
2. Eustacchio S, Leber K, Trummer M, Unger F, Pendl G. Gamma knife radiosurgery for glomus jugulare tumors. Acta Neurochir (Wien). 141(8): 811-8, 1999.
3. Liscak R, Vladyka V, Simonova G, Vymazal J, Janouskova L. Leksell gamma knife radiosurgery of the tumor glomus jugulare and tympanicum. 70 (suppl 1): 152-60, 1998.
4. Liscak R, Vladyka V, Wowra B, et al. Gamma Knife radiosurgery of the glomus jugulare tumor- early multicentre experience. Acta Neurochir (Wien). 141 (11): 1141-6, 1999.
5. Noble ER, Smoker WR, Ghatak NR. Atypical Skull Base Paraganglioma. AJNR : American Journal of Neuroradiology. 18(5) 986-90, 1997.
6. Flint EW, Classen D, Pang D, Hersch WL. Intrasellar and Suprasellar Paraganglioma: CT and MRI findings. AJNR Am J Neuroradiol. 14(5) : 1191-3 ,1993
7. Steel TR, Dailey HT, Born D, et al. Paraganglioma of the Sellar Region : Report of two cases. Neurosurgery. 32(5): 844-7, 1993.
8. Khamlichi A, Ouaharbi A Amrani F.,et al. Paraganglioma of the Cranial Vault. Aproros of a case. Neurachirurgie (French J.). 37(5) : 348-52,1991.

9. Bibao JM, Horvarth E, Kovaes K, et al. Intrasellar Paraganglioma associated with hypopituitarism. Arch Pathol Lab Med. 102 : 95-98 , 1998.
10. Cummings BJ, Beale FA, Garett PG, et al. The Treatment of Glomus Tumors in the Temporal Bone by Megavoltage Radiation. Cancer. 53 : 2653-40 , 1984.
11. Cole JM, Bulir D. Long-term Results of treatment for Glomus Jugulare and Glomus Vagale Tumor with Radiotherapy. Laryngoscope. 104 : 1461-65, 1994.
12. Evenson LJ, Mendenhall WM, Parsons JT, Cassisi NJ. Radiotherapy in the management of chemodectomas of the carotid body and glomus vagale. Head Neck. 20(7): 609-13, 1998.
13. Gstoettner W, Matula C, Hamzavi J, Kornfehl J, Czemy C. Long-term results of different treatment modalities in 37 patients with glomus jugulare tumors. Eur Arch Otorhinolaryngyngol. 256(7): 351-5, 1999.
14. Spector Gj, Compagno J, Perez, et al. Glomus jugulare tumors : Effects of radiotherapy. Cancer. 5 :1316-21, 1975.

COMPARISON OF LDR TO HDR IN TREATMENT OF CERVICAL CANCER.

SAIPIN TANGKARATT, M.D.[1]

Objective; To compare the treatment results between LDR and HDR in FIGO stage IIB cervical cancer, in terms of disease survival and late normal tissues complications.

Materials and methods; From Jan 1997 to Dec 1998, Prospective non-randomized study was conducted. About 161 patients with pathological diagnosis of FIGO stage IIB cervical cancer were included in the study. All patients were treated with combination of external beam radiation and brachytherapy. The patients were divided into 2 groups for difference brachytherapy protocols. The first group of patients was treated with 1-2 fractions of LDR, and the other group of patients was treated with 4-5 fractions of HDR. Total tumor dose to point A was 80-85 Gy.

Results; All of 161 patients had complete radiation treatment as planned. Ninety patients entered in LDR protocal, and 71 patients entered in HDR protocal.

The age of patients with LDR and HDR ranged from 29-82, and 29-80 years, respectively. The mean age was 45 years in both groups. The common subtype of both groups was squamous cell carcinoma, for LDR and HDR, accounted about 86% and 77%, respectively. The evaluable patients for LDR and HDR were 82 and 66, respectively. Three year survival of patients treated with LDR and HDR were 63.4% and 68% respectively. Fourteen of 52 responders patients (26.9%) with LDR had grade I proctitis, and 4 of 52 patients (7.7%) had grade I cystitis. About 6 of 45 responders patients with HDL had grade I proctitis, 1 of 45 patients had grade II proctitis, and 1 of 45 patients (2.2%) had cystitis.

Conclusion; The study has shown the comparable results with a slightly better survival of HDR than LDR (68.2% VS 63.4%) without significant difference ($p = 0.544$). About late normal tissue complications, the LDR showed more than HDR for proctitis and cystitis (26.9% VS 15.6% and 7.7% VS 2.2%), respectively. ($P = 0.062$)

Keywords; LDR (Low dose rate), HDR (High dose rate), Brachytherapy.

INTRODUCTION

Carcinoma of uterine cervix was the most common cancer in Thai women 1. Combination of external beam and brachytherapy was the standand treatment of cervical cancer 2. In the beginning of brachytherapy in 1903, radium-226 was the first radionuclide used in the treatment with satisfactory results. Because of the radiation hazard to medical personnels by decay radon gas and its long half life (1600 years), other radionuclides with short half life, such as cesium137, cobalt60, iridium192 etc were used instead of radium. In 1950, Dr.Henscke in Memorial Hospital developed manual after loading technique in brachytherapy. After 1970,

[1] Division of Radiation therapy, National Cancer Institute Bangkok, Thailand.

many technologies in radiation treatment were developed, such as advances in computer technology, modern imaging system (CT scans, MRI) and advances in physics dosimetry. Such development lead to rapid improvement in brachytherapy in terms of computerized remote after loading system and resulted in an improvement of accuracy with safty of brachytherapy.

Because of more HDR machine available with combination of computerized planning system many institutes shifted the installation from LDR to HDR. In our institute, the HDR machine (Nucletron Ir-192) was installed in Jan 1997, and was used to treat cervical cancer in parallel to the former LDR machine. Hence, we have conducted this study, with the aim to compare the results of both machines in treatment of FIGO stage IIB cervical cancer in terms of survival and late normal tissue complications.

METERIALS AND METHODS.

From Jan 1997-Dec 1998, patients with pathological proven FIGO stage IIB cervical cancer were included in the study. All patients were treated with combination of external beam and intracavitary brachytherapy.

External beam radiation. Co-60 machine or Linac 6 MV was used to the whole pelvis, anterior/posterior opposing fields. The superior border extended from upper border of lumbar 5 to 1 cm beyond the bottom of obturator foramina, the lateral fields were 2 cm from lateral pelvic walls, tumor dose was 4000 cGy, daily dose was 200 cGy. The lateral pelvic walls were boosted in additional 1000 cGy.

Intracavitary brachytherapy. The patients were divided into 2 groups for either LDR or HDR.

For LDR, one-two weeks after complete external beam, the patients were treated with 1-2 fractions of LDR, with Fletcher applicators, tumor dose to point A was 2800 cGy or 2 x 1500 cGy.

For HDR, the patients were treated with 4-5 fractions of HDR weekly during course of external beam radiation (external beam was omitted on the day of HDR). Tumor dose to point A was 5-6 Gy per fraction. Total tumor dose to point A, combination of external beam and brachytherapy (both LDR and HDR) was 80-85 Gy.

RESULTS

About 161 patients with pathological proven FIGO stage IIB cervical cancer were included in this study. All patients had complete the treatment as planned. Ninety patients entered in LDR protocol, and 71 patients entered in HDR protocol. The age of patients in LDR and HDR group ranged from 29-82 and 29-80 years, respectively. The mean age was 45 years in both groups. Squamous cell carcinoma was the most common subtype in both groups, accounted of 90 (86%), and 71 patients (77%), respectively. AS shown in table 1.

Table 1 Pathological classification Number of patients. (%)

	LDR	HDR
Squamous carcinoma	77 (85.5%)	55 (77.5%)
Adenocarcinoma	7 (7.8%)	14 (14.7%)
Adenosquamous carcinoma	5 (5.6%)	1 (1.4%)
Anaplastic carcinoma	1 (1.1%)	-
Malig neuroendocrine tumor	-	1 (1.4%)
Total	90 (100%)	71 (100%)

Duration of treatment for LDR and HDR ranged from 6-8 weeks, mean 6.8 weeks, and 5-6 weeks, mean 5.4 weeks, respectively.

Seven of 90 patients in LDR group lost to follow-up, and one patient died 14 months after complete radiation from congestive heart failure. Thirty of 82 evaluable patients (36.6%) had treatment failure (19 patients with locoregional recurrence, and 11 patients with distant metastasis). Five patients in HDR group lost to follow-up. Twenty-one of 66 evaluable patients (31.8%) had treatment failure (13 patients had locoregional recurrence, and 8 patients developed distant metastasis). As shown in table 2.

Table 2 Results of treatment. Number of evaluable patients (%)

	LDR	HDR
Locoregional recurrence	19 (23.2%)	13 (19.7%)
Distant metastasis	11 (13.4%)	8 (12.1%)
Complete response	52 (63.4%)	45 (68.2%)
Total	82 (100%)	66 (100%)

With minimal follow-up of 36 months, there were 14 and 4 patients of the 52 responders in LDR group (26.9,7.7%) developed grade I proctitis and grade I cystitis, respectively. Sixand 1 patient of the 45 responders in HDR group (13.3%,2.2%) developed grade I proctitis and grade I cystitis, respectively. Only one patient in HDR group had grade II proctitis. As shown in table 3.

Table 3 Late normal tissues complications Number of patients (%)

	LDR	HDR
Grade 0	34 (65.4%)	37 (82.2%)
Grade I proctitis	14 (26.9%)	6 (13.3%)
Grade II proctitis	0	1 (2.2%)
Grade I cystitis	4 (7.7%)	1 (2.2%)
Total	52 (100%)	45 (100%)

DISCUSSION

Radiation therapy with combination of external beam and brachytherapy has been the standard treatment of cervical cancer.[1,2] With LDR brachytherapy (radium-226 or cesium-137 source) and after manual loading technique, good treatment results were achieved with more safty to medial personnels.[3,4] After introduction of HDR with more advanced computerized planning

system and remote after loading system, many institutes have shifted the treatment from LDR to HDR.[5,6,7] There were several rationals for this change, the first was due to out-patient treatment basis that might reduce the hospital cost. The second was its reproducible planning, which might ensure more accurate dosimetry.[8] The third was the short treatment time, that caused more convenience and comfortable of the patients than overnight hospitalization etc.

Several published data suggested that dose-fractionation of HDR was the important factor in tumor control and late normal tissue complications[9,10,11] C.G.Orton & Armny had reported "An International Review on Patterns of Care in Cancer of the Cervix", including 56 facilities with 17,000 patients treated with HDR.[12] the mean of number of fraction and dose per fraction were 4.82 and 7.45 Gy, respectively. The crude 5 year-survival of this review was slightly better for HDR than LDR. In the survey data of Orton, the complictions of HDR is fewer than LDR. Studies from Japan,[5,7] the result in survival between HDR and LDR were comparable, with more severe and more frequent in late normal tissues complications. The difference results from reviewing study might due to variable of complications description, variable of treatment techniques, and variable of dose-fractionation.[13]

In our study, there was a slightly better 3 year-survival of HDR than LDR in terms of more locoregional control and less distant metastasis ($p = 0.544$). Rational for the better survival of HDR might due to its shorter overall treatment time than LDR. This result could be comparable to previous reported of the correlation between longer overall treatment time and worse prognosis.[14,15,16] In this study, fewer complications of HDR was noted, in both proctitis and cystitis without statistical significance ($p = 0.062$).

CONCLUSION

The HDR brachytherapy is comparable to former LDR treatment with minimal better survival and less normal tissue complications. More prospective randomized studies are needed to establish the optimal dose-fractionation schedule treatment in HDR to ensure the better results in treatment of cervical cancer.

REFERENCES

1. Perez CA,Camel HM,Kuske RR,et al : Radiation therapy alone in treatment of the uterine cervix : A 20 year experience. Gynecol Oncol 23:127,1986
2. Barillot I, Hariot J, Pigneux J: Carcinoma of the intact uterine cervix treated with radiotherapy alone: A french Cooperative Study Update and multivariant analysis of prognostic factors. Int J Radiat Oncol Biol Phys 38:969-978,1997
3. Fowler JF: The linear quadratic formula and progressive in fractionated radiotherapy : A review. Br J Radiol 62:679-694,1989
4. Fowler JF : The radiobiology of brachytherapy. In Martinez AA,Orton CG Mould RF, eds : Brachytherapy HDR and LDR, pp 121-137. Leeseem, The Netherlands, Nucletron International BV, 1990
5. Arai T, Nakano T, Morita R, et al: High dose remote after loading intracavitary radiation therapy for cancer of the uterine cervix. Cancer 69:175,1991
6. Patel F, Sharma S, Pritam S, et al : Low dose rate VS high dose rate brachytherapy in the treatment of the uterine cervix: A clinical trial. Int J Radiat Oncol Biol Phys 28:335,1993

7. Shigemastsu Y, Nishiyama K, Masaki N, et al: Treatment of carcinoma of the uterine cervix by remote controled after loading intracavitary radiotherapy with high dose rate : A Cooperative study with a low dose rate system. Int J Radiat Oncol Biol Phys 9:351,1983
8. Hoskin PJ, Cook M, Bouscale D, Camsdale J: Changes in applicator position with Fractionated high dose rate gynecologic brachytherapy. Radiother Oncol 3: 81-89,1987
9. Orton CG, Seyedsadr M, Somnay A: Comparison of high and low dose rate remote after loading for cervix cancer and the importance of fractionation, Int J Radiat Oncol Biol Phy 21:1425-1434,1991
10. Barendsen GW, Dose fractionation, dose rate and isoeffect relationship for normal tissue response. Int J Radiat Oncol Biol Phys 8:1931-1997,1982
11. Turesson I, Notter G: The influence of fraction size in radiotherapy on the late normal tissue reaction II. Comparison of the effects of daily and once week fractionation on human skin. Int J Radiat Oncol Biol Phys 10:599-618,1984
12. Orton CG,Somnay A: Brachytherapy from Radium to Optimization. In Mould RF, Battermann JJ, Martinez AA, Speiser BI, eds: Results of an international Review on Patterns of Care in Cancer of the Cervix, pp 49-54. Veenmann, The Netherlands, Nucletron International BV, 1994
13. Petercit DG, Pearcey R : Literature analysis of high dose rate brachytherapy fractionation schedule in the treatment of cervical cancer: Is there an optimal fractionation schedule. Int J Radiat Oncol Biol Phys 43: 359-366,1999
14. Lanciano R, Pajak T, Martz K et al: The influence of treatment time on outcome for squamous cell carcinoma of the uterine cervix treated with radiation: A Pattern of Care Study. Int J Radiat Oncol Biol Phys 25:391-397,1993
15. Fyler A, Keane T, Barton M, et al: The effect of treatment duration in the local control of cervix cancer. Radiother Oncol 25:273-279,1992
16. Perez CA, Gripsby P, Gripsby W, et al : Carcinoma of the uterine cervix: Impact of prolongation of overall treatment time and timing of brachytherapy outcome of radiation therapy. Int J Radiat Onclo Biol Phys 32:1275-1288,1995

HONG KONG COLLEGE OF RADIOLOGISTS
香 港 放 射 科 醫 學 院

Founder College of the Hong Kong Academy of Medicine

(Incorporated in Hong Kong with limited liability)

25th May 2002

Prof. Kawee TUNGSUBUTRA
President, The Radiological Society of Thailand
c/o Department of Radiology
Kaweevej Hospital, 318 Tarksin Road,
Dhonburi, Bangkok 10600
Thailand

Dear Prof. TUNGSUBUTRA,

Re: Request for free listing of the 10th Annual Scientific Meeting (19th – 20th October 2002, Hong Kong)

We would like to request for free listing of the 10th Annual Scientific Meeting organized by our College in your homepage and every issue of your publication(s) prior the event. Kindly include the information as shown below:

Name of the event	:	10th Annual Scientific Meeting
Date	:	19th – 20th October 2002
Venue	:	Hong Kong Academy of Medicine Jockey Club Building 99 Wong Chuk Hang Road Aberdeen, Hong Kong
Organizer	:	Hong Kong College of Radiologists
Contact	:	Ms Diane Lee, Executive Officer Hong Kong College of Radiologists Room 909, 9/F, Hong Kong Academy of Medicine Jockey Club Building 99 Wong Chuk Hang Road Aberdeen, Hong Kong Tel: (852) 2871 8788 Fax: (852) 2554 0739 E-mail: enquiries@hkcr.org Homepage: http://www.hkcr.org

A copy of the First Announcement is enclosed for your reference. Thank you for your attention. We look forward to your kind consideration.

Yours sincerely,

Diane Lee
Executive Officer

\\SERVER\ADMIN FILES\Education\Scientific\ASM\10th ASM + 2nd Joint Ceremonies for Admission of New Fellows\Corr\Free Listing\l_free listing_10thASM_merged.doc